universität
wien

# MASTERARBEIT / MASTER’S THESIS

Titel der Masterarbeit / Title of the Master‘s Thesis

## Environmental Fate of Clothianidin Nanopesticides

verfasst von / submitted by

Helene Walch, BSc

angestrebter akademischer Grad / in partial fulfillment of the requirements for the degree of

Master of Science (MSc)

Wien, 2016 / Vienna 2016

| | |
|---|---|
| Studienkennzahl lt. Studienblatt / degree programme code as it appears on the student record sheet: | A 066 229 |
| Studienrichtung lt. Studienblatt / degree programme as it appears on the student record sheet: | Environmental Sciences |
| Betreut von / Supervisor: | Univ.-Prof. Dr. Thilo Hofmann |
| Mitbetreut von / Co-Supervisor: | Mélanie Kah, PhD |

# i. Acknowledgments

I would like to express my gratitude to my co-supervisor Mélanie Kah, PhD for the confidence she had in me, allowing me to work autonomous within a given frame, while always being available to discuss the progress of my work and provide helpful and inspiring advice. I really appreciated her personal and scientific engagement throughout the learning process of my master's thesis.

Furthermore I would like to thank Univ.-Prof. Dr. Thilo Hofmann for creating a very constructive working atmosphere within the group and for always lending an ear in case of scientific or personal need.

Special thanks, also to Petra Körner who introduced me to the laboratory, techniques and analytics applied. She was always very helpful in organizing laboratory equipment and ensured a very good working atmosphere.

Last but not least I would like to thank my family for their financial and moral support, allowing me to focus on my studies, and of course my boyfriend and friends who were always there for me, helping me to keep my balance through busy periods. I am indescribably glad to have you on my side.

# ii. Declaration of Academic Honesty

Hereby, I declare and confirm with my signature that the present master's thesis is exclusively the result of my own autonomous work and has been composed without any other resources than the ones indicated. All thoughts taken directly or indirectly from external sources are properly denoted as such.

No part of this work has been previously submitted to another educational institution or published elsewhere yet.

Vienna, 9th October 2016

Helene Walch

Helene Walch, BSc

# iii. Summary

Nanotechnology reached the agricultural sector and the number of pesticide products containing nano-sized components (up to 1000 nm), so-called nanoformulations (NFs), increases. Especially polymer-based NFs are promising, as the nanocarriers (NCs) may be engineered for various aims with regards to the pesticide active ingredient (AI), e.g. slow/targeted release, protection against degradation, enhanced solubility. Tailored release NCs potentially change the environmental fate of the AI and might require adaptation of regulations with regards to environmental risk assessment. However, the current state of knowledge is not sufficient to assess NF impact on fate processes.

Thus, the present work investigates the influence of nanoformulations (1) on the aqueous photodegradation rate and (2) on the sorption behavior of the AI clothianidin (Clo), by means of comparative laboratory studies of three NFs (NFA, NFB, NFC) versus a commercially available formulation (Com) and a pure AI solution, to assess general formulation influences and nano-effects.

Clo analysis was performed by HPLC coupled with UV-Vis detection. Experimental Clo concentrations were based on maximum realistic application rates in foliar spray (for photodegradation) and in-furrow with the seed (for sorption). Both fate processes were investigated with AI/formulation solutions prepared in deionized water ($H_2O$-background) as well as in combination with PowerPhos liquid fertilizer (PP-background) to enhance the chance of AI-NC association due to salting out.

For photodegradation studies, solutions of the formulations/AI were irradiated with a xenon arc lamp. Generated degradation curves were used to determine degradation rates. To account for concentration effects, in $H_2O$-background additional concentrations below and above Clo solubility were tested.

The results showed a clear decrease in photodegradation rate constants with increasing Clo concentrations for all formulations and the AI. Furthermore, protective effects of nanoformulations (lower degradation rates than Com) emerged at concentration levels close to and above Clo solubility and increased with concentration. Since the release of Clo from the NC depended on Clo solubility, the protective effect was attributed to an increased AI-NC association at high Clo concentrations. The addition of PP fertilizer did not enhance the photoprotective effect of the NFs relative to Com/AI, but it strongly reduced the degradation rate of all formulations and the AI, probably due to a shading effect.

Sorption experiments were carried out on two contrasting soils (sand and loam) with two methods, a classical batch-equilibrium method (batchM), and a centrifugation method (centM), which allows assessment of sorption at a more realistic soil:solution ratio, as well as the investigation of sorption over time. Partitioning coefficients were determined to compare the various experimental setups.

Three-way ANOVA showed that the sorption behavior of all formulations and the AI was dominated by the soil type, which explained > 90 % of the $K_d$ variation in both methods: $K_d$ was always higher in loam than in sand, due to a higher content of organic matter. Other influencing factors (formulation, background solution and interactions) remained below 2.3 %. Sorption experiments did not reveal any general nano-effect, as the AI was immediately released from the NC upon dilution. Also the addition

of PP fertilizer did not enhance nano-effects. However, single NFs exhibited nano-effects in the batchM: NFC sorbed significantly stronger than Com throughout all soil-background-solution combinations (and stronger than AI in $H_2O$-backgrounds), and NFB sorbed more than Com/AI in loam ($H_2O$ and PP). As NFC was the formulation that aggregated the most in high ionic strength, physical capturing of the AI within aggregates might have been a reason. But absolute $K_d$ differences between formulations remained low and non-relevant when compared to other factors (e.g. soil).

Nevertheless, some insight into the different sorption methods and the relevance of soil-fertilizer interactions was gained. The influence of background solution was more pronounced in the centM and triggered contrary effects in sand and loam: for sand $K_d$ values were higher in $H_2O$, but for loam they tended to be higher in PP. The former may be explained by organic matter being dominated by fulvic and humic acids in sand, which were solubilized by $NH_4^+$ (introduced by PP) and caused co-mobilization of associated Clo. The latter may be explained by the impact of PP on soil aggregates in loam. Aggregates slow down equilibration and decrease accessibility of sorption sites. Thus, a higher sorption in loam-PP might arise from the destruction of these aggregates by monovalent $NH_4^+$, allowing for better equilibration. With longer incubation (in the centM) sorption generally increased because of a slow diffusion into aggregates and pores which offer further sorption sites. However, in loam-$H_2O$ sorption did not change with time probably due to a strong diffusion gradient in the aggregates caused by the pre-equilibration with deionized water.

When comparing the two methods, the calculated percentages of Clo adsorbed were higher with the centM for both soils, and so were $K_d$ values in loam. However, $K_d$ values in sand were higher with the batchM. Increased sorption in the centM for substances exhibiting rather low sorption (like Clo) is probably caused by physical capturing within aggregates and zones of immobile water at high soil:solution ratios.

Summing-up, the results indicate that the present NFs – as fast-release formulations – did not have any overarching nano-effect on photodegradation or sorption behavior when applied at maximum recommended concentrations for crops. With regards to environmental risk assessment, other factors like soil type and fertilizer addition had much stronger effects and nullified any formulation effect. However, this cannot be generalized, since a clear nano-effect was observed for photodegradation, when the concentrations were increased close to or above Clo solubility, causing the AI to stay associated with the NC. Such high Clo spray concentrations are e.g. applied for grapes and pome-fruits. This confirms the importance of the release behavior for NF risk assessment and shows that polymer-based NFs generally have the potential to influence fate processes in case of slow-release formulations.

With regards to sorption methods, it seems that the batchM underestimates percentages adsorbed under field conditions and is not able to reflect complex processes like fertilizer-humics interactions that would occur under more realistic conditions (like in the centM). Furthermore the centM proved to be suitable to study time-dependent sorption, which might be useful to study slow-release formulations.

# Table of Contents

**i. Acknowledgments**

**ii. Declaration of Academic Honesty**

**iii. Summary**

**iv. List of Tables**

**v. List of Figures**

**vi. Abbreviations**

**1. Introduction ........ 1**
- 1.1. Terms and Definitions ........ 1
- 1.2. State of Knowledge ........ 3
- 1.3. Research Focus and Experimental Plan ........ 5

**2. Materials ........ 7**
- 2.1. Soils ........ 7
- 2.2. Chemicals ........ 8
  - 2.2.1. Clothianidin Active Ingredient ........ 8
  - 2.2.2. Clothianidin Pesticide Formulations ........ 9

**3. Methods ........ 10**
- 3.1. Analytical Method ........ 10
- 3.2. Characterization of Nanoformulations ........ 10
- 3.3. Photodegradation ........ 12
- 3.4. Sorption to Soil ........ 14
  - 3.4.1. Batch Method ........ 15
  - 3.4.2. Centrifugation Method ........ 16
- 3.5. Clothianidin and Fertilizer Application Scenarios ........ 18
  - 3.5.1. Photodegradation: Foliar Spray Application Scenario ........ 18
  - 3.5.2. Sorption to Soils: In-Furrow Application Scenario ........ 19
- 3.6. Statistics ........ 20

**4. Results and Discussion ........ 21**
- 4.1. Characterization of Nanoformulations ........ 21
- 4.2. Photodegradation ........ 24
  - 4.2.1. Formulation Influence on Photodegradation in $H_2O$-Background ........ 28
  - 4.2.2. Photodegradation in the Foliar Spray Application Scenario ........ 30
- 4.3. Sorption to Soils ........ 32
  - 4.3.1. Effect of Soil Type ........ 34
  - 4.3.2. Effect of Time (Centrifugation Method only) ........ 34
  - 4.3.3. Effects of Background Solution ........ 36

4.3.4. Effect of Sorption Experimental Method ........ 40
4.3.5. Effects of Formulations ........ 44
**5. Conclusions and Outlook ........ 51**
5.1. Nanoformulation Characterization ........ 51
5.2. Photodegradation ........ 51
5.3. Sorption to Soil ........ 53
5.4. Future Research Perspectives ........ 55

**vii. Literature Cited**
**viii. Annex**

# iv. List of Tables

Table 1. Main characteristics of the studied soils (±SD) ........ 7
Table 2. Dry-weight factors and water contents of the experimental soils (±SD) ........ 7
Table 3. pH dependence of Clo water solubility, octanol-water partitioning coefficient ($K_{ow}$) & hydrolysis ........ 8
Table 4. Composition of the Clo formulations ........ 9
Table 5. Clo content in formulations and Clo recovery (±SD) ........ 9
Table 6. HPLC method mobile phase gradient ........ 10
Table 7. Experimental fertilizer/Clo concentrations in soil solution and respective working solutions ........ 15
Table 8. Summary: experimental concentrations of $NH_4$, $P_2O_5$ and Clo for foliar spray application case ........ 19
Table 9. Calculation of N concentration ($c_N$) in soil dry weight in case of in-furrow fertilizer application ........ 20
Table 10. Summary: experimental concentrations ($c_{soil}$) of $NH_4$, $P_2O_5$ and Clo for in-furrow application case ........ 20
Table 11. NFs characterization: hydrodynamic diameter, polydispersity index and zeta potential in $H_2O$ (±SD) 21
Table 12. Photodegradation: summary of half-lives ( ± SD) derived from degradation curve fits ........ 25
Table 13. Photodegradation rates k of NFs relative to k of Com ........ 30
Table 14. $K_d$ values (±SD) in loam & sand derived with the batch (after 24h) and centM (after 1 & 7 days) ........ 33
Table 15. Results of three-way ANOVA calculated for the batchM and for the centM at day1 and day7 ........ 33
Table 16. Changes (Δ) of solution pH (±SD, n=27) due to equilibration with soils (soil:solution ratio 1:2) ........ 37
Table 17. Clo percentage adsorbed (A ± SD) in loam & sand in the batch (after 24h) and centM (after 1 & 7 d) 43
Table 18. Differences of $K_d$ values between formulations (<, >, n.s.; read row vs. column) ........ 49

# v. List of Figures

Figure 1. Three scenarios to assess NC influence on fate processes based on AI release kinetics and fate process time scales (modified after Kah & Hofmann 2014)....4
Figure 2. Overview on experimental testing....6
Figure 3. Chemical structure of clothianidin (EC-SANCO 2005)....8
Figure 4. Modes of colloidal stabilization (steric, electrostatic, electrosteric) (modified after Liu et al. 2014)....11
Figure 5. (a) Atlas Suntest CPS+, (b) samples/controls within the aging chamber....13
Figure 6. Model of first order exponential decay (GraphPad Software Inc 2014)....14
Figure 7. (a) incubation of spiked soils at 60% MWHC, (b) AcN-extraction for total cClo, (c) centrifugation to gather soil solution....17
Figure 8. Planting device with in-furrow pesticide/fertilizer application (modified after Fish et al. 2001)....19
Figure 9. NFs characterization: change in particle size and zeta potential in $H_2O$ and 75 mM $CaNO_3$....22
Figure 10. NFs release of the AI: stabilization of filtrate concentration (0.2 µm filters) at cClo < solubility....22
Figure 11. NF release behavior tested by syringe filters at cClo below and above solubility....23
Figure 12. NF release behavior tested by syringe filters at max. experimental cClo and fertilizer concentration....23
Figure 13. Example of degradation curves: NFB at cClo ~544 mg/L....24
Figure 14. Linear regression of NFC dark control samples at cClo ~544 mg/L....24
Figure 15. Photodegradation: relations of rate (k), cClo and pH....26
Figure 16. Non-linear relation of photodegradation rate (k) and initial testing substance concentration ($C_0$) (data from Hessler et al. 1993)....27
Figure 17. Photodegradation: comparison of slopes from linear regression of rate (k) vs. cClo....28
Figure 18. Photodegradation rate constants (k) of the formulations at various Clo concentration levels.....29
Figure 19. Photodegradation rate (k) at cClo ~136 mg/L in aqueous and fertilizer background....30
Figure 20. The area of spectrally active elements in the periodic table[a] (Wozniak & Dera 2007, p 73)....30
Figure 21. Photodegradation rate (k) comparison of the different formulations in fertilizer background....32
Figure 22. CentM: influence of time on $K_d$ of formulations in all soil-background-solution combinations....34
Figure 23. CentM: AcN extractable Clo per $kg_{dw}$ soil (a) and cClo in solution (b) after 1 & 7 days (compiled data of all formulations and the AI)....35
Figure 24. BatchM: pH values of initial solutions before equilibration with soils....37
Figure 25. CentM: background solution dependence of soil-solution color....37
Figure 26. Chemical properties of humic substances (Stevenson 1982)....38
Figure 27. Influence of background solution on centM and batchM $K_d$ values of formulations and the AI....39
Figure 28. Sorption experiments: comparing batchM and centM at equilibrium....41
Figure 29. Sorption $K_d$ comparisons between formulations and the AI in the batchM and centM....45
Figure 30. CentM: patterns of $K_d$ values in loam at day 1 (a), Kd values in loam-day 1 ordered by size (b)....48
Figure 31. Zoomed-into $K_d$ differences between formulations in the batchM....50

# vi. Abbreviations

| | |
|---|---|
| AcN | acetonitrile |
| AI(s) | active ingredient(s) |
| batchM | batch method |
| cClo | concentration of clothianidin |
| CEC | cation exchange capacity |
| centM | centrifugation method |
| Clo | clothianidin |
| Com | commercial formulation |
| HPLC | high-performance liquid chromatography |
| k | photodegradation rate |
| $K_d$ | distribution (sorption) coefficient |
| mAU | milli absorption units |
| MWHC | maximum water holding capacity |
| NC | nanocarrier |
| NF(s) | nanoformulation(s) |
| NFA | nanoformulation A |
| NFB | nanoformulation B |
| NFC | nanoformulation C |
| PP | PowerPhos liquid fertilizer |
| SD | standard deviation |

# 1. Introduction

The present master's thesis investigates the sorption to soils and photodegradation of new kinds of pesticide formulations, so-called polymer-based nanopesticides. Sorption and photodegradation are two major processes with regards to environmental risk assessment. To see whether a nanoformulation can influence the environmental behavior of the active ingredient (clothianidin), comparative studies of three nanoformulations, a commercially available formulation and the pure active ingredient solution were conducted.

To get into the topic, the following sections give some important definitions, summarize the current state of knowledge and introduce the research focus and experimental plan.

After that, the chapter on materials (2) comprises information on the soils (2.1) and chemicals used (2.2), and is followed by a chapter on methods (3), giving details on the analytical method used (3.1), the characterization of the nanoformulations (3.2) and the experimental procedures for photodegradation (3.3) and sorption to soils (3.4). For the latter two, the experimental concentrations were based upon application scenarios, which are elaborated in 3.5, and the last section (3.6) is dedicated to the statistics performed.

Subsequently, the results are presented and discussed based on scientific literature (chapter 4) in the following order: 4.1 Characterization of Nanoformulations, 4.2 Photodegradation and 4.3 Sorption to Soils. Whereby the photodegradation and sorption sections are structured according to the major influencing factors (e.g. background solution, soil type, formulation...).

Finally, chapter 5 gives conclusions on the main findings and includes future research perspectives.

## 1.1. Terms and Definitions

Pesticide: A pesticide either prevents/destroys/controls harmful organisms (pests) or diseases, or protects plants/plant products during production, storage and transport. This includes e.g. herbicides, fungicides, insecticides, acaricides, nematicides, molluscicides, rodenticides, growth regulators, repellents and biocides (EC 2016b). Pesticide products are mixtures of chemicals which allow to effectively control a pest and consist of active ingredient(s) and inert substances (formulants) (US-EPA 2016; Bindhu et al. 2016).

Plant Protection Product: A plant protection product is a pesticide aiming to protect crops or plants, as used in the agricultural sector, forestry, horticulture, amenity areas and home gardens. It narrows down the term pesticides to plant/crop uses, excluding other uses e.g. biocides. Plant protection products either protect plants/crops against pests/diseases (before and after harvest), against other undesired plants, or they influence the life process of plants (e.g. growth regulators) (EC 2016b).

Pesticide Active Ingredient (AI): The EC (2016b) defines an active substance as *"any chemical, plant extract, pheromone or micro-organism (including viruses), that has action against 'pests' or on plants,* *parts of plants or plant products".* Similarly, the US-EPA (2016) defines an active ingredient (as opposed to an inert ingredient) as *"a substance that prevents, kills, or repels a pest or acts as a plant regulator, desiccant, defoliant, synergist, or nitrogen stabilizer".* And summarizes: AIs *"are the chemicals in a pesticide product that act to control the pests".*

Pesticide Formulation: An AI is formulated to a pesticide product by addition of inert ingredients (formulants or forming agents). The formulation aims to improve storage, handling, safety, application, or effectiveness of the AI (Ware 1994). Forming agents can be inert carriers, emulsifiers, wetting agents, solvents, thickeners, encapsulants etc. (Bindhu et al. 2016).

Nanomaterial: A nanomaterial generally is a material with external dimensions or internal structures at a nanoscale size range (Kah et al. 2013). In the nanomaterial definition of the EU (EC 2016a), this includes sizes from 1-100 nm. However, in nanopesticide research sizes up to 1000 nm were usually termed "nano" (Kah et al. 2013; Kah & Hofmann 2014).

Nanocarrier (NC): A nanocarrier can be defined as a nanomaterial (here organic or inorganic nanoparticles) that functions as a carrier or transporter for molecules (AIs). NCs are used for medical, cosmetic, food, or agricultural applications and often have dimensions > 100 nm (Kah et al. 2013).

Nanoformulation (NF): There are various types of NFs including emulsions (AI dissolved in oil droplets spread in aqueous solution by surfactants/co-surfactants), dispersions (crystalline/amorphous pure AI particles dispersed in liquids, sometimes using surfactants or polymeric stabilizers), solid-lipid based NFs (like emulsions, but the AI is captured in solid lipid particles), mineral-based NFs (porous silica, layered hydroxides or clays provide a mineral matrix for AI loading), nano-metals/oxides (either incorporated e.g. into nanopolymers as catalysts for photodegradation, coated by pesticides or exhibiting pesticidal activity themselves) and finally polymer-based NFs (various, cited in Kah et al. 2013). The latter typically were either nanospheres (with unknown AI distribution) or nanocapsules (with the AI inside a polymer capsule) (Kah et al. 2013), but more recently also nanogels and nanofibers received attention in pesticidal applications (Kah & Hofmann 2014). Nanospheres are insoluble solid colloidal nanoparticles providing a matrix for the AI, nanogels are nano-sized 3D cross-linked networks of hydrophilic polymers loaded with the AI and nanocapsules exhibit a typical core-shell structure (various, cited in Talevi et al. 2014).

Deionized Water, H2O: In the present study the terms "deionized water", "$H_2O$" and "aqueous" generally mean (based on) deionized (MilliQ) water. The terms are used interchangeably.

## 1.2. State of Knowledge

Nanotechnology made its way into agriculture over the past decade. Especially nanoformulations of plant protection products, so-called nanopesticides, gain importance (Kah & Hofmann 2014).

A practically oriented definition of nanopesticides was given by Kah et al. (2013), comprising *"any pesticide formulation that (a) intentionally includes entities in the nanometer size range (*[…] *up to 1000 nm), (b) is designated with a "nano" prefix (e.g., nanohybrid, nanocomposite), and/or (c) is claimed to have novel properties associated with the small size."*

There are various types of NFs, but polymer-based NFs received a lot of attention in the last years and were judged to be the most promising (Kah & Hofmann 2014; Kookana et al. 2014). Hence, the present work also focuses on polymer-based NFs.

The advantage of polymer-based NFs is that they offer a huge potential to be engineered for various aims with regards to the AI e.g. slow release and prolonged or delayed effect, protection against premature degradation (e.g. enhanced photostability), enhanced solubility for formulation issues, increased uptake by plant or pest and enhanced efficacy, reduced losses (e.g. due to volatilization, leaching, hydrolysis, plant wash-off), reduced residues on crops (e.g. including a photocatalyst) and targeted release and decreased toxicity to non-target organisms (Kah & Hofmann 2014; Kah et al. 2013).

Thus, NFs can enhance properties of plant protection products and potentially also improve their environmental compatibility e.g. using biodegradable polymers to protect less stable natural AIs (Kah & Hofmann 2014) , reducing application frequency due to combination of conventional formulations and delayed release NFs (Kang et al. 2012), reducing total applied amounts due to decreased losses or increased efficacy, or substituting other toxic additives like surfactants, emulsifiers and solvents (Kah et al. 2013). However, also negative effects of these engineered NF properties on the environmental fate and behavior of an AI cannot be excluded and might have implications for environmental risk assessment.

Nanopesticides, when used as plant protection products, are outstanding in terms of environmental risk as compared to other nanoparticle applications: They are released on a large scale (diffuse source), intentionally and repeatedly. Kah et al. (2013) pointed out that EU regulations might need adaption, since so far environmental risk assessment is usually based on testing the AI only (e.g. for sorption, photolysis, hydrolysis studies), assuming that formulants have no long-term effect on the fate and behavior of the AI. However, considering the above engineering aims, nanoformulations might have a substantial influence on transport, bioavailability and persistency of an AI.

The potential of a NF to influence those fate processes might to a large extent depend on its release behavior. Kah & Hofmann (2014) proposed the generalization of a concept previously developed to assess the colloid/nanoparticle-facilitated transport of contaminants (Hofmann & von der Kammer 2009; Hofmann & Wendelborn 2007; Kretzschmar et al. 1999), and assess fate processes of nanoformulated AIs by comparing the release kinetics of the AI from the NC to the rate or time scale of the fate process (e.g. transport, photo-/biodegradation). Based on this, three types of conditions can be differentiated (Figure 1): equilibrium conditions (rapid release; the AI behaves like a solute), decoupled conditions (slow release; fate processes have to be assessed for two decoupled pools of NC-associated AI and dissolved AI) and kinetic conditions (release and fate process proceed over similar time scales; release kinetics are needed to asses transfer from the associated to the dissolved AI). However, Kah & Hofmann (2014) also pointed out that degradation of the NC-associated AI cannot be excluded so far. Nevertheless, these considerations underline the importance of the release behavior in terms of environmental fate.

The AI can be released from the polymer NC by desorption form the surface, diffusion out of the polymer matrix or by dissolution/erosion of the NC itself (Kah & Hofmann 2014).

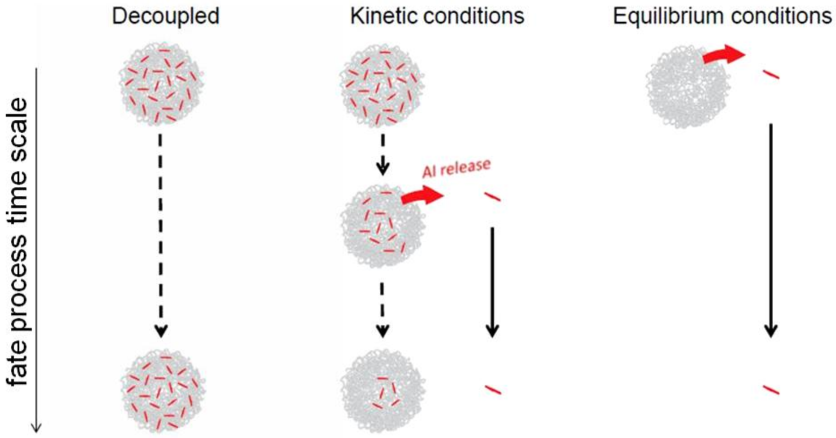

**Figure 1. Three scenarios to assess NC influence on fate processes based on AI release kinetics and fate process time scales (modified after Kah & Hofmann 2014)**

Next to release, particle size, size distribution, surface chemistry and functionalization are key properties of NFs (Kah et al. 2013) which might be decisive for the occurrence of nano-effects on environmental fate and behavior. Thus, characterization of the NCs receives increased attention, including measurements of size distribution, polydispersity indices (heterogeneity of sizes) and zeta potentials (surface charge) (Kah & Hofmann 2014). Such measurements can e.g. be used to asses colloidal stability of the formulation, which might also affect the fate of the AI: After application the NF might aggregate/agglomerate in soil solution or be separated into its constituents by dilution (Kah et al. 2013).

Two major environmental risk assessment tests for pesticides include sorption studies in soils and photodegradation in water (OECD 2000; OECD 2008). Both have only rarely been investigated for polymer-based NFs, not allowing for general conclusions on the impact of NFs. For example, sorption studies with slow-release formulations of paraquat (dos Santos Silva et al. 2011) and atrazine (Kah et al. 2014) showed contrasting effects of the NF on sorption behavior. Photodegradation studies often comprised photocatalytic NFs (e.g. including $TiO_2$) designed to reduce residues on crops (e.g. Guan et al. 2010; Cao et al. 2005). Photoprotective effects of polymer-based NFs, on the other hand, were shown by Shang et al. (2013) and Deng et al. (2016).

## 1.3. Research Focus and Experimental Plan

Studies on the environmental fate of nanopesticides are rather scarce, especially as far as organic particles are concerned (Kah et al. 2013). Thus, the present study aims at shedding more light onto the environmental fate of polymer-based NFs, with the main hypothesis being that nanoformulations can affect the aqueous photodegradation or soil-sorption behavior of the AI with possible consequences on the environmental fate of the AI.

To test this hypothesis, we received three polymer-based NFs of clothianidin (Clo), a neonicotinoid insecticide, currently being developed by a North American company, as well as a commercially available formulation called “Belay”. The NFs were subjected to a basic characterization, including size and zeta potential measurements by dynamic & electrophoretic light scattering and an investigation of the release behavior by filtration.

Since Clo is very persistent to biodegradation but susceptible to photodegradation (University of Hertfordshire 2016), sorption to soils and photodegradation were the environmental fate processes of choice. Thus, the main hypothesis was split into two research questions: Does the NF influence (1) the sorption behavior of the AI towards soils and (2) the aqueous photodegradation rate of the AI. Both questions were investigated by means of comparative studies of the three NFs, the commercial formulation (Com) and a pure AI solution, whereby Com served as control for nanoformulation effects and the AI as control for general formulation effects.

Photodegradation studies were carried out at several concentrations above and below solubility of Clo to account for concentration effects. Additionally, a “worst case” application scenario was developed based on maximum Clo application rates in foliar spray in combination with a liquid fertilizer, intended to enhance the NC-association of the AI by salting out, which is the reduced solubility of organic molecules in high salt concentration (Delle Site 2001).

Concerning sorption to soils, Kah et al. (2013) questioned the applicability of standard test protocols (e.g. OECD 2000) on NFs, because experimental setups (e.g. low soil:solution ratios, vigorous shaking, etc.) might affect the properties of the nanopesticides and therefore not allow for conclusions on their behavior under more realistic conditions. Additionally, NFs might require considerations of property changes over time (Kah et al. 2013). Hence, sorption experiments were carried out using two methods, a classical batch-equilibrium method (batchM) (OECD 2000) and a centrifugation method (centM), as developed by Walker & Jurado-Exposito (1998) and adapted/applied by Allen Walker (2000), Kah & Brown (2007) and Kah et al. (2014). The centM allows to assess sorption under more realistic conditions (lower soil:solution ratios, structured soil, no shaking) as well as changes over time. To cover different soil properties, sorption studies were conducted with two contrasting soil types (a sand and a loam). Additionally, similar to photodegradation, an application scenario provoking high Clo soil concentrations (in-furrow application) and possibly salting out (fertilizer addition) was assumed to increase the chances of NF-effects. Thus, for sorption and photodegradation experiments, two background solutions (aqueous and fertilizer) were used.

For clothianidin analysis, a high-performance liquid chromatography (HPLC) method was developed and validated. Photodegradation experiments were carried out with Atlas Suntest CPS+ measuring remaining Clo concentrations (cClo) in solution at increasing time intervals and calculating photodegradation rate constants (k). For sorption experiments, distribution coefficients ($K_d$=$cClo_{soil}$/$cClo_{solution}$) were determined measuring remaining cClo in solution and calculating cClo in soil by subtraction from total initial Clo concentrations. Photodegradation rates and $K_d$ values could then be compared between formulations, background solutions and/or soils to assess their influences or interactions.

Figure 2 gives an overview on the experimental testing scheme.

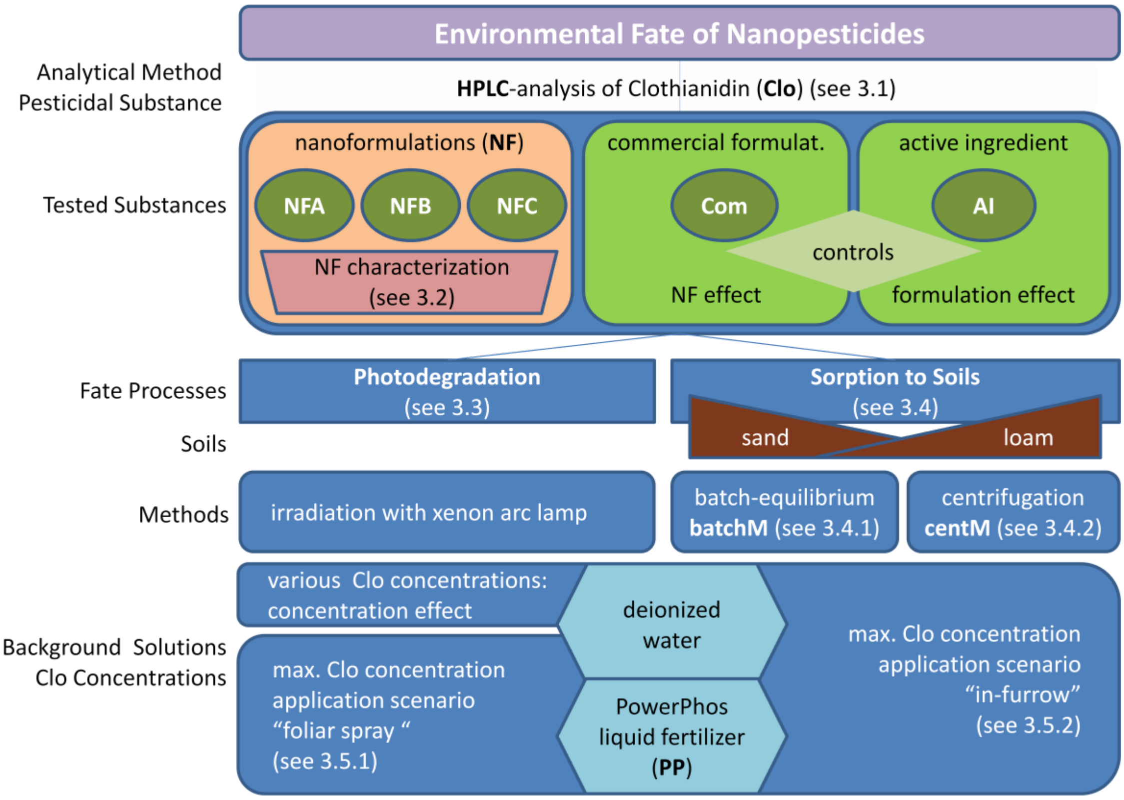

**Figure 2. Overview on experimental testing**

# 2. Materials

The following section provides information on the origin and characteristics of the soils (2.1) and chemicals used (2.2). Concerning the nanoformulations, only the information obtained from the provider is given in this section, further characterization results are presented in section 4.1.

## 2.1. Soils

Two standard soils were obtained from LUFA (Landwirtschaftliche Untersuchungs- und Forschungsanstalt) Speyer, Germany. Both were sampled in about 20 cm depth according to ISO standards and good laboratory practices in March 2013 in the region of Rheinland-Pfalz, Germany. Soil 2.1 (sand) was taken from an uncultivated field in Dudenhofen, whereas soil 2.4 (loam) was taken from a meadow with apple trees in Leimersheim. No pesticides or fertilizers were applied to the soils for a period of minimum four years before sampling. The soils were air-dried, sieved at 2 mm and analyzed by LUFA Speyer. Analysis results are summarized in Table 1.

**Table 1. Main characteristics of the studied soils (±SD)**

| soil Nr. | soil type[a] | OC[b] [%] | N [%] | pH[c] | CEC [meq/100g] | clay[a] (<2 µm) [%] | sand[a] (0.05-2 mm) [%] | MWHC[d] [g/100g] | density [g/dm³] |
|---|---|---|---|---|---|---|---|---|---|
| 2.1 | sand | 0.65±0.1 | 0.05±0.01 | 5.1±0.3 | 4.3±0.5 | 2.8±1.1 | 87.0±1.5 | 31.1±2.1 | 1474±28 |
| 2.4 | loam | 2.26±0.5 | 0.20±0.04 | 7.2±0.2 | 31.4±4.6 | 25.9±2.1 | 33.6±1.8 | 44.1±1.2 | 1288±36 |

[a] according to USDA

[b] difference in carbon content (heat-conductivity detector) before and after combustion of the soil samples at 425°C (Kah et al. 2014)

[c] determined at a soil:solution mass-ratio of 10:25 in 0.01 M $CaCl_2$

[d] amount of water a soil sample can hold against gravity when left to drain for 2h on a saturated sand bath (ISO 11268-2 2012)

The water contents of both soils were determined by weight loss upon drying at 105°C in triplicates using muffled porcelain cups. Oven-dry weights were stable over four subsequent days and soil dry weights ($m_{sd}$) were calculated as means over all 4 days. The dry-weight factors and water contents were determined according to Equations 1 and 2. Results are shown in Table 2.

**1)**

$$dry\ weight\ factor = \frac{m_{sd}}{m_{sad}}$$

$m_{sd}$ .....mass of oven-dry soil
$m_{sad}$ ....mass of air-dry soil

**2)**

$$water\ content\ [\%] = \frac{m_{sad} - m_{sd}}{m_{sd}} \times 100$$

$m_{sd}$ .....mass of oven-dry soil
$m_{sad}$ ....mass of air-dry soil

**Table 2. Dry-weight factors and water contents of the experimental soils (±SD)**

| soil | dry-weight factor | water content [%] |
|---|---|---|
| sand | 0.9960±0.0013 | 0.40±0.13 |
| loam | 0.9731±0.0002 | 2.77±0.02 |

## 2.2. Chemicals

Acetonitrile (AcN) analytical-grade (HiPerSolv Chromanorm®) was purchased from VWR. PowerPhos (PP) liquid fertilizer (NPK 10-34-0) was bought from Hechenbichler. It has a density of 1.38 kg/L, a pH of 6.4 and contains 138 g/L $NH_4$, 469 g/L $P_2O_5$ and traces of Fe (0.1 %). Analytical-grade Pestanal® standard of clothianidin ((E)-1-(2-chloro-5-thiazolylmethyl)-3-methyl-2-nitroguanidine) was bought from Sigma Aldrich and the three NFs (NFA, NFB, NFC) as well as the commercial formulation of Clo (insecticide "Belay") were provided by a North American company.

### 2.2.1. Clothianidin Active Ingredient

Clothianidin is a neonicotinoid systemic insecticide acting against Hemiptera (true bugs), Thysanoptera (thrips), Coleoptera (beetles), Lepidoptera (butterflies, moths), and Diptera (flies). It has been co-developed by today's Sumomito Chemical Co. and Bayer CropScience, was first registered in 2001 and is now available in more than 40 countries. The major product names are Dantotsu, Belay, Clutch and Poncho (Uneme 2011). The chemical structure of Clo ($C_6H_8ClN_5O_2S$) is shown in Figure 3. Characteristic are a thiazole ring and an open-chain guanidine skeleton (Uneme 2011).

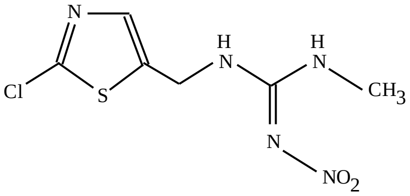

**Figure 3. Chemical structure of clothianidin (EC-SANCO 2005)**

Table 3 shows some pH dependent properties of Clo. It is rather soluble in water and solubility increases with pH. The octanol-water partitioning coefficient ($K_{ow}$) also varies with pH, being lower at pH 4 and 10 than at pH 7. Hydrolysis does not play a role at pH 4-9 at 20°C but occurs at alkaline pH and elevated temperatures. The dissociation constant $pK_a$ is 11.09 (EC-SANCO 2005; University of Hertfordshire 2016).

**Table 3. pH dependence of Clo water solubility, octanol-water partitioning coefficient ($K_{ow}$) & hydrolysis**

| pH | Clo water solubility [mg/L] at 20°C | log $K_{ow}$ at 25°C | hydrolysis half-life at 50°C |
|---|---|---|---|
| 4 | 304 | 0.893 | stable |
| 7 | 327 | 0.905 | stable |
| 9 | | | 14.4 d |
| 10 | 340 | 0.873 | |

(data from EC-SANCO 2005)

### 2.2.2. Clothianidin Pesticide Formulations

The composition of the provided formulations is given in Table 4 and the ingredients are briefly described below.

**Table 4. Composition of the Clo formulations**

| ingredient | NFA | NFB | NFC | Com |
|---|---|---|---|---|
| water | + | + | + | - |
| acrylates polymer | + | + | + | - |
| sodium methyl oleoyl taurate | - | + | - | - |
| sodium alkylnaphthalenesulfonate, formaldehyde condensate | + | - | + | - |
| propylene glycol | - | - | - | + |

Sodium methyl oleoyl taurate is a long-chain anionic surfactant with good wetting properties. It is stable across a wide pH range and resistant to hard water (Innospec 2015; Visek 1990). Chemically, it is the Na-salt of the oleic acid amide of N-methyl taurine. It can be used as surfactant, antistatic, cleansing agent, foaming agent and detangler (EWG 2016).

Sodium naphthalenesulfonate formaldehyde condensate is the Na-salt of naphthalene sulfonate, polymerized with formaldehyde (Chemtrade International 2007). It is an anionic dispersant with a high stabilizing effect (Bergstrom & Strandberg 2014), often used as water-reducing admixture or superplasticizer (improves dispersion of particle mixtures at low water contents) (Zhejiang NetSun Co. Ltd. n.d.). As a polymeric surfactant it is used e.g. as base for spreaders in agrochemicals or as dispersant for synthetic rubbers/resins during emulsion polymerization (Kao Corp. 2016).

Propylene glycol is a synthetic organic substance that absorbs water. It is used in the chemical pharmaceutical and food industries, to absorb extra water or maintain moisture, as a solvent or as antifreeze agent (ATSDR 1997). In pesticide formulations is used as carrier or antifreeze agent (L.V. Lomas 2014). Propylene glycol is water miscible and can be used as co-solvent (Rutesh 2008).

The Clo contents given on the labels of the formulations were 19.19, 20.50, 19.11 and 23.60 %wt for NFA, NFB, NFC and Com, respectively. These were checked by triplicate extractions of à ~200 mg formulation in 10 mL AcN, which were then diluted 1:500 (V:V) with $H_2O$ and measured by HPLC. According to the formulation provider, AcN completely separates the AI from the NC. Recoveries ranged from 93.5 % to 101.7 % (Table 5). For all working solution preparations, the measured Clo contents were used.

**Table 5. Clo content in formulations and Clo recovery (±SD)**

| formulation | expected cClo [%wt] | measured cClo [%wt] | Clo recovery [%] |
|---|---|---|---|
| NFA | 19.19 | 18.76±0.16 | 97.74±0.82 |
| NFB | 20.50 | 20.76±0.19 | 101.28±0.94 |
| NFC | 19.11 | 19.43±0.21 | 101.69±1.09 |
| Com | 23.60 | 22.07±0.10 | 93.52±0.44 |

# 3. Methods

This chapter provides detailed information on the analytical (3.1) and experimental methods including data evaluation (3.2 Characterization of Nanoformulations, 3.3 Photodegradation and 3.4 Sorption to Soils). Furthermore, the Clo and fertilizer application scenarios are developed (3.5) and the statistics used are introduced (3.6).

To ex-ante preclude any unwanted error sources, several preliminary tests were conducted (see Annex A), which confirmed that Clo is not susceptible to hydrolysis or losses to materials used in the lab. Also photodegradation under work-bench light conditions could be excluded. Based on this knowledge the following methods were developed.

## 3.1. Analytical Method

To ensure quantification of Clo throughout all the experimental setups, the following high-performance liquid chromatography (HPLC) method was developed and validated (for validation results see Annex B).

The HPLC (Agilent 1100 series) equipped with a ZORBAX Eclipse XDB-C18 column (4.6×150 mm, 5 µm pore size, Agilent) was coupled with UV-Vis detection. Column temperature was regulated to 30°C and flow rate was 1 mL/min. The mobile phase consisted of a gradual mixture of $H_2O$ and AcN from 0-100 % AcN in 7 min (Table 6).

**Table 6. HPLC method mobile phase gradient**

| cumulative time [min] | AcN [%] | $H_2O$ [%] |
|---|---|---|
| 0 | 0 | 100 |
| 7 | 100 | 0 |
| 9 | 100 | 0 |
| 11 | 0 | 100 |
| 13 | 0 | 100 |

Retention time was around 5.5 min, and Clo was quantified at a wavelength of 269 nm (FAO 2015) with calibration curves consisting of 9 standards, ranging from 0.1 to 15 mg/L, prepared in AcN ($R^2 > 0.999$). The limits of detection and quantification were determined to be 0.02 and 0.08 mg/L, respectively (see Annex B).

## 3.2. Characterization of Nanoformulations

### Particle Size, Size Distribution, Zeta Potential, Mode of Stabilization

Important NF characteristics are particle size, size distribution (polydispersity index) and zeta potential (Kah & Hofmann 2014). The zeta potential is the electric potential at the shear plane (which includes the particle and the adsorbed counterions) and the polydispersity index is a measure for heterogeneity of particle sizes (Bhattacharjee 2016).

Since NFs are colloidal systems, they need to be stabilized to avoid aggregation. The major modes of stabilization (Figure 4) include polymeric (steric), electrostatic, and electrosteric stabilization (Liu et al. 2014).

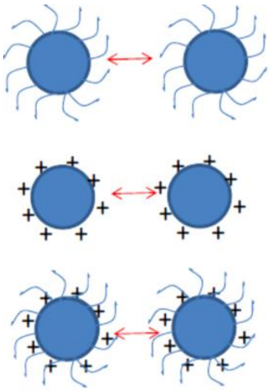

**Figure 4. Modes of colloidal stabilization (steric, electrostatic, electrosteric) (modified after Liu et al. 2014)**

The mode of stabilization can be concluded from the aggregation behavior of the particles in high ionic strength and values of zeta potential based on the DLVO theory: Electrostatically stabilized colloids aggregate at increased ionic strength (Meunier & Elaissari 2003) and surface charge is higher for electrostatic and electrosteric than for steric stabilization.

Size distribution and hydrodynamic diameter of the present NFs were determined by dynamic light scattering (DLS)[1] and zeta potential by electrophoretic light scattering (ELS)[2] with a Zetasizer Nano (Malvern), at a fixed scattering angle of 173°. Measurements were conducted with all NFs in 1:400 dilutions (V:V) with $H_2O$ and 75 mM $CaNO_3$ (high ionic strength), respectively. Size was determined in three subsamples, whereas zeta potential was measured in one sample only.

### Release of the Active Ingredient from the Nanocarrier

Another important characteristic of NFs is their AI-release behavior (Kah & Hofmann 2014). Release was tested with syringe filters (nylon, 25 mm diameter, Yeti Syringe Filters, Merz Brothers GmbH) at cClo above and below solubility, to test for concentration influences, as well as in fertilizer background.

First, NF-solutions at concentrations of 34 mg NF per L (cClo 6.0-7.5 mg/L) were prepared in $H_2O$ and filtered as fast as possible upon dilution (within max. 5 min) through 0.2 µm pore size filters – sufficient to separate NC-associated and dissolved Clo according to the determined particle sizes (see Table 11). The first 10 mL were discarded to flush the filters. From mL 11 on, every second mL was

---

[1] For DLS, a laser beam passes through the sample solution containing particles which scatter the light. The scattered light is detected in short time intervals by a fast photon detector at a known scattering angle. Intensity fluctuations of the scattered light contain information about particle motion (Doppler shift) and allow calculation of the diffusion coefficient. Finally, the diffusion coefficient can be used to calculate the particles' hydrodynamic diameter via the Stokes-Einstein equation (LS Instruments 2016).

[2] The principle for ELS is similar to DLS, just that an electrical field is applied and thus directed electrophoretic movement is superimposed to diffusion (random Brownian motion). The particle motion within the electric field depends on the zeta potential (McNeil-Watson 2013).

collected and cClo was measured directly by HPLC. AI solutions at a similar concentration served as reference for losses to the filters. Triplicates of each NF-solution were extracted 1:1 (V:V) with AcN to assure release from the NC and served as unfiltered controls.

In a second step, the filtration test was repeated at cClo > solubility. The first attempt was done with NFB at a formulation concentration of > 8600 mg NF/L. Since this solution could be hardly pushed through the 0.2 µm filters, 0.45 µm was used. Tests for NFA and NFC were then conducted at reduced concentrations of 3400 mg NF/L (cClo 638-661 mg/L). After flushing, again every second mL of filtrate was collected (10 in total). Filtrates and controls needed dilution for HPLC measurement (NFB 1:250, NFA & NFC 1:100).

Furthermore, the possible influence of high ionic strength (due to PP liquid fertilizer addition) on release behavior was tested with NFC at PP and Clo concentrations similar to the maximum-reached experimental soil-solution concentrations (which occur in sand in the centM, see Table 7). $NH_4$ and $P_2O_5$ concentrations were ~1986 and 6753 mg/L, respectively and cClo at around 80-100 mg/L (depending on preparation mode). Two different ways to prepare NFC-solutions were compared: In the first case NFC was added to the PP-background as aqueous spiking solution (cClo 117 mg/L), in the second case an appropriate amount of pure NFC was weighed in directly and diluted with PP-background solution. Aliquots (30 mL) of both solutions were pushed through 0.45 µm syringe filters immediately after preparation, mL Nr. 23, 26 and 29 were collected, diluted (1.5:10, V:V) and measured by HPLC. The cClo of the unfiltered solutions were determined in duplicate AcN extractions. The procedure was repeated with AI-solution at a similar cClo (73 mg/L), which proved that no losses of Clo to the filter occurred.

## 3.3. Photodegradation

The following experimental setup was optimized based on a preliminary study (see Annex C). Photodegradation experiments were carried out with Atlas Suntest CPS+ (Figure 5a), equipped with a xenon lamp and an optical daylight filter (coated quartz filter), cutting off UV light at 290 nm (in compliance with OECD 2008). The irradiance[3] was regulated to 65 W/m² in the wavelength range of 300-400 nm and the black standard temperature[4] was set to 99°C. 65 W/m² corresponds to natural summer irradiance at 300-400 nm in Basel (CH) at 50°N latitude (OECD 2002).

The study duration was 6 h to make sure it covers more than two degradation half-lives[5] (OECD 2008). Sampling intervals were after 10, 40, 90, 160, 250 and 360 min. For each interval, triplicates of transparent screw-cap HPLC vials (Markus Bruckner Analysetechnik) were filled up to the top (à 1.8 mL) with the different formulation/AI solutions and put horizontally, in random order on the sample tray of the aging chamber. Since the chamber temperature[6] could not be controlled, temperature

---

[3] incident radiation energy on a surface

[4] maximum surface temperature allowed for a black body (that would fully absorb the incident radiation)

[5] time to degrade 50% of a substance

[6] air temperature in the test chamber

controls were introduced (test solutions in aluminum-foil wrapped amber HPLC vials) (Figure 5b). Sample and control vials were taken out of the aging chamber at each interval and stored in the dark fridge. Triplicates to determine real initial cClo were stored in the fridge right from the start. At the end of the degradation period samples were AcN-extracted, diluted (if necessary) and cClo was measured by HPLC in all samples and dark controls.

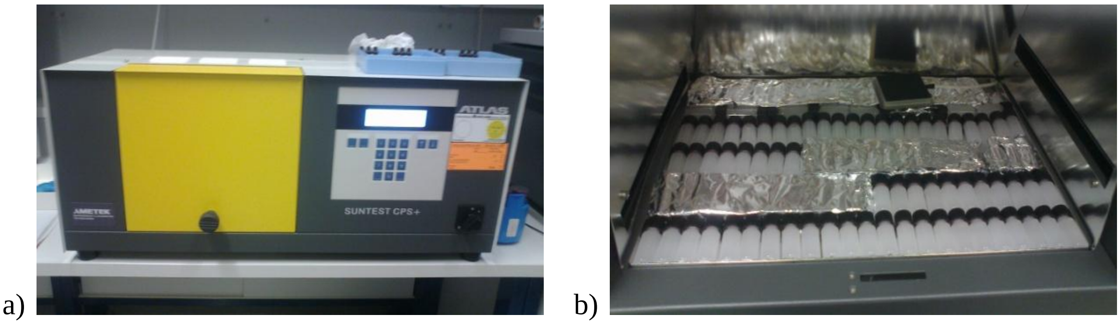

**Figure 5. (a) Atlas Suntest CPS+, (b) samples/controls within the aging chamber**

This test was first carried out with unbuffered aqueous formulation- and AI-solutions (a pre-test with a phosphate buffer showed, that the buffer influenced the degradation rates, see Annex C). Since pH was not controlled, initial test-solution pH values were measured to account for a possible pH influence. The solutions were prepared at various concentrations above and below Clo solubility limit (nominal cClo: 544, 408, 136, 102 and 13.6 mg/L), to check for concentration effects. The higher four concentrations needed dilution for HPLC measurement: 1:50, 1:10, 13:100 and 3:100, respectively. For NFC and Com, photodegradation rates (k) were additionally determined at cClo 204 and 306 mg/L, to establish the relation of k and cClo.

In a second step, photodegradation of a combination of PP liquid fertilizer and Clo at maximum realistic use concentrations was studied. Those concentrations were 136, 18400, 62560 and 184 mg/L, for Clo, $NH_4$, $P_2O_5$ and Fe, respectively based on a foliar spray application scenario (see 3.5.1). To avoid any Clo salting out in the pipette tips, testing solutions were prepared directly in each HPLC vial: à 1.65 mL of formulation/AI working solution (cClo 157 mg/L) were pipetted into each vial before injection of à 0.24 mL pure PP fertilizer using a glass syringe. This gave a final amount of 1.8 mL solution in each vial with the planned experimental Clo and PP concentrations. Samples were diluted 1:10 in $H_2O$ before HPLC measurement.

The measured remaining cClo in solutions were plotted over time and fit by a least sum-of-squares first-order exponential decay fit “one phase decay” (GraphPad Software Inc. 2016). The model and its parameters are explained in Equation 3 and Figure 6.

**3)**

$$y = (y_0 - plateau) * e^{(-k*x)} + plateau$$

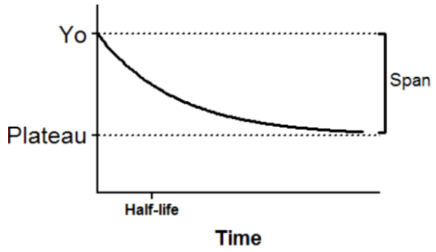

$y_0$............. y at x = 0
plateau...... y at x = ∞
k .............. rate constant [$time^{-1}$]
half-life .... decay time of 50 % substance = ln(2)/k.
span.......... difference of $y_0$ and Plateau

**Figure 6. Model of first order exponential decay (GraphPad Software Inc 2014)**

The fit was used fixing initial concentrations ($y_0$) to the measured initial cClo values and the plateau to 0 mg/L, precluding degradation below zero. The k values and calculated errors from the fits were then compared using unpaired t tests (see 3.6 Statistics).

To evaluate degradation in the dark-control samples, least sum-of-squares linear regression (GraphPad Software Inc. 2016) was applied. Occurrence of dark-degradation was only concluded, when the slope was significantly non-zero[7] ($p < 0.05$) and also peaks of degradation products occurred in the chromatograms.

## 3.4. Sorption to Soil

Sorption experiments were carried out with two methods. A classical batch-equilibrium method with a low soil:solution ratio, based on the OECD guideline Nr. 106 (OECD 2000) and a centrifugation method (Walker & Jurado-Exposito 1998; Walker 2000a; Kah & Brown 2007) with a realistic soil:solution ratio. For both methods two different background solutions were used: deionized water and PP-solution. The OECD guideline specifies a 0.01 M $CaCl_2$ background solution, but preparation of the PP-solution in $CaCl_2$-background led to $CaPO_4$ precipitation. To avoid precipitation and let fertilizer be the only difference between the experimental solutions, $CaCl_2$ was left away in both backgrounds.

The experimental concentrations of Clo and PP were chosen based on maximum realistic application rates in soil. Maximum concentrations are achieved by an application in-furrow while seeding (see 3.5.2) and amount to 13, 320, 1088 and 3.2 mg/kg dry soil for Clo, $NH_4$, $P_2O_5$ and Fe, respectively.

The soil concentrations were translated into equivalent soil-solution concentrations for the batchM and centM using the respective experimental soil:solution ratios (Table 7).

The concentrations in the respective working/spiking solutions for both methods are also shown in Table 7 and were adjusted in a way that the final intended soil-solution concentrations are reached during the experimental procedure.

---

[7] GraphPad Prism determines significance of the slope by an extra sum-of-squares F test which compares the relative increase in sum-of-squares and the relative increase in degrees of freedom of hypothesis (the slope corresponds to the fitted value) and null hypothesis (the slope is zero). The slope is significant if the relative increase in sum-of-squares is larger than the relative increase in degrees of freedom (GraphPad Software Inc. 2014a)

**Table 7. Experimental fertilizer/Clo concentrations in soil solution and respective working solutions**

| substance | | $c_{soil}$ [mg/kg] | $c_{soil\text{-}solution}$ [mg/L] | | | $c_{working\text{-}solutions}$ [mg/L] | |
|---|---|---|---|---|---|---|---|
| | | | batchM | centM | | batchM | centM |
| | | | | sand | loam | | |
| PP | $NH_4$ | 320 | 160 | 1714.9 | 1209.4 | 168.42 | 3840 |
| | $P_2O_5$ | 1088 | 544 | 5830.7 | 4111.9 | 572.63 | 13056 |
| | Fe | 3.2 | 1.6 | 17.15 | 12.09 | 1.68 | 38.4 |
| Clo-AI | | 13 | 6.5 | 69.67 | 49.13 | 130 | 130 |
| Clo-formulation | | 13 | 6.5 | 69.67 | 49.13 | 1300 | 1300 |

All working solutions were prepared in volumetric flasks by weighing in the respective amounts of PP fertilizer or formulation and filling up with deionized water.

Clo concentrations in formulation working solutions were chosen to be 4 × above Clo solubility in water, in order to minimize release of Clo from the NC before actual soil contact (see 4.1 release behavior). The pure AI working solution can of course not be prepared above Clo solubility limit, thus cClo in the AI working solution was 130 mg/L. Since the concentration of PP working solution differs between the methods they are termed $PP_{batch}$ and $PP_{cent}$ accordingly.

### 3.4.1. Batch Method

For the batch experiments, PTFE tubes (50 mL, Semadeni) were filled with à 10 g (+ max. 1%) of air-dry soil and 19 mL of either $PP_{batch}$ or $H_2O$ and pre-equilibrated in the dark on the side-to-side shaker (125 rpm) for > 16 h (overnight). The next day, suspensions were spiked with

- 1 mL of AI-solution (130 mg/L in $H_2O$) or
- 0.1 mL of formulation-solution (cClo 1300 mg/L in $H_2O$) + 0.9 mL $H_2O$,

each in triplicates, giving a final soil:solution ratio of 1:2 and the intended cClo (6.5 mg/L) and salt concentrations (160 mg/L $NH_4$ and 544 mg/L) (see Table 7). The soil:solution ratio was chosen to be 1:2 according to OECD (2000) (see Annex D). Triplicate blanks for each soil (pre-equilibrated soils spiked with 1 mL $H_2O$) confirmed the absence of background and triplicate controls for each formulation and the AI (19 mL $PP_{batch}$ spiked with 1 mL AI-solution or 0.1 mL NF-solution + 0.9 mL $H_2O$) served as initial solution concentration for $K_d$ calculations.

The samples were equilibrated through side-to-side shaking at 125 rpm in the dark for 24 h and then centrifuged for 30 min at 4000 g. Equilibration time and centrifuge settings were chosen based on a preliminary study (see Annex D). In accordance with OECD (2000) pH in solution was measured before (in controls) and after sorption (in supernatants). Clo concentrations in solutions were measured directly by HPLC.

The produced data were used to calculate $K_d$ values and percentages absorbed (A) according to (OECD 2000). The different experimental settings were compared based on the derived $K_d$ values (±SD).

The distribution coefficient ($K_d$) relates the soil concentration ($c_{soil}$) of a chemical to its solution concentration ($c_{solution}$) at chemical equilibrium conditions (Equation 4).

**4)**

$$K_d\ [\mathrm{L/kg}] = \frac{c_{soil}\ [\mathrm{mg/kg}]}{c_{solution}\ [\mathrm{mg/L}]}$$

The solution concentration was measured directly, whereas $c_{soil}$ was derived by subtracting the Clo mass in soil solution ($mClo_{ss}$) from the initial Clo mass ($mClo_{ini}$), which was determined from controls (without soil) (Equation 5).

**5)**

$$c_{soil}\ [mg/kg]\ = \frac{m_{Clo_{ini}} - m_{Clo_{ss}}}{m_{sd}}$$

$mClo_{ini}$... mass of Clo initially added [mg]
$mClo_{ss}$.... mass of Clo in soil solution at equilibrium [mg]
$m_{sd}$......... mass of oven-dry soil [kg]

The percentage adsorbed is the fraction of $mClo_{ini}$ which was adsorbed to soil at equilibrium (Equation 6).

**6)**

$$A\ [\%] = \frac{m_{Clo_{soil}}}{m_{Clo_{ini}}} \times 100$$

$mClo_{soil}$ .... mass of Clo adsorbed to soil at equilibrium [mg]
$mClo_{ini}$ ..... mass of Clo initially added [mg]

For all presented calculation results (section 4.3), error values (standard deviations) were propagated according to Harvard University (2007).

### 3.4.2. Centrifugation Method

For the centM, the chosen soil moisture was 60% of the MWHC based on a preliminary test (see Annex E). The moisture content was adjusted by weighing. Thus, in the case of PP-background, the mass of introduced fertilizer salts was accounted for, to let the 60% MWHC be solely solution without salts (see Annex E). The MWHC of 60 % gave a soil:solution ratio of ~3.78:1 for sand and ~5.36:1 for loam.

For incubation (Figure 7a), 120 g (dry weight) of each soil were weighed into 250 mL glass bottles with screw caps (Schott Duran). Soils were brought close to 60% of the MWHC with either 10 mL $PP_{cent}$ + $H_2O$ or just $H_2O$. After careful mixing, samples were pre-equilibrated for three days in the dark fridge at 4°C. Then the soils were spiked with 1.2 mL formulation-solution (cClo 1300 mg/L) or 12 mL AI-solution (cClo 130 mg/L) and adjusted to the final 60% MWHC by $H_2O$ addition. Blanks for each soil were adjusted to 60% MWHC with just $H_2O$. Samples were carefully mixed with a spatula and incubated in the dark fridge (4°C). Weighing and readjusting weight by $H_2O$ addition allowed for compensation of possible moisture losses during the incubation periods.

After 24 h and after 7 days of incubation, triplicate subsamples of à 10 g (+ max. 1 %) were weighed into the inserts of PVDF centrifuge tubes (VectaSpin 20, 50 mL, Whatman International Ltd.). The original filter was replaced by a polycarbonate membrane pore size 0.4 µm (Whatman) to retain NCs, plus a glass microfiber filter pore size 1.6 µm (Whatman GF/A, Ø 25 mm) to retain soil particles and avoid scaling of the membrane. Filter and membrane were pre-wetted with 0.1 mL of $H_2O$. The tubes were then centrifuged for 30 min at 1500 g to receive an amount of soil solution between 0.18±0.01 and 1.01±0.04 mL, for loam and sand respectively (Figure 7b). Centrifugation subjected the soil to a pressure of 200 kPa, which is the border between "mobile" and "immobile" water[8] (Addiscott 1977, cited in Kah et al. 2014). Recovered soil solutions of sand needed to be diluted 1:3 with $H_2O$ for HPLC measurement, whereas soil solutions of loam could be measured directly.

Further triplicate subsamples were taken at the same time intervals (24 h and 7 days) to determine the total cClo, which served as initial concentrations for $K_d$ calculations. À 10 g (+ max. 1 %) of incubated soil were weighed into PTFE tubes and extracted with 20 mL AcN in the dark on the side-to-side shaker (1 h, 125 rpm). The tubes were then put upright and left for 1 h to let the soil settle down (Figure 7c). Finally, 1 mL of each extract was transferred to an HPLC vial to measure cClo. The mean extraction recovery of all soil-solution combinations (based on nominal concentrations) was 103 %, with a range of 93-113 % (for derivation see Annex E).

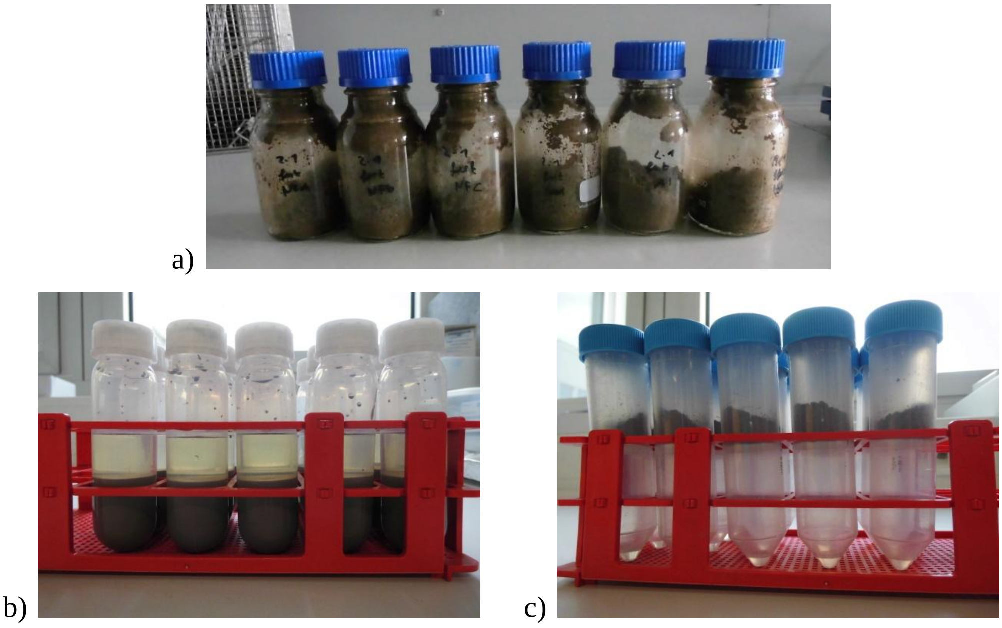

**Figure 7. (a) incubation of spiked soils at 60% MWHC, (b) AcN-extraction for total cClo, (c) centrifugation to gather soil solution**

To compare the various experimental settings, produced data were used to calculate $K_d$ values (Equation 4) and percentages adsorbed (A). In the case of PP-background, corrections for the introduced salt mass were made (see Annex E).

AcN extracts served for calculation of the initial cClo in soil ($cClo_{ini}$, Equation 7), which was used to derive $c_{soil}$ for $K_d$ calculations.

$$c_{Clo_{ini}}[\text{mg/kg}] = \frac{c_{Clo_{measured}}(m_{ss\_extr} + V_{AcN})}{m_{sd\_extr}} \tag{7}$$

$cClo_{measured}$ ... conc. of Clo in AcN extracts [mg/L]
$m_{ss\_extr}$ .......... mass of soil solution in extracted soil [kg]
$V_{AcN}$ ............ volume of AcN for extraction [L]
$m_{sd\_extr}$ .......... mass of oven-dry soil extracted [kg]

---

[8] water that is not participating in gravitational flow

Multiplication of $cClo_{ini}$ with the calculated oven-dry weight of the centrifuged soil subsamples ($m_{sd\_cent}$) gave the initial mass of Clo present ($mClo_{ini}$). Subtracting the Clo mass in soil solution ($c_{solution} \times m_{ss}$) and dividing by $m_{sd}$ gave the equilibrium cClo in soil ($c_{soil}$) needed for $K_d$ calculation (Equation 8)

**8)**

$$c_{soil}\ [mg/kg] = \frac{m_{Clo_{ini}} - c_{solution} \times m_{ss\_cent}}{m_{sd\_cent}}$$

$c_{soil}$ ..........conc. of Clo in soil at equilibrium [mg/kg]
$mClo_{ini}$ ....mass of Clo initially present [mg]
$c_{solution}$......conc. of Clo in solution at equilibrium [mg/L]
$m_{ss\_cent}$.....mass of soil solution in centrifuged soil [kg]

The concentration measured in the centrifugate ($c_{cent}$) needed to be corrected for the $H_2O$ amount (0.1 mL) added by pre-wetting the filters ($m_{H2O}$) to arrive at $c_{solution}$ (Equation 9). For that it was assumed, that $m_{H2O}$ diluted the total mass of soil solution in the soil subsamples weighed in for centrifugation ($m_{ss\_cent}$)[9].

**9)**

$$c_{solution} = \frac{c_{cent} \times (m_{ss\_cent} + m_{H2O})}{m_{ss\_cent}}$$

$c_{solution}$.... concentration of Clo in solution at equilibrium [mg/L]
$c_{cent}$........ concentration in centrifugate [mg/L]
$m_{ss\_cent}$ ... mass of soil solution in centrifuged soil [kg]
$m_{H2O}$...... mass of $H_2O$ for filter pre-wetting [kg]

$K_d$ was finally calculated according to Equation 4. For all presented calculation results (in section 4.3), error values (standard deviations) were propagated according to Harvard University (2007).

## 3.5. Clothianidin and Fertilizer Application Scenarios

Since NFs might be decomposed upon dilution (Kah et al. 2013) and the AI release can depend on solubility, maintenance of nanoproperties might be enhanced at high concentrations of Clo in combination with high ionic strength (salting-out effect).

### 3.5.1. Photodegradation: Foliar Spray Application Scenario

A scenario where high fertilizer/Clo concentrations are exposed to sunlight is application as foliar spray. Maximum PP fertilizer applications as foliar spray are 40 L/ha (applied before full coverage on corn and sugar beet) in a water amount of min. 300 L/ha (Hechenbichler GmbH 2012) which would result in the salt concentrations shown in Table 8.

Clo application of the insecticide Belay (AI content: 2.13 lbs/gal = 255.23 g/L) as foliar spray amounts to a maximum of 6 fl.oz./A for most crops in a water amount of min. 100 gal/A (Valent USA Corp. 2014), giving a spray concentration of 120 mg/L. For pome fruits and grapes maximum spray concentrations would be even higher: 480 mg/L and 200 mg/L, respectively (Valent USA Corp. 2014;

---

[9] This assumption is probably not correct, however it would be neither correct to assume $m_{H2O}$ just diluted the gathered centrifugate which passed through the pre-wetted filter, since in a pre-test at MWHC 50 % (see Annex E) the centrifugate amount gained from loam (0.073 mL) was less than the $m_{H2O}$ (0.1 mL) introduced by pre-wetting. Thus, it seems that $m_{H2O}$ is not fully relocated to the centrifugate, but part of it remains in the filter or is taken up by the soil in the insert.

APVMA 2009). However, those are rather special cultivars and thus cClo was chosen to be around the crop application (Table 8).

**Table 8. Summary: experimental concentrations of $NH_4$, $P_2O_5$ and Clo for foliar spray application case**

| substance | $c_{spray}$ [mg/L] |
|---|---|
| $NH_4$ | 18400 |
| $P_2O_5$ | 62560 |
| Fe | 184 |
| Clo | 136 |

### 3.5.2. Sorption to Soils: In-Furrow Application Scenario

The highest local fertilizer and Clo concentrations in soil occur during application in-furrow while sowing (Figure 8): A furrow in some cm depth is opened by a wheel (18). The seed drops out of the seed tube (24) into the furrow, is positioned by the rebounder (26) and covered with a liquid pesticide-fertilizer mixture out of the delivery tube (40) before the furrow is closed again (22).

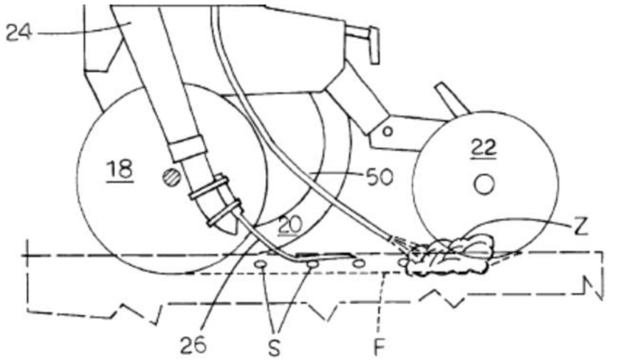

18....furrow opening device
20....gauge wheel assembly
22....furrow closing device
24....seed tube
26....rebounder™
50....liquid pesticide delivery tube
F......furrow
S......seed
Z......zone of turbulence

**Figure 8. Planting device with in-furrow pesticide/fertilizer application (modified after Fish et al. 2001)**

Experimental concentrations of Clo and PP fertilizer were based on maximum realistic usage. When PP fertilizer is incorporated as basic soil fertilization, the label recommends using 40 L/ha e.g. in corn, potatoes, sunflowers, oil-pumpkins and sugar beets (Hechenbichler GmbH 2012). As Clo is often used for seed treatment of corn, the scenario was developed for corn. Applying 40 L/ha in-furrow would lead to very high local salt concentrations, possibly causing salt injury of the seeds. However, the recommended safe amount for 10-34-0 fertilizer in-furrow application on corn would be 5 gallons per acre (≈ 47 L/ha) in 30-inch (≈ 76 cm) rows (Hergert et al. 2012). Thus the scenario is still realistic.

With an average number of 10 plants per m² and 75 cm row distance, planting distance within rows needs to be ~13 cm (LWK Nordrhein-Westfalen 2015). Each plant accounts for 13 cm of furrow, so the total furrow length is 10 plants × 13 cm = 130 cm/m². It was assumed that 3 × 3 cm of soil is influenced along the furrow length. The volume of influenced soil would then be 11.7 m³/ha.

PP fertilizer should be mixed with a minimum of 300 L water per ha (Hechenbichler GmbH 2012), giving a total of 340 L/ha. Since PP fertilizer contains 138 g/L N, the assumptions results in a N concentration ($c_N$) of 315 mg/kg in dry soil, assuming a soil bulk density of 1.5 kg/dm³ (as calculated in Table 9).

**Table 9. Calculation of N concentration ($c_N$) in soil dry weight in case of in-furrow fertilizer application**

| N applied [g/ha] | $c_N$ in soil volume [g/m³] | $c_N$ in dry soil [mg/kg] |
|---|---|---|
| 40 L/ha × 138 g/L = 5520 | 5520 g/ha : 11.7 m³/ha ≈ 472 | 472 mg/dm³ : 1.5 kg/dm³ ≈ 315 |

315 mg/kg were rounded up to 320 mg/kg N and concentration of $P_2O_4$ in dry soil was derived from the NPK ratio (10-34-0) to be 1088 mg/kg.

Similar considerations were made for Clo concentration: The in-furrow application of the commercial insecticide Belay (e.g. against corn wireworm) amounts up to 12 fl.oz./A (= 0.8769 L/ha). The insecticide contains 2.13 lbs Clo per gallon (= 255.23 g/L) (Valent USA Corp. 2014), so the maximum application amounts to 223.81 g/ha. With the above calculated 11.7 m³/ha of influenced soil, the soil concentration gives 19.13 g/m³ which translates into ~13 mg/kg using a soil density of 1.5 g/cm³. Table 10 shows a summary of the experimental Clo and fertilizer concentrations in soil.

**Table 10. Summary: experimental concentrations ($c_{soil}$) of $NH_4$, $P_2O_5$ and Clo for in-furrow application case**

| substance | $c_{soil}$ [mg/kg] |
|---|---|
| $NH_4$ | 320 |
| $P_2O_5$ | 1088 |
| Fe | 3.2 |
| Clo | 13 |

## 3.6. Statistics

Statistics, curve fits and graphs were produced using GraphPad Prism 6 (GraphPad Software Inc. 2016). Conducted analysis included linear regression, t tests and "one phase decay" curve fits.

The significance level was always set to $\alpha$=0.05. In graphs, significant differences are indicated by *, non-significant ones by "n.s." and error bars always represent standard deviations of means (usually n=3). Groups of statistically equal values were denoted by letters (a, b, c, ab,..). Statistically non-different values share at least one letter, whereas significantly different values do not share any letter.

Whether values are significantly different was determined by unpaired t tests (independent samples), assuming a Gaussian distribution of the data and equal SD of the compared groups. An unpaired t test compares the differences between the means of the groups with the standard error of the differences, which combines the standard errors of the compared groups (GraphPad Software Inc. 2014b).

As GraphPad Prism is not able to perform three-way ANOVA, such analysis was calculated manually in Excel according to Zaiontz (2016). The percentages of variance explained by each factor/interaction were determined as eta squared ($\eta^2$) which is the sum-of-squares of the factor/interaction considered divided by the total sum-of-squares of all data, given in percent.

# 4. Results and Discussion

In this major part of the thesis the results yielded from the previously introduced experiments are presented and discussed based on a comprehensive literature research. The sections comprise Characterization of Nanoformulations (4.1), Photodegradation (4.2) and Sorption to Soils (4.3).

## 4.1. Characterization of Nanoformulations

**Particle Size, Size Distribution, Zeta Potential, Mode of Stabilization**

The results of size and zeta potential measurements in deionized water are shown in Table 11. The measured hydrodynamic particle diameters ranged from 560 nm to 801 nm, which excludes the present formulations from the definition of nanomaterials (up to 100 nm) by the European Commission (EC 2016a) and confirms that NFs often exceed this size range (Kah et al. 2013).

Particle size measurements by dynamic light scattering start to be less reliable at a polydispersity index > 0.3 and are not trustworthy anymore if the value exceeds 0.5 (NanoComposix 2015). The determined polydispersity indices were well below 0.3. As the measured diameters were rather large, particle sedimentation could impact on the reliability of the data (Shaw 2013). However, polymer-based particles have a rather low density and sedimentation in aqueous background should be negligible within the short measuring period, even for larger particles. Thus, the dynamic light scattering data can be considered reliable.

The polydispersity indices ranged from 0.12 to 0.22 and indicate moderate polydispersity for all NFs, according to the following classification: ≤ 0.1 high monodispersity, 0.1–0.4 moderate polydispersity and > 0.4 high polydispersity (Bhattacharjee 2016).

Zeta potentials were in the “highly stable” range (> ± 30 mV) for NFB and NFC and close to unstable for NFA, with values of 0-10, 10-20, 20-30 and > 30 mV classifying nanoparticle dispersions as highly unstable, relatively stable, moderately stable and highly stable, respectively (Bhattacharjee 2016).

**Table 11. NFs characterization: hydrodynamic diameter, polydispersity index and zeta potential in $H_2O$ (±SD)**

| | hydrodynamic diameter [nm] | polydispersity index | zeta potential [mV] |
|---|---|---|---|
| NFA | 801.3 ± 28.0 | 0.22 ± 0.04 | -12.7 |
| NFB | 744.3 ± 15.7 | 0.12 ± 0.03 | -59.0 |
| NFC | 559.6 ± 26.1 | 0.15 ± 0.04 | -57.9 |

The changes in hydrodynamic diameter and zeta potential due to increased ionic strength (75 mM $CaNO_3$) are depicted in (Figure 9). NFC displayed a much larger particle size (due to aggregation) in $CaNO_3$-background as compared to $H_2O$ and its zeta potential was lowered to −10 mV (highly unstable) in high ionic strength. This indicates an electrostatic stabilization: High ion concentration shields the surface charges that would repel each other and aggregation occurs. NFA did not aggregate at all, even though the zeta potential was very small in both background solutions. Ionic strength had no influence on colloidal stability, therefore a steric stabilization can be assumed. NFB shows a mixed behavior: while the zeta potential decreased dramatically in high ionic strength, aggregation was very low (but still significant) which indicates electrosteric stabilization.

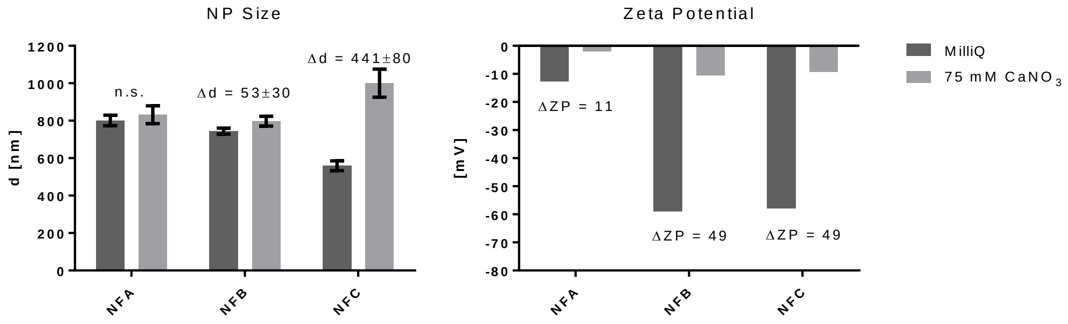

**Figure 9. NFs characterization: change in particle size and zeta potential in $H_2O$ and 75 mM $CaNO_3$**

## Release of the Active Ingredient from the Nanocarrier

During filtration at cClo < solubility, Clo concentrations in the filtrates stabilized from 20 mL onwards (Δ cClo < 0.04 mg/L), as shown in Figure 10. Thus, means of the last three collected milliliters were compared to the unfiltered controls. At cClo > solubility, concentrations were stable right from the start and averages of all 10 collected mL were used for comparison.

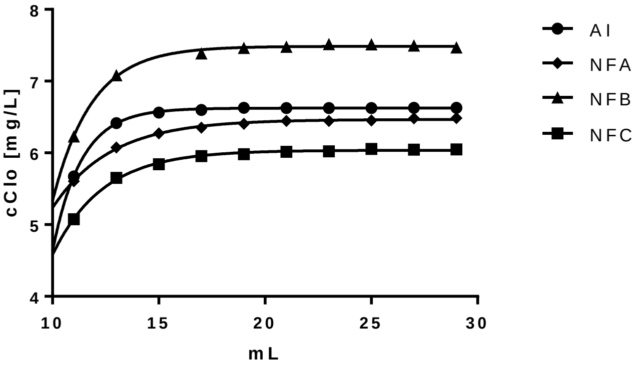

**Figure 10. NFs release of the AI: stabilization of filtrate concentration (0.2 µm filters) at cClo < solubility**

The results of the syringe filter based release tests at cClo below and above solubility are shown in Figure 11. At cClo below solubility, filtered and control samples were not significantly different, except for NFC, but the tiny difference of 0.03 mg/L can be considered non-relevant. These results suggested that the AI is released very quickly upon dilution and NC-association is solubility controlled. The repetition of the test at cClo > solubility resulted in filtrate Clo concentrations being lower than controls. Irrespectively of the initial concentrations (cClo was much higher in case of NFB), filtrates always displayed Clo concentrations close to its water solubility, which is 327 mg/L (US-EPA 2005). This proves the dependency of the AI release on solubility limits.

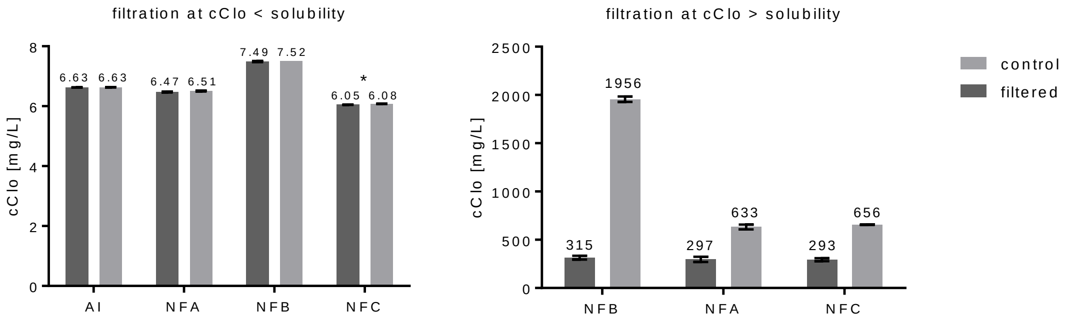

Figure 11. NF release behavior tested by syringe filters at cClo below and above solubility

Filtration in PP-background at maximum experimental concentrations (still below solubility) (Figure 12) indicates that, once diluted, the AI does not reattach to the NCs when salt concentration is increased ($NFC_{H2O}$), but a small fraction of the AI stays associated to the NCs (at least for a short period) and can be filtered off, when NFC is directly added to high-salt background ($NFC_{direct}$). Thus, PP has the potential to decrease AI release and NF spiking solutions should be prepared at high cClo (>> solubility) to avoid premature release.

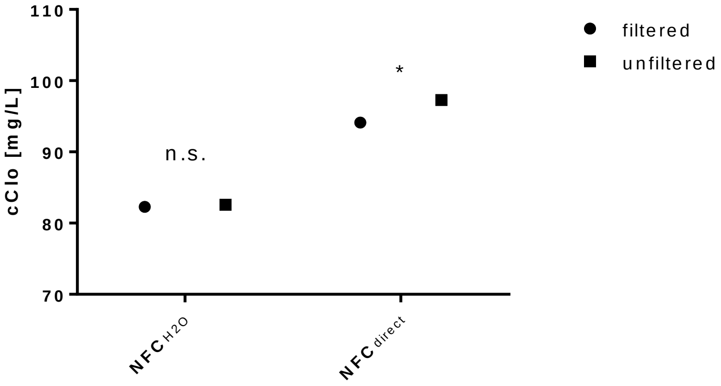

Figure 12. NF release behavior tested by syringe filters at max. experimental cClo and fertilizer concentration

Overall, the NF characterization allows to conclude, that the formulations were designed to enhance the solubility of the AI and/or tank-mix compatibility e.g. with liquid fertilizers (Kah et al. 2013).

## 4.2. Photodegradation

The following comprises the results and discussion of the photodegradation experiments. After some general paragraphs (dealing with photodegradation kinetics, half-lives and pH/concentration effects), the two experimental settings are discussed in detail: 4.2.1 Formulation Influence on Photodegradation in $H_2O$-Background and 4.2.2 Photodegradation in the Foliar Spray Application Scenario.

**Photodegradation Kinetics and Degradation in the Dark**

Figure 13 shows a representative example of the photodegradation curves produced. The radiated samples followed a first-order exponential decay fit (see 3.3) with a range of $R^2$ from 0.970 to 0.996. In the dark controls no significant degradation occurred except in NFC at cClo ~544 mg/L. Linear regression for NFC dark control samples at cClo ~544 mg/L (Figure 14) showed a significantly negative slope ($p = 0.0122$). Even though the fit is not convincing ($R^2 = 0.39$), there were also small peaks of degradation products detected in the dark control chromatograms of the last sampling interval. Therefore, the degradation curve of NFC was corrected for degradation in the dark using the equation of the linear regression fit.

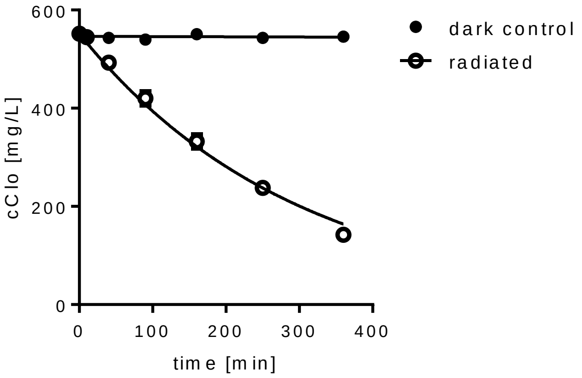

**Figure 13. Example of degradation curves: NFB at cClo ~544 mg/L**

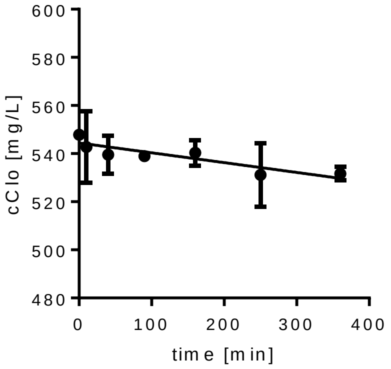

**Figure 14. Linear regression of NFC dark control samples at cClo ~544 mg/L**

First-order kinetics of Clo photodegradation have been previously reported (Gong et al. 2012; Zabar et al. 2012; Mulligan et al. 2016). Degradation in the dark is not expected, as Clo is stable to hydrolysis, except at high pH and increased temperature (University of Hertfordshire 2016).

The slight degradation in the dark control samples observed in NFC was probably caused by hydrolysis, since NFC at this concentration had the highest occurring pH value (8.08±0.02) and ageing chamber temperatures reached up to 70°C.

### Photodegradation Half-lives

The half-lives derived from the degradation curve fits are summarized in Table 12. Half-lives increased with concentration and ranged from 0.92 to 3.61 h for aqueous background. In PP-background they were quite higher (5.9 h on average) for all formulations and the AI.

**Table 12. Photodegradation: summary of half-lives ( ± SD) derived from degradation curve fits**

| nominal cClo [mg/L] | half-lives [h] | | | | |
|---|---|---|---|---|---|
| | NFA | NFB | NFC | Com | AI |
| 13.6 in $H_2O$ | 1.00 ± 0.05 | 0.97 ± 0.06 | 1.06 ± 0.07 | 0.96 ± 0.06 | 0.92 ± 0.05 |
| 102 in $H_2O$ | 1.28 ± 0.06 | 1.25 ± 0.07 | 1.28 ± 0.10 | 1.25 ± 0.07 | 1.17 ± 0.07 |
| 136 in $H_2O$ | 1.49 ± 0.10 | 1.44 ± 0.09 | 1.47 ± 0.10 | 1.30 ± 0.08 | 1.33 ± 0.08 |
| 203 in $H_2O$ | | | 1.68 ± 0.11 | 1.39 ± 0.07 | 1.35 ± 0.10 |
| 306 in $H_2O$ | | | 2.06 ± 0.11 | 1.77 ± 0.09 | |
| 408 in $H_2O$ | 2.49 ± 0.17 | 2.31 ± 0.08 | 2.46 ± 0.11 | 2.15 ± 0.07 | |
| 544 in $H_2O$ | 3.47 ± 0.26 | 3.43 ± 0.15 | 3.61 ± 0.14 | 2.99 ± 0.13 | |
| 136 in PP | 5.61 ± 0.29 | 6.49 ± 0.19 | 4.72 ± 0.23 | 6.25 ± 0.14 | 6.44 ± 0.21 |

Reported photodegradation half-lives for Clo in deionized water range from 0.69 h at cClo 1.1 mg/L (Mulligan et al. 2016) to 3.7 h at cClo 10 mg/L (Gong et al. 2012). Further reported values include 0.1 d, 3.1 h and 3.4 h (US-EPA 2005; University of Hertfordshire 2016). The authors did not always specify the irradiance used, and the procedure used in the present study (e.g. test vessels out of normal glass, not quartz glass) is not exactly comparable, nevertheless the observed half-lives in aqueous background were within the same range.

Equivalent days of natural summer sunlight can be calculated by multiplying the xenon lamp half-life [h], which corresponded to Basel summer sun conditions (see 3.3), by 1/(0.75*12), because the average daily solar radiation intensity can be assumed to be 75% of the maximum intensity over 12h (OECD 2002). This yields a half-life range of 0.1-0.4 d for aqueous background experiments in Basel summer sun conditions.

### Effect of pH and Concentration on Photodegradation Rates

As shown in Figure 15, degradation rate (k) and cClo were negatively correlated for all formulations and the AI, meaning that increasing cClo reduced the photodegradation rate. Also pH varied with cClo: In NFA pH and cClo were negatively related, whereas in NFC and Com the relation was positive. Since for the AI no data could be generated for cClo > solubility, no clear relationship could be established. For NFB, pH seemed to be concentration independent.

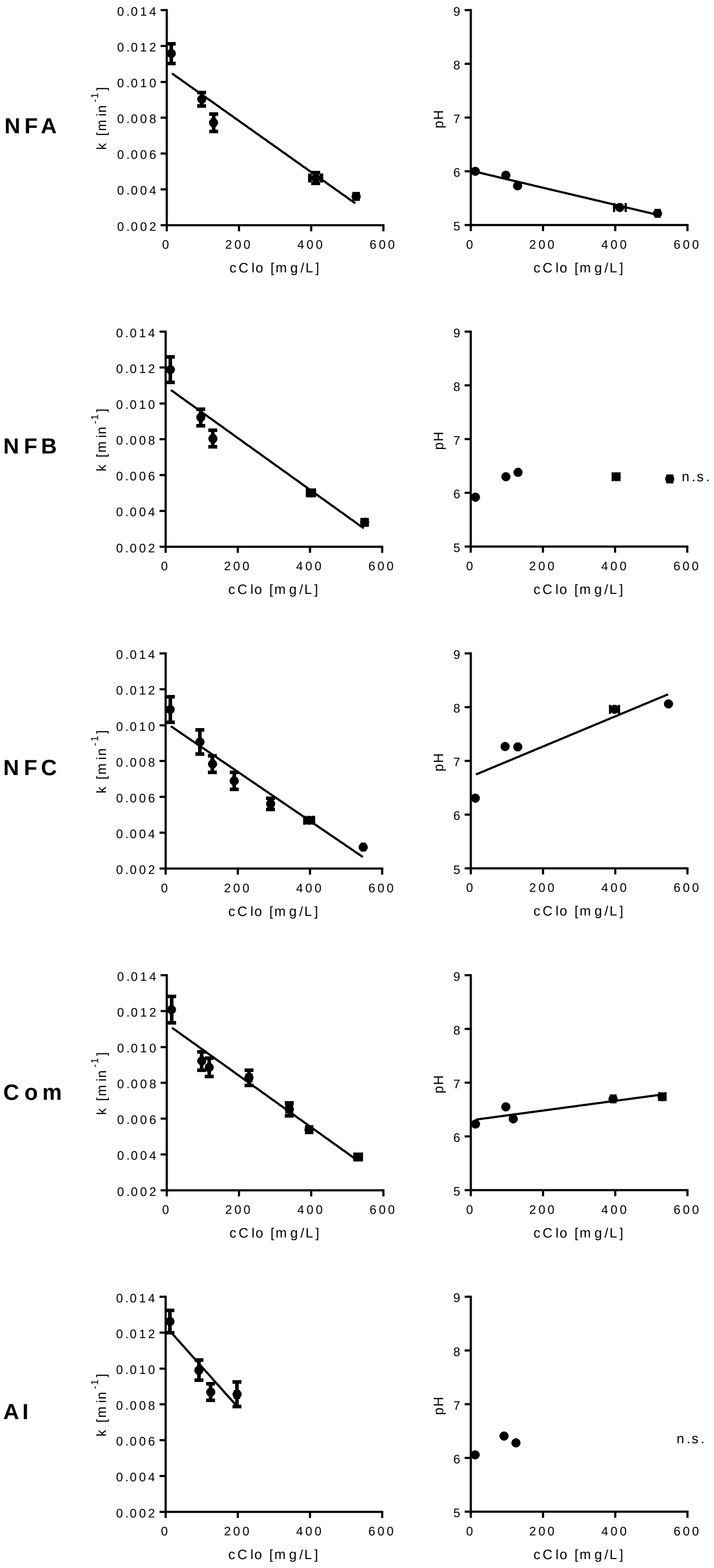

Figure 15. Photodegradation: relations of rate (k), cClo and pH

A decrease in photodegradation rate with increasing concentrations has been previously observed for various organic pollutants (Shu et al. 2013; Li et al. 2014; Hessler et al. 1993; Huang et al. 2006; Zheng & Ye 2001). Zheng & Ye (2001) supposed that at a fixed light energy amount available in a certain volume, a lower concentration allows for higher energy absorption by each molecule. Li et al. (2014) proposed that the relation of rate vs. initial concentration ($C_0$) is linear, but present data suggests that the slope flattens with increasing cClo.

Non-linearity could be attributed to the testing solutions not being optically dilute at decadic absorbances larger than 0.02 or concentrations > $10^{-4}$ mol/L (OECD 2008). In optically thin solutions absorption is negligible, whereas in optically dense solutions total absorption is assumed (Hessler et al. 1993; OECD 2008). Using the $10^{-4}$ mol/L threshold for optically thin solutions (OECD 2008), the Clo concentrations should be < 25 mg/L, but present testing solution concentrations were higher – except for the lowest cClo (13.6 mg/L).

In optically dilute solutions first-order photolysis kinetics can be assumed, whereas in dense solutions a zero-order rate prevails (OECD 2008). Hessler et al. (1993) found decreased quantum yields and degradation rates at increased atrazine and metazachlor concentrations coinciding with increased absorbance and attributed this to a transition from first-order kinetics (exponential degradation curve) to zero-order kinetics (linear degradation curve).

This can be underpinned, considering the shape of the k:cClo relations (Figure 15). With increasing cClo, slope zero would be reached for k:cClo relations in a totally dense solutions, where k becomes independent of cClo. Hence, a gradual change from first to zero-order rates should be indicated by flattening slopes of k:cClo relations, finally approaching zero. In the present study, slopes seemed to be non-linear and tended to flatten, but more data would be needed to clearly exclude linearity. However, plotting k:$C_0$ relations for the data generated by Hessler et al. (1993) clearly underpins this argumentation (Figure 16).

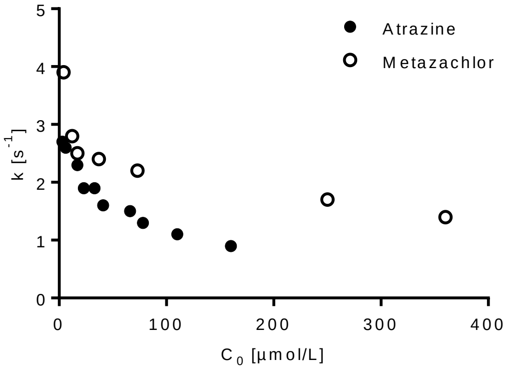

**Figure 16. Non-linear relation of photodegradation rate (k) and initial testing substance concentration ($C_0$) (data from Hessler et al. 1993)**

No studies on the influence of pH on the direct photolysis rate of Clo were found. Whether pH (co-)affected k might be deduced from following considerations: If pH had an influence on k (additional to cClo), this should be visible in the slopes of the k:cClo relations, because pH was as well a function of cClo (for NFA, NFC, Com). A comparison of the k:cClo slopes by an extra-sum-of-squares F test (GraphPad Software Inc. 2016) revealed that the slopes were not significantly different for all formulations (Figure 17), not even between NFA and NFC, which showed the strongest differences in pH:cClo relation (Figure 15). Therefore, it can be concluded that initial solution pH did not affect the rate constants.

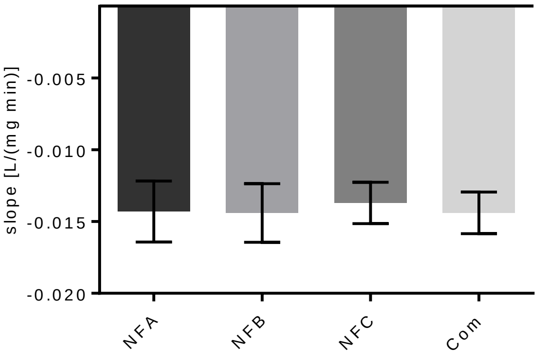

**Figure 17. Photodegradation: comparison of slopes from linear regression of rate (k) vs. cClo**

### 4.2.1. Formulation Influence on Photodegradation in $H_2O$-Background

The rate constants (k) of the degradation curve fits were used to compare the different formulations at all experimental cClo levels (Figure 18).

As expected, at initial cClo close to and above solubility a protective effect of the NFs compared to Com was observed. (The AI could not be included at cClo > solubilitiy, as it would not dissolve above solubility.) The significance of differences increased with concentrations: At cClo ≤ 102 mg/L NFs did not differ from Com, at cClo 136 mg/L k of NFA was already lower than that of Com, followed by NFA and NFB at cClo 408 mg/L and at the highest cClo finally all NFs were significantly more resistant to photodegradation than Com. This indicates that an increased NC-association at increasing cClo is the reason for the protection. Interestingly, at the lowest concentration level NFC degraded slower than the AI. However the rate did not differ from Com.

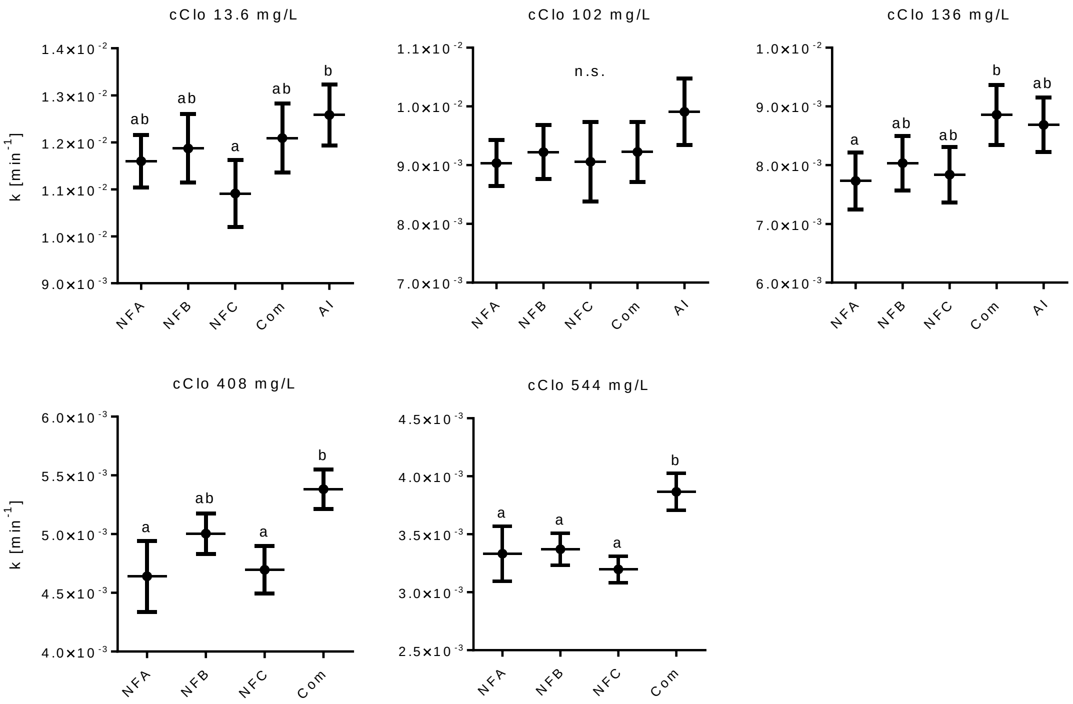

**Figure 18. Photodegradation rate constants (k) of the formulations at various Clo concentration levels.**

The significantly reduced photodegradation rates of NFs as compared to the commercial formulation at cClo > solubility indicate a clear nano-effect through protection of the AI from photodegradation due to increased NC-association.

Nanoformulations can aim at slower or faster (e.g. combined with catalysts) photodegradation (Kah et al. 2013). Shang et al. (2013) demonstrated a decreased photodegradation of an AI (emamectin benzoate) formed in polyacrylate nanoparticles by emulsion polymerization – similar to the present NFs – and attributed this to a partial protection of the AI embedded within the nanoparticles. However, they tested at a concentration level of 1% AI (~10000 mg/L) which was higher than emamectin benzoate solubility (0.1-320 mg/L at pH 5-7) (FAO and WHO 2012).

Decreased photodegradation has also been shown for other types of polymer based formulations like microcapsules containing neem oil (Riyajan & Sakdapipanich 2009). The authors prepared three types of microcapsules and found that all of them reduced photodegradation rate compared to the non-encapsulated neem. The microcapsule type which provided best protection, also showed the slowest release rate, indicating that the AI was protected only within the capsule.

Table 13 quantifies the photodegradation rate comparisons relative to Com. Having a look at the numbers, NFA and NFC were always more distant from Com than NFB. This pattern is also reflected in the graph above (Figure 18), but no significant differences between NFB and NFA/NFC were detected. However, those formulations contain the same ingredients (Table 4) and might thus exhibit more structural NC similarity and similar protective behavior.

**Table 13. Photodegradation rates k of NFs relative to k of Com**

| nominal initial cClo [mg/L] | $k_{NF}/k_{Com}$ [%] | | | |
|---|---|---|---|---|
| | NFA | NFB | NFC | Com |
| 544 | 86.19 | 87.17 | 82.70 | 100 |
| 408 | 86.20 | 92.96 | 87.24 | 100 |
| 136 | 87.28 | 90.71 | 88.48 | 100 |
| 102 | 97.94 | 99.98 | 98.20 | 100 |
| 13.6 | 95.95 | 98.18 | 90.24 | 100 |

### 4.2.2. Photodegradation in the Foliar Spray Application Scenario

The repetition of the experiments in fertilizer background (foliar spray application scenario) at cClo ~136 mg/L resulted in an about four times slower photodegradation of all formulations (Figure 19). Again no degradation occurred in the dark control samples.

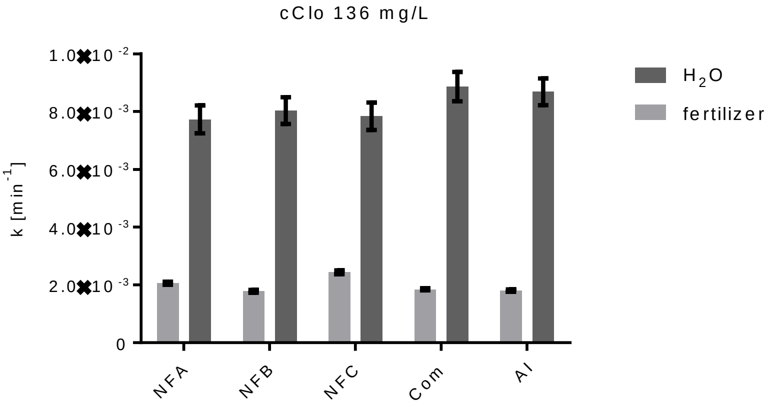

**Figure 19. Photodegradation rate (k) at cClo ~136 mg/L in aqueous and fertilizer background**

The reason for reduced degradation in high salt concentration was probably an increased radiation attenuation (shading). Attenuation can happen either by absorption or scattering.

The absorption of many salts (incl. phosphate salts) is very low in the relevant wave length range (> 290 nm) – with nitrite and nitrate salts being a slight exception – and increases rapidly in the farer UV regions (Buck et al. 1954). This has to do with components of most salts not being spectrally active elements in the near UV (> 300 nm) range (Figure 20).

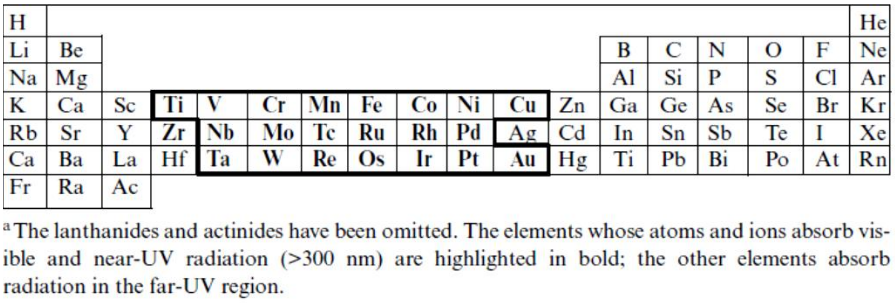

| | | | | | | | | | | | | | | | | | |
|---|---|---|---|---|---|---|---|---|---|---|---|---|---|---|---|---|---|
| H | | | | | | | | | | | | | | | | | He |
| Li | Be | | | | | | | | | | | B | C | N | O | F | Ne |
| Na | Mg | | | | | | | | | | | Al | Si | P | S | Cl | Ar |
| K | Ca | Sc | Ti | V | Cr | Mn | Fe | Co | Ni | Cu | Zn | Ga | Ge | As | Se | Br | Kr |
| Rb | Sr | Y | Zr | Nb | Mo | Tc | Ru | Rh | Pd | Ag | Cd | In | Sn | Sb | Te | I | Xe |
| Ca | Ba | La | Hf | Ta | W | Re | Os | Ir | Pt | Au | Hg | Ti | Pb | Bi | Po | At | Rn |
| Fr | Ra | Ac | | | | | | | | | | | | | | | |

[a] The lanthanides and actinides have been omitted. The elements whose atoms and ions absorb visible and near-UV radiation (>300 nm) are highlighted in bold; the other elements absorb radiation in the far-UV region.

**Figure 20. The area of spectrally active elements in the periodic table[a] (Wozniak & Dera 2007)**

Still, the absorption coefficient of marine-salt solution (37.8 PSU ≈ 37.8 g/kg$_{water}$) was found to be slightly higher than that of pure $H_2O$ in the relevant UV range (>290 nm) (Copin-Montegut et al. 1971 and Kopelevitch 1983, cited in Wozniak & Dera 2007). The absorption of salts as a fraction of total absorption in artificial sea water (salinity 35 PSU ≈ 35 g/kg$_{water}$) was found to be still ~ 70 % at 280 nm and decreased to < 10 % at 400 nm (Wozniak & Dera 2007). Since experimental salt concentrations were very high (in total > 80 g/L, see Table 8), even tiny absorption could lead to significant radiation attenuation and therefore reduce the radiation available for absorption by and degradation of Clo. Furthermore complexes of transition metals which are spectrally active in the near UV and visible range (Figure 20), especially Mn and Fe (Alekin 1970 and Kondratev et al. 1990, cited in Wozniak & Dera 2007) might increase absorbance. The Fe content in experimental solution was considerable (~ 184 mg/L) and it is likely that dissolved Fe formed complexes with phosphate/phosphoric acid or $OH^-$. Additionally, the experimental solutions were slightly colored (yellowish-greenish) which indicates an absorption in the visible range.

The second radiation attenuation mechanism – scattering – is also increased by salt concentrations: e.g. sea salts in the ocean are responsible for ~ 30 % of total molecular scattering in sea water (Morel 1974, Kopelevitch 1983, cited in Wozniak & Dera 2007). Scattering increases non-linearly with shorter wavelengths and linearly with salt concentration (Röttgers et al. 2010). The energy of the radiation is decreased by scattering and with it the likeliness of Clo photodegradation.

Reduced photodegradation of organic pollutants due to salt addition has been reported previously (Mateus et al. 2000; Quivet et al. 2006; Nayak 2015), whereby explanations ranged from quenching of exited states by salt ions, via stabilization of the compound due to chelation with metal ions (e.g. Cu), to direct competition in photon absorption. The mechanisms of Clo photodegradation, identified by Gong et al. (2012), included a.o. radical denitration. In PP-background, radicals might have been quenched by salt ions (phosphate or ammonium). Also chelation with metal ions might have played a role, since there was also some Fe present in PP.

However, the influences of ammonium, phosphate and iron on Clo photodegradation have not been investigated so far. In the photodegradation preliminary study, phosphate buffer was observed to increase degradation rates of Clo (see Annex C). Thus, inhibiting effects were probably mainly due to simple shading by increased optical solution density in high salt concentrations and/or due to some interactions (quenching or complexation) by $NH_4^+$ or Fe.

Regarding the effect of NF on photodegradation rates in PP-background, the high salt concentration did not trigger the expected protective effect due to an increased AI-NC association: Comparing the rate constants of the formulations shows that NFB, Com and the AI did not differ, whereas NFA and NFC even degraded significantly faster than the former (Figure 21).

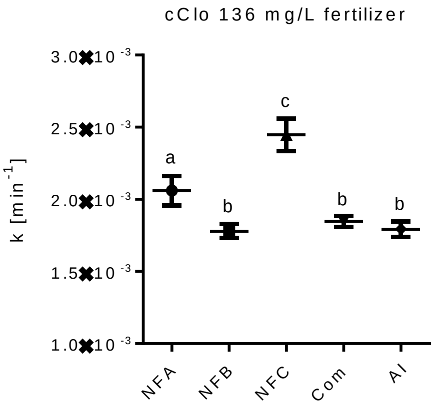

**Figure 21. Photodegradation rate (k) comparison of the different formulations in fertilizer background**

A protection due to NC-association might have been concealed by the strong shading effect of high salt concentrations (see above). Furthermore one has to consider that, the introduction of salt ions as well as high temperatures might also have changed/destroyed the structure of the polymer carriers, not allowing for AI protection anymore.

The slightly increased degradation rate of NFA and NFC could be due to similarity of those formulations: NFA and NFC both contain sodium alkylnaphthalenesulfonate formaldehyde condensate, an anionic surfactant which is often used stabilizer in the emulsion polymerization processes (see section 2.2.2). Emulsion polymerization is frequently used to produce acrylic polymers (as contained in the NFs) and is often initiated by persulfate (Chern 2006). Persulfate was shown to participate as oxidant in photo-Fenton degradation of Clo: catalyzed by $Fe^{2+}$, $SO_4^-$ radicals are produced which effectively enhance indirect photolysis of Clo (Ahmed et al. 2014). In the present study, persulfates might have been artifacts from formulation preparation and PP fertilizer introduced soluble Fe to the system, triggering additional indirect photolysis of NFA and NFC. However, this catalyzing effect was negligible compared to the general decrease of photodegradation rate by fertilizer addition.

## 4.3. Sorption to Soils

The $K_d$ values generated by both methods are presented in Table 14 and ranged from 0.245 to 1.717 L/kg in the centM and from 0.42 to 1.17 L/kg in the batchM.

Previously reported $K_d$ values for Clo ranged from 0.52-4.14 L/kg for various soils (US-EPA 2005) and were higher under simulated rice field conditions: 5.1-10.8 L/kg (Mulligan et al. 2015). With the batchM $K_d$ values corresponded to the lower edge of the reported range. There were no studies found on Clo sorption using the centM.

**Table 14. $K_d$ values (±SD) in loam & sand derived with the batch (after 24h) and centM (after 1 & 7 days)**

| | | $K_d$ [L/kg]<br>NFA | NFB | NFC | Com | AI | average |
|---|---|---|---|---|---|---|---|
| BatchM | loam PP 1d | 1.094 ± 0.021 | 1.147 ± 0.027 | 1.146 ± 0.034 | 1.075 ± 0.021 | 1.071 ± 0.033 | 1.062 ± 0.036 |
| | loam $H_2O$ 1d | 1.103 ± 0.051 | 1.099 ± 0.026 | 1.121 ± 0.024 | 1.022 ± 0.020 | 0.741 ± 0.103 | |
| | sand PP 1d | 0.466 ± 0.010 | 0.441 ± 0.010 | 0.463 ± 0.010 | 0.420 ± 0.015 | 0.430 ± 0.024 | 0.449 ± 0.014 |
| | sand $H_2O$ 1d | 0.449 ± 0.009 | 0.462 ± 0.024 | 0.478 ± 0.012 | 0.449 ± 0.009 | 0.430 ± 0.017 | |
| CentM | loam PP 1d | 1.125 ± 0.219 | 1.359 ± 0.160 | 1.167 ± 0.337 | 0.990 ± 0.338 | 1.214 ± 0.045 | 1.283 ± 0.193 |
| | loam $H_2O$ 1d | 1.400 ± 0.208 | 1.202 ± 0.209 | 1.431 ± 0.138 | 1.604 ± 0.151 | 1.339 ± 0.123 | |
| | loam PP 7d | 1.583 ± 0.039 | 1.535 ± 0.093 | 1.632 ± 0.076 | 1.559 ± 0.133 | 1.717 ± 0.017 | 1.508 ± 0.079 |
| | loam $H_2O$ 7d | 1.337 ± 0.083 | 1.333 ± 0.089 | 1.484 ± 0.064 | 1.444 ± 0.114 | 1.452 ± 0.083 | |
| | sand PP 1d | 0.249 ± 0.008 | 0.251 ± 0.013 | 0.249 ± 0.011 | 0.245 ± 0.006 | 0.246 ± 0.009 | 0.255 ± 0.008 |
| | sand $H_2O$ 1d | 0.267 ± 0.011 | 0.266 ± 0.007 | 0.260 ± 0.005 | 0.251 ± 0.004 | 0.264 ± 0.003 | |
| | sand PP 7d | 0.282 ± 0.007 | 0.281 ± 0.004 | 0.293 ± 0.008 | 0.291 ± 0.014 | 0.295 ± 0.009 | 0.310 ± 0.008 |
| | sand $H_2O$ 7d | 0.324 ± 0.004 | 0.334 ± 0.008 | 0.332 ± 0.008 | 0.325 ± 0.010 | 0.347 ± 0.007 | |

Those calculated $K_d$ values were used to compare the different experimental settings with regards to sorption, shedding light onto the importance of the various influencing factors.

To get an overview of the influencing factors on sorption (soil type, background solution and formulation) and their relative importance, three-way ANOVAs (see statistics 3.6) were calculated separately for the batchM, centM-day 1 and centM-day 7. The results are shown in Table 15 and show an overarching effect of soil type, accounting for > 90 % of the variation in both methods and irrespective of equilibration time.

At equilibrium conditions (in the batchM and assumed in the centM after 7 days), background solution had a significant influence, accounting for 0.39 % of the variance. After one day of equilibration in the centM background solution still made up 1.2 %.

The formulation influence was important in the batchM where it came on second place (after soil), explaining 2.29 % of the variation, but was very low or insignificant in the centM.

Some interactions also seemed to be important e.g. in the batchM the soil×formulation interaction constituted 1.26 % of the variance. In the centM after one day of equilibration, the soil×background-solution×formulation interaction accounted for 1.35 %, which was non-significant after 7 days.

Some of the interactions had more influence than the single factor (e.g. for background solution), which already indicates the complexity of the systems. The factors/interactions will be picked up and further discussed on the pages to come.

**Table 15. Results of three-way ANOVA calculated for the batchM and for the centM at day1 and day7**

| source of variation | batch method<br>% of total variation | P value | | centrifugation method<br>day 1<br>% of total variation | P value | | day 7<br>% of total variation | P value | |
|---|---|---|---|---|---|---|---|---|---|
| A (soil) | 92.87 | <0.0001 | * | 90.08 | < 0.0001 | * | 97.42 | < 0.0001 | * |
| B (backgr.-sol.) | 0.39 | <0.0001 | * | 1.20 | 0.0038 | * | 0.39 | < 0.0001 | * |
| C (formulation) | 2.29 | <0.0001 | * | 0.01 | 0.9991 | n.s. | 0.26 | 0.0086 | * |
| A × B | 0.61 | <0.0001 | * | 0.95 | 0.0094 | * | 0.97 | < 0.0001 | * |
| A × C | 1.26 | <0.0001 | * | 0.02 | 0.9960 | n.s. | 0.18 | 0.0433 | * |
| B × C | 0.97 | <0.0001 | * | 1.29 | 0.0544 | n.s. | 0.04 | 0.6214 | n.s. |
| A × B × C | 0.92 | <0.0001 | * | 1.35 | 0.0465 | * | 0.07 | 0.4170 | n.s. |

### 4.3.1. Effect of Soil Type

Looking at the $K_d$ values of the different soil types in the above table (Table 14) and at the ANOVA results (Table 15), one can see on the first glance that sorption was much stronger in loam than in sand, irrespective of the method, background solution, sampling time or formulation. T tests confirmed significance in all cases.

This was expected, since loam is the more sorptive soil by its properties (higher CEC, higher clay content and higher organic C content). Clo has a $pK_a$ of 11.09 which means it should be mostly protonated and therefore uncharged in the pH values that occurred during the experiments, which suggests organic content to be decisive for higher adsorption in loam.

In general, sorption of organic contaminants is mostly governed by organic matter content (Ciou 2002). This has also been found for the commercial formulation of Clo “Belay” (Tjeerdema et al. 2014).

### 4.3.2. Effect of Time (Centrifugation Method only)

Figure 22 shows the influence of time on $K_d$ values derived by the centM. For sand, a clear increase of sorption with time occurred in both background solutions. In loam with PP-background sorption also tended to increase with time, even though significant differences were only observed for NFA and the AI. However, in $H_2O$-background $K_d$ values did not significantly change with time.

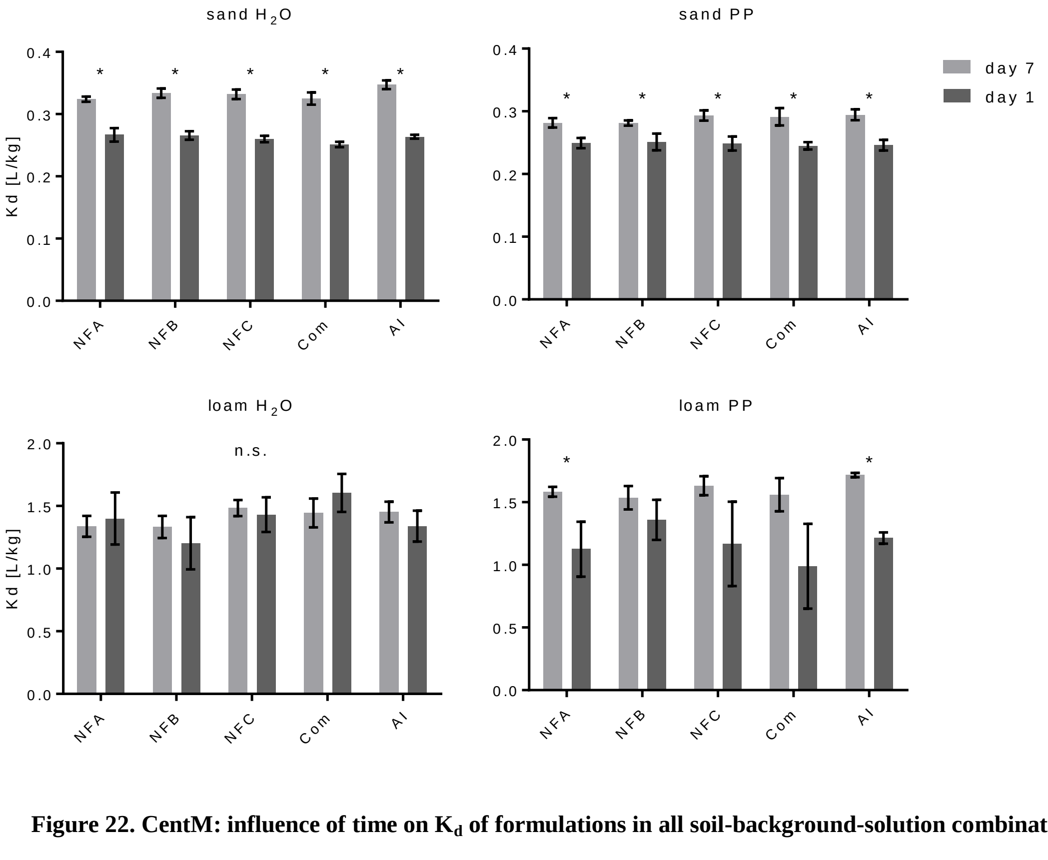

Figure 22. CentM: influence of time on $K_d$ of formulations in all soil-background-solution combinations

A temporal increase in sorption during the centM was also reported in literature (Kah & Brown 2007; Walker & Jurado-Exposito 1998; Kah et al. 2014).

One explanation for an increase of $K_d$ with time during the centM could be biodegradation. Microbes preferably degrade the fraction in solution (i.e. the denominator decreases) which increases $K_d$, provided that re-equilibration from the sorbed fraction is slower than degradation (Duffy et al. 1993, cited in Walker & Jurado-Exposito 1998).

The soils were incubated in the dark at 4°C, which should minimize biological activity. Furthermore, Clo is very resistant to biodegradation with a half-life of 121 and 545 days in the field and lab (20°C) respectively (University of Hertfordshire 2016). Comparing the total amounts of Clo recovered by AcN extraction after one and seven days (Figure 23 a) shows that, depending on soil type and background solution, the extractable amount either increased, decreased or didn't change with time. The fact that it didn't decrease in all soil-solution combinations, plus the aforementioned, allows preclusion of any occurrence of biodegradation.

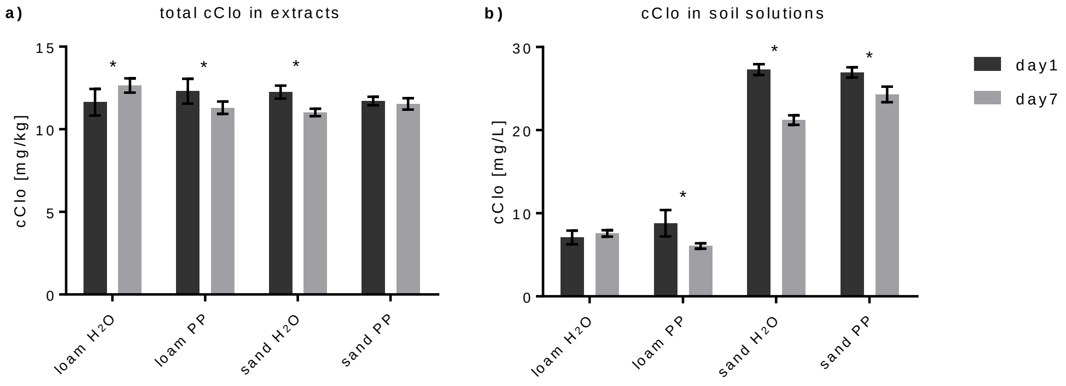

**Figure 23. CentM: AcN extractable Clo per kg$_{dw}$ soil (a) and cClo in solution (b) after 1 & 7 days (compiled data of all formulations and the AI)**

Another explanation for $K_d$ increase, proposed by Walker & Jurado-Exposito (1998), is an increase in sorbed amounts with time. Since degradation can be excluded, a decrease in measured solution concentration with time can be directly interpreted as an increase in sorption (Figure 23 b): sorption increased in sand for both background solutions and in loam-PP.

A higher sorption with time can be explained by the time needed by the compound to diffuse into soil aggregates, organic matrices or particle pores and reach more inaccessible sorption sites (Walker & Jurado-Exposito 1998; Pignatello & Xing 1996).

At high soil:solution ratios a physical non-equilibrium arises, with zones of mobile and immobile water (Pignatello & Xing 1996). Immobile water is mainly associated with aggregated soils, but can also be in a thin liquid film around a soil particle, in a dead-end pore or in an isolated zone under unsaturated conditions; the solute exchange between immobile and mobile water is diffusion limited (various, cited in Gamerdinger & Kaplan 2000). Diffusion in(to) those zones is slower than in bulk water e.g. because of tortuous flow paths, higher retention of solutes in fine pores and higher viscosity of liquids in fine pores (Pignatello & Xing 1996) and not to forget physical isolation.

For loam soil aggregates, it was shown by Walker (2000) that equilibration was slowed down with increasing aggregate size and even more so, when aggregates were previously wetted with 0.01 M $CaCl_2$. In his study for example, equilibrium was not reached after 70 h for isoproturon in soil:solution ratio of 1:1.

In the present work, diffusion into aggregates might be especially relevant for loam, which formed visible aggregates. Pre-equilibration with PP-solution might have had a similar effect as wetting with 0.01 M $CaCl_2$.

However, loam in $H_2O$-background displayed the opposite behavior: the extractability increased significantly with time and solution concentration did not decrease (Figure 23). This might be due to a fast uptake of pesticide spiking solution into soil aggregates and pores upon spiking (Kah & Brown 2007), especially in aqueous background. The pre-equilibration with deionized water probably induced a strong diffusive gradient, speeding up Clo diffusion into the aggregates, removing the diffusion limitation discussed above and allowing for high level sorption right from the start.

With time, equilibration with aggregates that were not directly hit by spiking droplets could have triggered a back-out diffusion, increasing extractability and – in some cases – solution concentrations (significant for Com, insignificant increase for NFC & NFA; data not shown).

The decreased extractabilities for loam-PP and sand-$H_2O$ (Figure 25 a) might furthermore indicate an increased sorption strength with time: sorbates might diffuse into a complex matrix (e.g. soil organic matter, soil aggregates) and sorb to less accessible sites, causing them to be trapped; or initially weak interactions (e.g. van der Waals, hydrophobic bonding) can be transformed into stronger bonds (H-bonds, ion bonds or covalent bonds) (Von Oepen et al. 1991, cited in Delle Site 2001).

### 4.3.3. Effects of Background Solution

Before discussing the effect of background solution on $K_d$ values for both methods, related changes of solution pH (during the batchM) and solution color (during the centM) are presented.

**Change of Solution pH by Equilibration with Soils in the Batch Method**

The pH values measured in the initial solutions (control samples) were significantly higher in PP-background than in $H_2O$-background for all formulations (Figure 24). The initial solution of the AI in $H_2O$ had the lowest pH and t tests confirmed its significant difference from the other formulations in $H_2O$ (as indicated in red).

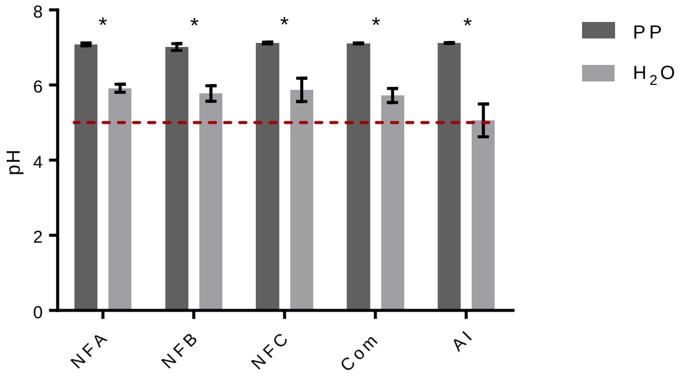

**Figure 24. BatchM: pH values of initial solutions before equilibration with soils**

The average initial pH values for PP- and $H_2O$-background were 7.09 ± 0.06 and 5.67 ± 0.41, respectively (compiling all formulations and the AI). After equilibration with the soils, average pH values were 7.26±0.07 in loam and 6.88±0.04 in sand and no more relevant differences between background solutions or formulations could be spotted, indicating that pH was buffered by the soils.

The changes in pH due to equilibration with soils are shown in Table 16 and were only small for PP-background, but more pronounced in $H_2O$-background. Considering the dissociation constant of Clo ($pK_a$ 11.09), changes in pH were not strong enough to cause marked dissociation of Clo. Hence, sorption of Clo should not be dependent on surface charge.

**Table 16. Changes (Δ) of solution pH (±SD, n=27) due to equilibration with soils (soil:solution ratio 1:2)**

| background solution | pH initial solution | Δ solution pH due to soil | |
|---|---|---|---|
| | | sand | loam |
| $H_2O$ | 5.67 ± 0.41 | 1.21 ± 0.41 | 1.59 ± 0.41 |
| PP | 7.09 ± 0.06 | -0.21 ± 0.07 | 0.18 ± 0.09 |

### Background Solution Dependence of Soil-Solution Color in the Centrifugation Method

During the centM an interesting observation was made: the centrifugate color depended on the background solution in sand, whereas in loam the gathered solution was transparent in both backgrounds (Figure 25). Thus, the soils are probably characterized by different types of organic matter and a different mobilization of those types by each background solution.

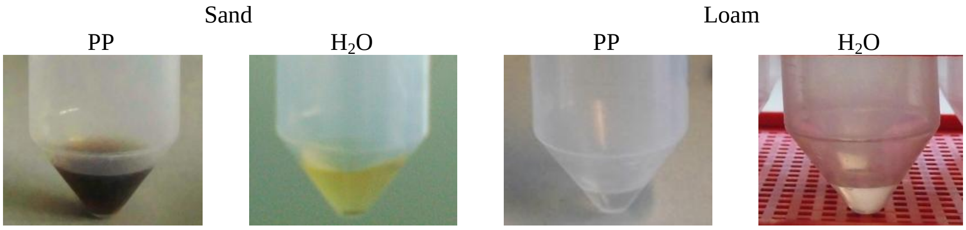

**Figure 25. CentM: background solution dependence of soil-solution color**

Assessing the colors soil solution of sand displayed according to Figure 26, suggests that $H_2O$ mobilized fulvic acids, whereas PP (additionally) mobilized humic acids.

Soil solution gathered from loam did not have any color in both background solutions. This could mean that the organic matter content was dominated by particulate or high molecular weight fractions, which were either held back by the filter membrane (0.4 µm) or were non-soluble per se; e.g. humins, which are strongly incorporated into aggregates and not water soluble (Kahn 1980).

Those findings comply with the rule that more acidic, leached soils (often sandy) typically contain organic matter in form of fulvic acids, whereas in neutral/alkaline, less weathered soils (like loam) organic matter is dominated by high molecular weight humic acids and humin (Pettit 2008).

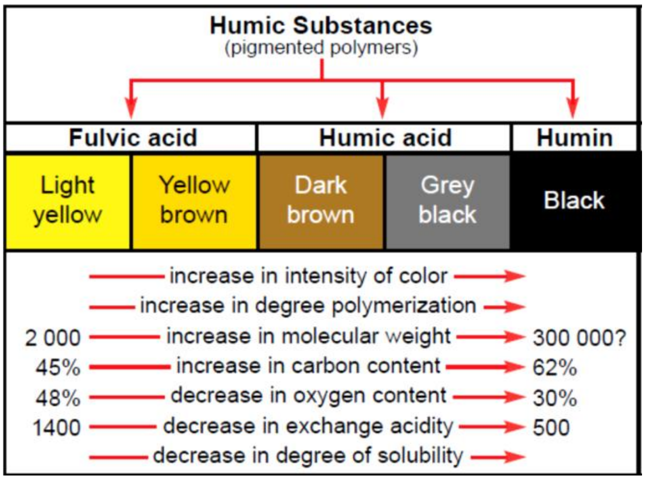

**Figure 26. Chemical properties of humic substances** (Stevenson 1982)

But why does PP cause such a strong mobilization of humic acid in sand? It cannot be an ionic strength effect, since solubility of humic acid should decrease with increasing ionic strength (Weng et al. 2007).

A pH effect cannot be excluded: Humic acids as opposed to fulvic acids are less soluble at low pH (Pettit 2008). Extrapolating from the initial solution pH in the batchM (see above) to the centM suggests that pH is lower in $H_2O$-background (pH 5.67) than in PP-background (pH 7.09), which would favor the observed higher humic acid content in PP compared to $H_2O$. However aqueous solution pH was buffered to around neutral after equilibration with sand. Still, in the centM physical non-equilibrium might have slowed down equilibration.

A more likely explanation is the solubilization of humic acids in PP due to the high concentration of $NH_4^+$. Ammonia, as a monovalent cation, can increase the dispersion of soil aggregates and thus release organics into solution (de Jonge & Wollesen de Jonge 1999) or it can directly solubilize humic acids by formation of soluble salts – ammonia humates – via an ion exchange reaction (Shulgin 2013). The latter is more likely, since there were no visible aggregates in sand. Also phosphate ions, as present in PP, can increase dispersion of clays (and release organics): E.g. Lagaly & Ziesmer (2003) showed that montmorillonite suspensions were more stable in presence of phosphate.

### Influence of Background Solution on $K_d$ Values

Comparing $K_d$ values in the different background solutions (Figure 27) shows that in sand sorption tended to be stronger in $H_2O$-background, whereas in loam the opposite trend could be discerned, at least at equilibrium conditions (as prevailing in the batchM and assumed after 7 days in the centM). Since fertilizer influences on $K_d$ values were not directed the same way in both soils and appeared equally for NFs, Com and the AI, they cannot be attributed to any nano-effect but probably rather to background-solution×soil interactions.

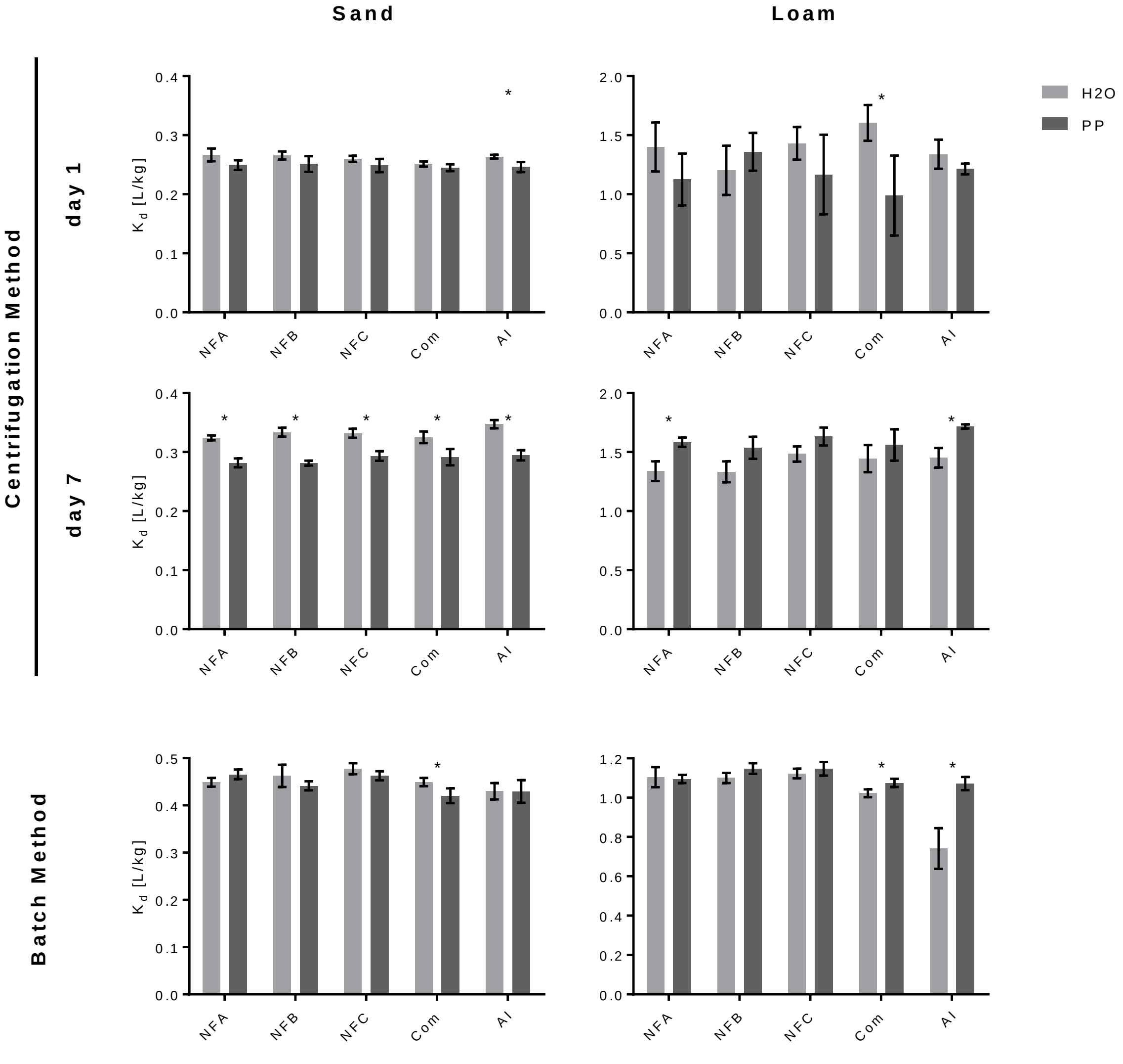

Figure 27. Influence of background solution on centM and batchM $K_d$ values of formulations and the AI

In sand, significantly higher sorption in $H_2O$ evolved with time for all formulations and the AI in the course of the centM. When the batchM was applied, the difference was only significant for Com, but the same trend was observed for NFB and NFC. Considering the increased mobilization of humics in sand by PP as compared to aqueous background (see above), lower $K_d$ values in PP could be explained by an increased dissolution of humic substances and with it mobilization of associated Clo. Sorption of the Clo containing insecticide “Belay” was shown to be dominated by organic substances (Tjeerdema et al. 2014). Hence, an increased dissolved organic content in PP-background probably increased cClo in solution, yielding lower $K_d$ values. Ping et al. (2006), for example, found an increased sorption of imidacloprid due to addition of humic acid and a decrease in $K_d$ due to addition of fulvic acid, probably because the latter is more water soluble.

In loam after one day of equilibration during the centM, the interplay between formulation, soil and background solution, as indicated by 3-way ANOVA (see Table 15) probably masked the sole background solution effect, but after 7 days $K_d$ values of NFA and the AI were significantly higher in PP than in $H_2O$ and NFB, NFC & Com displayed an insignificant tendency in the same direction. This can be the combined effect of (1) a different organic matter quality in loam (e.g. humin) which could not be solubilized by PP, avoiding co-mobilization of Clo, and (2) the dispersion of soil aggregates by $NH_4^+$ which made OM more accessible for sorption.

Comparing the methods with regards to background-solution effects at assumed equilibrium, the $K_d$ differences between background solutions were less pronounced in the batchM, probably because of more intense equilibration. Considering sand, fulvic and humic acids should be both soluble in water at the experimental pH values (Pettit 2008), but in the centM humic acids were only mobilized in PP-background. In the batchM vigorous shaking might have favored solubilization to an equal extent in both background solutions. Additionally, in the batchM the system is more dilute (lower soil:solution ratio), which probably reduced the power of PP fertilizer to mobilize humics.

### 4.3.4. Effect of Sorption Experimental Method

The methods were compared, each at their (assumed) sorption equilibrium: batchM vs. centM at day 7. (However, the trends would have been the same for $K_d$ comparisons between the batchM and the centM at day 1.) Significant $K_d$ differences between the methods were found in all experimental setups and for all formulations: in sand $K_d$ values were higher applying the batchM, whereas in loam higher $K_d$ values were produced with the centM irrespective of background solution (Figure 28). Absolute differences were larger for loam (ranging from 0.23 to 0.71 L/kg) than for sand (ranging from 0.08 to 0.18 L/kg)

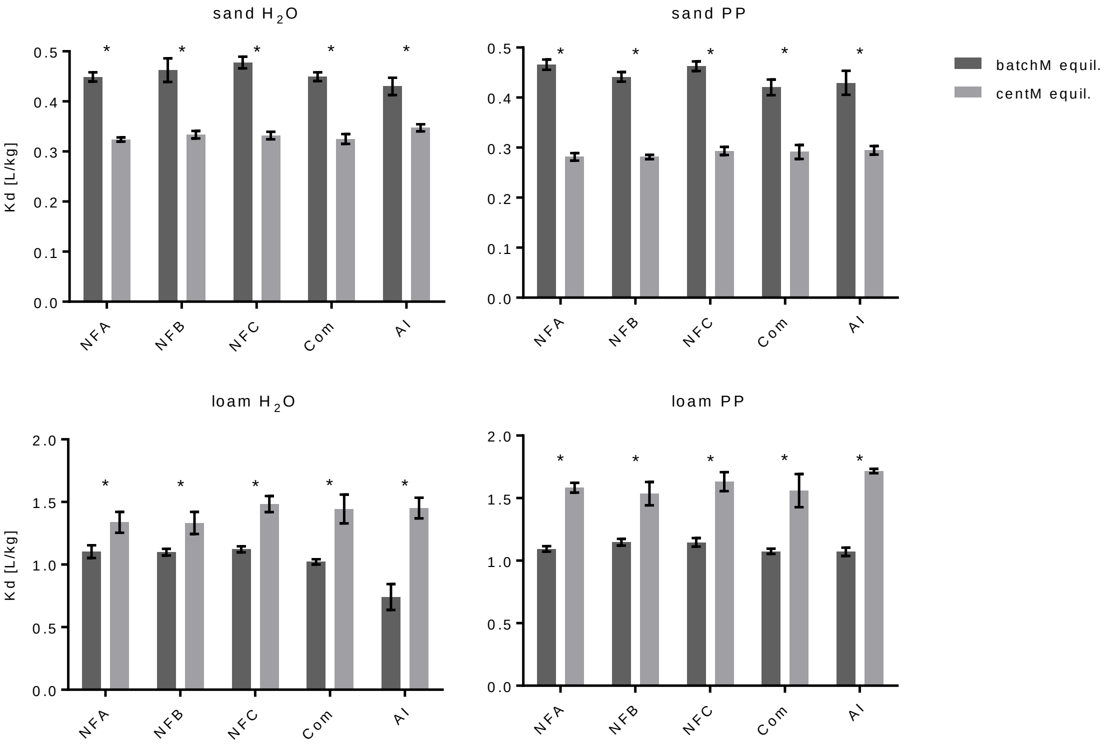

Figure 28. Sorption experiments: comparing batchM and centM at equilibrium

In literature, batchM $K_d$ values were often found to be higher than those derived by the centM, especially when compared to centM-$K_d$ determined after one day of equilibration (Kah & Brown 2007; Yazgan et al. 2005). A higher $K_d$ in the batchM was explained by increased availability of, and contact with sorption sites due to better mixing and destruction of soil aggregates by shaking (Walker & Jurado-Exposito 1998; Kah & Brown 2007; Kah et al. 2014). In the present study this rule might apply to sand, but loam behaved differently.

Data in literature were also not always consistent (Walker & Jurado-Exposito 1998; Kah & Brown 2007; Kah et al. 2014), and Kah & Brown (2007) suggested that for strongly sorbing molecules in highly sorbing soils $K_d$ values are higher in the batchM, whereas for less sorbing molecules they are higher in the centM. To explain higher $K_d$ values in the centM, Kah & Brown (2007) suggested a rapid uptake of spiking solution into soil aggregates could lead to a physical protection and therefore higher $K_d$ values in the centM. Loam has a high affinity for water and formed aggregates which were only saturated to 60 % of the MWHC, therefore a rapid absorption of spiking solution into aggregates is very likely.

Physical protection could be due to pesticide diffusion into sites of immobile water, since during the centM centrifugation force was chosen to separate mobile and immobile water (Addiscott 1977, cited in Kah et al. 2014). Gamerdinger & Kaplan (2000) found that the fraction of immobile water increased with decreasing moisture saturation of the soil. In their study, at similar saturation, the immobile frac-

tion was furthermore higher in loam than in sand. Hence, this protection mechanism is more likely for loam than sand.
Another mechanism creating higher $K_d$ values in the centM than in the batchM might be a preferential sorption to dissolved organics or fine colloids: In the batchM those can stay in solution after centrifugation, which would be measured as a decreased distribution coefficient (de Jonge & Wollesen de Jonge 1999). Gooddy et al. (2007) found increased diuron concentrations in size fractions > 0.1 µm and > 0.45 µm relative to unfiltered samples of soil suspension. Also atrazine was found to be associated with colloidal organic matter ranging from 0.45 µm to 5000 g/mol (Wijayaratne & Means 1984). Clo was shown to be scavenged by polymers via H-bonds (Yang et al. 2014). Hence, H-bonds, next to hydrophobic interactions, are probably also a major mechanism of Clo sorption. Via H-bonds organic pesticides can also bind to surface oxygen or edge hydroxyls of clay minerals (Bailey et al. 1968, cited in Kahn 1980). Since loam contained much more fine material < 2 µm (25.9 ± 2.1 % of the total weight vs. 2.8 ± 1.1 % in sand, see Table 1), it might be more prone to produce high colloid concentrations upon equilibration. If Clo had some affinity to those colloids, this fraction could have been interpreted as "in solution" by the batchM, whereas in the centM the filtermembrane (0.4 µm), physical protection within soil aggregates or screening of colloidal fractions when migrating through structured soil samples might have avoided high colloid concentrations in centrifugates.
Furthermore, the possibility of precipitation of the AI due to exceedance of solubility limits at high soil:solution ratios was proposed to increase $K_d$ values in the centM (Kah & Brown 2007; Kah et al. 2014). Soil-solution cClo in the centM reached ~ 49 mg/L in loam (see Table 7) which is more than 6 × lower than solubility limit. Still precipitation could have played a role locally, e.g. due to accumulation on the surface of particles/aggregates. Furthermore, high salt concentration (as in PP-background) typically decreases solubility of neutral organics due to "salting out" (Delle Site 2001). However, precipitation is probably not a major factor since soil-solution cClo in sand was even higher in the centM (~ 70 mg/L, see Table 7), but in sand $K_d$ was higher in the batchM.

The calculated percentages of Clo adsorbed in both methods are shown in Table 17. Average percentages adsorbed in the batchM were around 34 % in loam and 18 % in sand. In the centM, the values were higher for both soils, with averages of 85 % in loam and 62 % in sand (at equilibrium).

**Table 17. Clo percentage adsorbed (A ± SD) in loam & sand in the batch (after 24h) and centM (after 1 & 7 d)**

| | | A [%] | | | | | |
|---|---|---|---|---|---|---|---|
| | | NFA | NFB | NFC | Com | AI | average |
| BatchM | loam PP | 34.6 ± 0.4 | 35.6 ± 0.5 | 35.6 ± 0.7 | 34.1 ± 0.4 | 34.0 ± 0.7 | 33.9 ± 1.0 |
| | loam $H_2O$ | 35.8 ± 2.0 | 34.4 ± 0.5 | 35.5 ± 1.1 | 32.7 ± 0.4 | 26.5 ± 2.7 | |
| | sand PP | 18.9 ± 0.3 | 18.1 ± 0.3 | 18.8 ± 0.3 | 17.4 ± 0.5 | 17.6 ± 0.8 | 18.3 ± 0.5 |
| | sand $H_2O$ | 18.3 ± 0.3 | 18.8 ± 0.8 | 19.3 ± 0.4 | 18.3 ± 0.3 | 17.7 ± 0.6 | |
| CentM | loam PP 1d | 80.7 ± 3.1 | 83.6 ± 1.6 | 80.9 ± 4.7 | 77.9 ± 6.2 | 82.1 ± 0.5 | 82.4 ± 2.4 |
| | loam $H_2O$ 1d | 84.0 ± 2.0 | 81.7 ± 2.6 | 84.3 ± 1.3 | 85.8 ± 1.2 | 83.4 ± 1.3 | |
| | loam PP 7d | 85.7 ± 0.3 | 85.3 ± 0.8 | 86.0 ± 0.6 | 85.4 ± 1.1 | 86.6 ± 0.1 | 85.0 ± 0.7 |
| | loam $H_2O$ 7d | 83.4 ± 0.9 | 83.4 ± 0.9 | 84.8 ± 0.6 | 84.5 ± 1.0 | 84.5 ± 0.7 | |
| | sand PP 1d | 57.2 ± 0.8 | 57.4 ± 1.3 | 57.1 ± 1.1 | 56.8 ± 0.6 | 56.9 ± 0.8 | 57.6 ± 0.7 |
| | sand $H_2O$ 1d | 58.7 ± 1.0 | 58.6 ± 0.6 | 58.1 ± 0.5 | 57.3 ± 0.4 | 58.4 ± 0.3 | |
| | sand PP 7d | 60.1 ± 0.6 | 60.1 ± 0.4 | 61.1 ± 0.7 | 61.0 ± 1.1 | 61.2 ± 0.7 | 62.3 ± 0.6 |
| | sand $H_2O$ 7d | 63.3 ± 0.3 | 64.0 ± 0.5 | 63.9 ± 0.5 | 63.4 ± 0.7 | 64.9 ± 0.5 | |

Regarding the percentages adsorbed, it is interesting that, unlike $K_d$ values, they were higher for both soils in the centM than in the batchM. This confirms the influence of sorbent concentration on sorption behavior as proposed by many authors (cited in Delle Site 2001). However, those authors usually related the $K_d$ values to the soil:solution ratio, suggesting that $K_d$ increases with higher soil:solution ratios, especially for compounds with large $K_d$ (Delle Site 2001). In the present study $K_d$ did not generally increase with soil:solution ratio (only for loam a $K_d$ increase was observed), but the percentage adsorbed were higher in the centM in all experimental settings and might indicate an increase in the percentage adsorbed with increasing soil:solution ratio.

When basing the method comparison on the percentages adsorbed, this study confirms the idea of stronger sorption in the centM for less strongly sorbing compounds (like Clo) as proposed by Kah & Brown (2007).

The discrepancies arising for sand when basing the method comparison on $K_d$ or percentage adsorbed might be an artifact from the experimental setup in the centM. The centrifugate was corrected for the amount of $H_2O$ used for filter pre-wetting, assuming a dilution of the whole soil-solution amount in the 10 g of moist soil weighed in (see 3.4.2), which of course had a different impact on sand and loam due to their different MWHC. The impact of this “dilution” should be quite low for sand, as for sand ~1.01 mL centrifugate were recovered and the pre-wetting amount was only 0.1 mL $H_2O$. However, also AcN extraction efficiency varied between the soil-background-solution combinations. If the error introduced by AcN extraction was larger than the error introduced by “dilution”, the formula for $K_d$ reacts more sensitive than that for the percentage adsorbed: The AcN-extract cClo enters the $K_d$ calculation only in the nominator (to calculate the amount of Clo in soil), whereas it enters the percentage adsorbed formula in the nominator and the denominator (see 3.4.2) and the error is kind of cancelled out by that. Since the absolute $K_d$ differences between the methods were rather small in sand (0.08-0.18 L/kg, see above), this sensibility might have been enough to cause this discrepancy.

#### 4.3.5. Effects of Formulations

Figure 29 compares the $K_d$ values of the different formulations and the AI. In the batchM there were significant differences in all experimental settings, whereas in the centM several settings did not yield any significant difference: sand-PP (at day 1 & day 7), loam-$H_2O$ (at day 1 & day 7) and loam-PP at day 1. Only the results of soil-background-solution combinations with significant differences are shown.

This indicates that for the present formulations, the batchM had more power to detect formulation influences. However, for a slow-release formulation Kah et al. (2014) found equally pronounced impacts of NF on sorption with both methods.

Those differences that were found to be significant were rather small in both methods. The $K_d$ range (= max – min) between the formulations in the batchM was < 0.1 L/kg in various experimental settings and also never exceeded 0.2 L/kg in the centM at assumed equilibrium (after 7 days). The only exception in the batchM was loam-$H_2O$, where the range reached 0.4 L/kg (due to the much lower $K_d$ of the AI). Similarly, in the centM after just one day of equilibration the $K_d$ range was still up to 0.4 L/kg in the various settings.

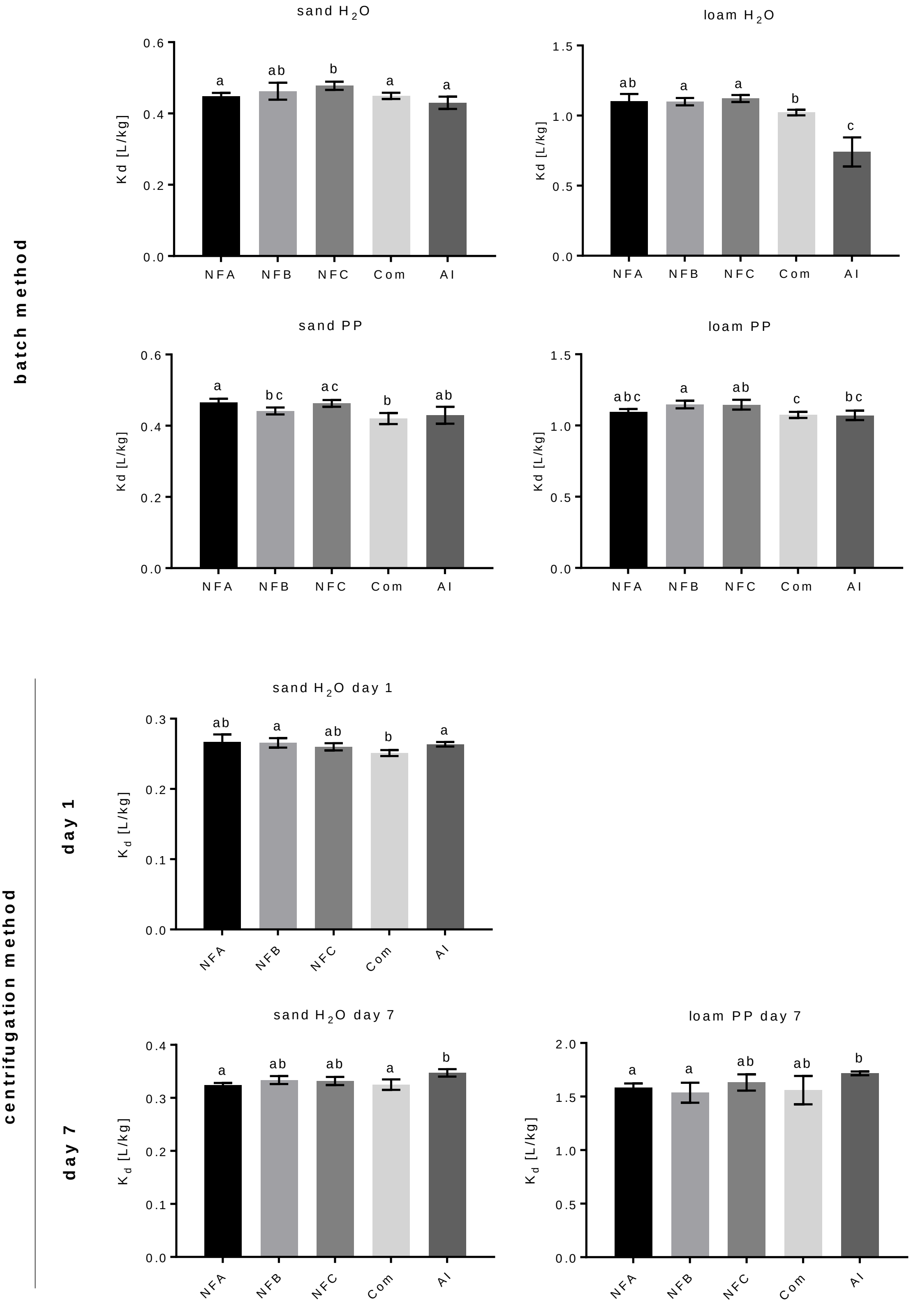

**Figure 29. Sorption $K_d$ comparisons between formulations and the AI in the batchM and centM**

## General Influence of Formulation

Figure 29 shows that in only one scenario – loam with aqueous background in the batchM – the $K_d$ value of the AI was different (lower) from that of all the formulations, indicating a general formulation influence.

Since this was not observed in PP-background (where aggregates were probably destroyed by $NH_4^+$), the reason might again be a lower accessibility of sorption sites due to water-stable aggregates in $H_2O$-background. As a matter of fact, it was observed that during batch experiments not all the aggregates in loam were destroyed by shaking. However, stable aggregates in loam-$H_2O$ should reduce the sorption-site accessibility not only for the AI but also for the formulations, yet the $K_d$ values of the formulated pesticides were not reduced in loam-$H_2O$ as compared to loam-PP (Figure 29). The reasons for this could be either an enhanced loam aggregate stability in the AI aqueous solution (as compared to the formulation solutions) or vice versa a decreased loam aggregate stability in the formulation solutions vs. the AI solution (or a combination of both).

The first might be explained by the fact that AI-$H_2O$ solution displayed a lower initial solution pH as compared to the formulations (see Figure 24), which was not observed in PP-background, and a low pH enhances clay aggregate stability (de Jonge & Wollesen de Jonge 1999).

The second might be a result of simple (non-nano) formulation effects, for which two mechanisms can be hypothesized:

First, an impact of forming agents on soil aggregate stability, making sorption sites more available also in $H_2O$-background: all NFs contained (anionic) surfactants/dispersants (see 2.2.2). Sorption of anionic surfactants can increase negative surface charge and thus dispersion of soil particles (Ishiguro & Koopal 2016). This dispersion (eg. by sodium dodecylbenzenesulfonate = SDBS) can act on micro- and macroaggregate levels, meaning clay dispersion and dispersion of water-stable aggregates respectively (Piccolo & Mbagwu 1989). Rao et al. (2006) found that an anionic surfactant (SDBS) increased the dispersion of a Ca-saturated soil and proposed three mechanisms for that: Negative charge added by anionic surfactants leads to increased repulsive forces in soil aggregates, adsorption of surfactant decreases interface tension leading to dispersion of particles (Tumeo 1997, cited in Rao et al. 2006) and/or monovalent $Na^+$ added with the surfactant increases dispersion (substituting $Ca^{2+}$) (Levy et al. 1999, cited in Rao et al. 2006). Also Lagaly & Ziesmer (2003) found an increased dispersion of montmorillonite by sodium dodecyl sulfate. An increased dispersion of soil aggregates might again increase accessibility of sorption sites and therefore $K_d$ values in the NFs as compared to the AI. Analogously, since humic substances have a polyelectrolyte nature (Ishiguro & Koopal 2016), sorption of anionic surfactants might increase negative surface charge and lead to an expansion of humic substances, increasing accessibility of sorption sites. The influence of propylene glycol (the carrier in Com) on soil properties has not been studied so far.

Second, a formulant-mediated sorption/precipitation of the AI. Usually surfactants tend to sorb to the soil components below their critical micelle concentration. E.g. Beigel et al. (1998) investigated sorption of low level anionic and non-ionic surfactants to a loamy clay soil and found that all surfactants significantly sorbed to the soil, probably due to hydrophobic interactions. Micelles themselves do not sorb to soils (Wang & Keller 2009) but sorbed monomers can form admicelles on soil surfaces (various, cited in Wang & Keller 2009), and organics might partition into those admicelles. Sánchez-Camazano et al. (1995) showed that the anionic surfactant lauryl sulfate at concentrations below the critical micelle concentration decreased mobility of pesticides (diazinon, atrazine, metolachlor, acephate) and explained this by hydrophobic bonding to sorbed surfactant monomers or admicelles. Similarly, formulants (e.g. polymers) might also just increase the organic content of the soil and thus enhance sorption due to hydrophobic interactions (Sun et al. 1995, cited in Beigel et al. 1998). The type of cation dominating the CEC might also have an important influence on surfactant sorption/precipitation and co-sorption of pesticides. Rao et al. (2006) found that the anionic surfactant SDBS strongly sorbed to Ca-saturated soil (in Na-saturated soil sorption decreased when the critical micelle concentration was reached). This was explained by surface complexation of $DBS^-$ with divalent cations and possibly precipitation of $CaDBS_2$. Similarly, Wang & Keller (2009) showed that linear alkylbenzene sulfonate (LAS) did not just partition into organic matter, but was also sorbed to negatively charged soil particles via divalent cation bridges or precipitated by those cations, since partitioning was strongly correlated to exchangeable divalent cation concentration. Additionally, they observed that pesticides (diuron and atrazine) sorbed to those LAS precipitates. It is likely that in loam $Ca^{2+}$ and $Mg^{2+}$ concentration on the CEC was substantial (as compared to sand which was more acidic) (Washington State University 2004). Hence, such mechanisms are possible and perhaps more likely in loam-$H_2O$, as loam-PP contained much monovalent $NH_4^+$, which might cover the CEC.

Another indication for some formulation influence might be the interaction between the factors soil, background solution and formulation, as visualized in Figure 30: Even though the $K_d$ values were not significantly different, the centM after one day of equilibration yielded an opposing pattern of $K_d$ values in PP-background as compared to $H_2O$-background (Figure 30 a). Reordering the $K_d$ values by size revealed that $K_d$ decreased in $H_2O$ and increased in PP following the same order of formulations/AI (Figure 30 b), so the formulation with the highest $K_d$ in $H_2O$ displayed the lowest $K_d$ in PP etc.

Of course this might just be a random product of slower equilibration in loam-$H_2O$ (where stable aggregates were likely), but it might also indicate a systematic loam×background-solution×formulation interaction (as already suggested by 3-way ANOVA, see Table 15).

Whether some formulation influences were the reason for that cannot be concluded. However, the only significant $K_d$ difference between a NF and Com in the centM was also found after day 1 (NFB > Com, in sand-$H_2O$) and the $K_d$ range (= max – min) in the centM was still larger at day 1 (up to 0.4 L/kg) than at day 7 (up to 0.2 L/kg). Altogether this indicates that any formulation-dependent interactions might be only visible shortly after formulation application and could be perhaps detected with more frequent and shorter sampling intervals in the centM.

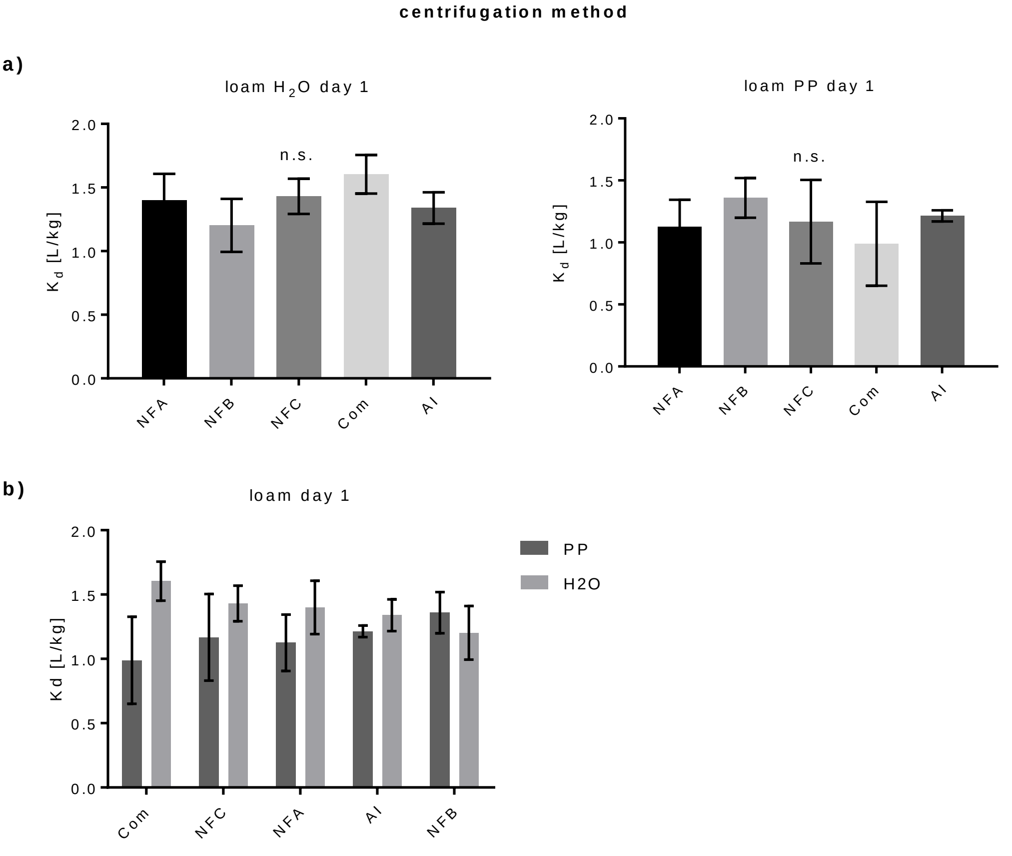

**Figure 30. CentM: patterns of $K_d$ values in loam at day 1 (a), Kd values in loam-day 1 ordered by size (b)**

### Influence of Nanoformulation

To assess the influence of nanoformulations, Table 18 again summarizes the significant differences of $K_d$ between the formulations/AI (as already depicted in Figure 29).

Regarding the effect of nanoformulation, no general nano-effect can be concluded. Even though in the batchM, in all settings at least one NF sorbed significantly stronger than Com, there was no setting in which all NFs sorbed more than Com. In the centM, the only significant difference between a NF and the commercial formulation (NFB>Com) was observed in sand-$H_2O$ at day one. This is consistent with the observed immediate release of the AI from the NC (see 4.1). Kah et al. (2014) conducted similar experiments with a slow-release formulation of atrazine and found clearly higher $K_d$ values for NFs compared to the pure AI-solution.

Also fertilizer did not provoke the expected increase in NC-association of Clo due to following lines of evidence: (1) in the centM, where NCs could not pass through the filter membranes, NC-association in PP would have led to increased $K_d$ values of the NFs (as compared to Com/AI) and the effect should have been even more evident in sand, since soil-solution concentrations of Clo were higher in sand than in loam (see 3.4) – however, none of this was observed (Table 18); (2) also in the batchM the $K_d$ values of the NFs were similar in PP and $H_2O$-background and $K_d$ differences between the NFs and Com/AI were not more pronounced in PP.

All those considerations indicate, that PP did either not increase NC-association at all, or the effect was minor and masked by other effects of the fertilizer (like mobilization of certain humic substances (see 4.3.3). Furthermore, equilibration with soil might have nullified initial ionic strength differences. E.g. Kah et al. (2014) found similar $K_d$ values for deionized $H_2O$ and 0.01 M $CaCl_2$-background in the batchM and concluded that soil solutes compensated ionic strength differences.

**Table 18. Differences of $K_d$ values between formulations (<, >, n.s.; read row vs. column)**

| | | batch method | | | | | | | | | | |
|---|---|---|---|---|---|---|---|---|---|---|---|---|
| | | sand $H_2O$ | | | | | | sand PP | | | | |
| | | NFA | NFB | NFC | Com | AI | | NFA | NFB | NFC | Com | AI |
| | NFA | | n.s. | < | n.s. | n.s. | NFA | | > | n.s. | > | n.s. |
| | NFB | | | n.s. | n.s. | n.s. | NFB | | | n.s. | n.s. | n.s. |
| | NFC | | | | 🟨 > | 🟦 > | NFC | | | | 🟨 > | n.s. |
| | Com | | | | | n.s. | Com | | | | | n.s. |
| | | loam $H_2O$ | | | | | | loam PP | | | | |
| | | NFA | NFB | NFC | Com | AI | | NFA | NFB | NFC | Com | AI |
| | NFA | | n.s. | n.s. | n.s. | > | NFA | | n.s. | n.s. | n.s. | n.s. |
| | NFB | | | n.s. | 🟫 > | 🟫 > | NFB | | | n.s. | 🟫 > | 🟫 > |
| | NFC | | | | 🟨 > | 🟦 > | NFC | | | | 🟨 > | n.s. |
| | Com | | | | | > | Com | | | | | n.s. |
| | | centrifugation method | | | | | | | | | | |
| | | sand $H_2O$ | | | | | | loam PP | | | | |
| | | NFA | NFB | NFC | Com | AI | | NFA | NFB | NFC | Com | AI |
| day 1 | NFA | | n.s. | n.s. | n.s. | n.s. | NFA | | n.s. | n.s. | n.s. | n.s. |
| | NFB | | | n.s. | > | n.s. | NFB | | | n.s. | n.s. | n.s. |
| | NFC | | | | n.s. | n.s. | NFC | | | | n.s. | n.s. |
| | Com | | | | | 🟩 < | Com | | | | | n.s. |
| | | sand $H_2O$ | | | | | | loam PP | | | | |
| | | NFA | NFB | NFC | Com | AI | | NFA | NFB | NFC | Com | AI |
| day 7 | NFA | | n.s. | n.s. | n.s. | < | NFA | | n.s. | n.s. | n.s. | < |
| | NFB | | | n.s. | n.s. | n.s. | NFB | | | n.s. | n.s. | < |
| | NFC | | | | n.s. | n.s. | NFC | | | | n.s. | n.s. |
| | Com | | | | | 🟩 < | Com | | | | | n.s. |

shadings indicate consistencies within each method:
yellow.....in all soil/solution combinations
blue ........in same background solution
brown ....in same soil
green ......at both sampling times in the same soil/solution combination

Even though no overall nano-effect could be shown, Table 18 comprises some significant nano-effects for single formulations and indicates consistencies observed between soils or background solutions. There were no consistencies in formulation influences between the two methods. In the centM, the only consistency observed was a consistency over time: in sand-$H_2O$ the AI sorbed stronger than Com. However, this is probably just an artifact of different spiking volumes in the centM, which were 12 mL and 1.2 mL, for the AI (due to solubility limit) and the formulations respectively. A higher spiking amount might have allowed for a faster and better mixing with the soils and therefore increased contact to sorption sites. Excluding the AI, there remain no significant $K_d$ differences between formulations in the centM, except NFB > Com in sand-$H_2O$ at day1.

Within the batchM results, one consistent nanoformulation-effect was found throughout all soil-background-solution combinations: NFC sorbed significantly stronger than Com (marked in yellow). However, it only sorbed stronger than the AI in aqueous background solution (blue). Perhaps there was some salting-out of the AI in PP-background. Another single nano-effect was observed in loamy soil: NFB sorbed stronger than Com and the AI irrespective of background solution (brown).

Zooming into the $K_d$ differences between the formulations in the batchM (Figure 31) reveals that $K_d$ of NFC was not just always higher than that of Com, it was generally found on the higher edge (indicated in red), whereas the AI and Com were on the lower edge. NFA and NFB varied their relative positions. Since NFC was the formulation that aggregated the most (see 4.1), its special behavior could be due to aggregation of nanocarriers in the dilute soil suspension upon spiking (Kah et al. 2013), which might have slightly increased the $K_d$ by physical capturing of some still associated AI within aggregates, preventing total release. In the centM, aggregation of NCs in solution might have been physically impossible due to high soil:solution ratios.

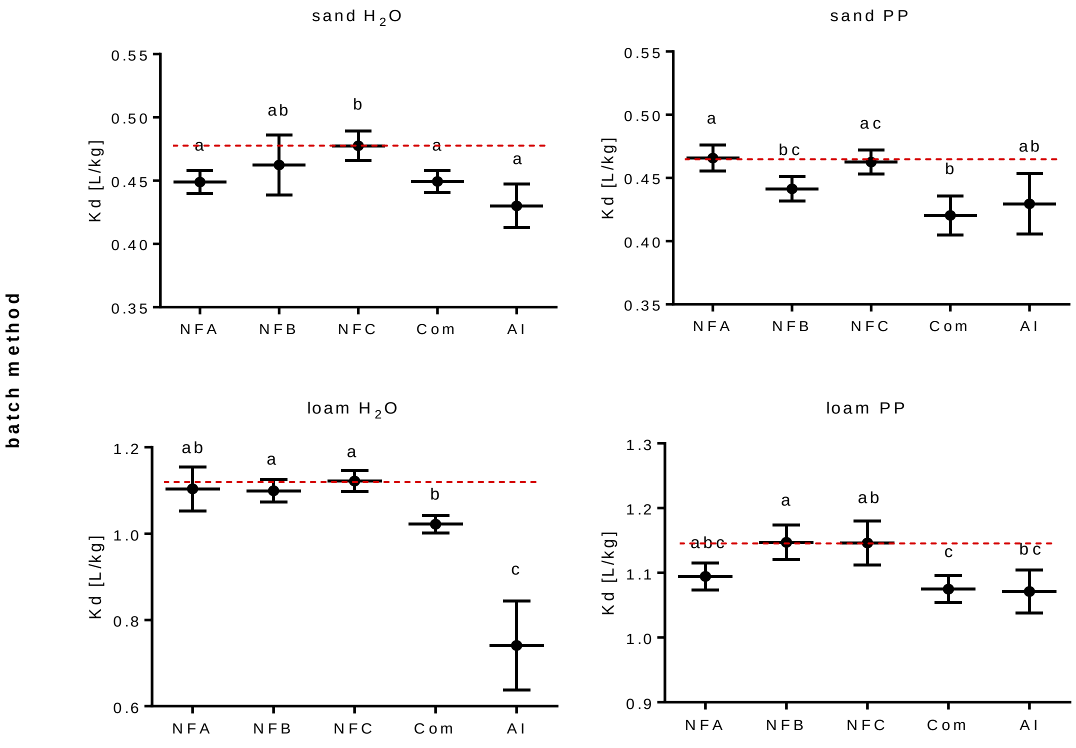

**Figure 31. Zoomed-into $K_d$ differences between formulations in the batchM**

# 5. Conclusions and Outlook

The present study, to the best of my knowledge, is the first one investigating the environmental fate and behavior of Clo nanopesticide formulations. The following summarizes and concludes on the major findings of this study and gives some hints on further research necessities.

## 5.1. Nanoformulation Characterization

The aim of the present NFs probably was to increase solubility of the AI in aqueous solution, not any slow or targeted release. AI association with nanopolymers increases solubility limits and helps to minimize package sizes and storage space needed. It also allows for improved mixing properties when preparing tank mixes e.g. with addition of liquid fertilizer.

The NFs immediately released the AI into solution when diluted to cClo below solubility and it might be sufficient to separately assess the fate of the NC and the AI at the usually low concentrations reached in the environment.

The polymer particles were in the upper nano-size range when measured in deionized water and quickly aggregated in case of NFC in increased ionic strength. However, NFA did not aggregate at all and NFB only slightly. Due to their size, the particles are probably not very mobile in soils (being screened when migrating through soils). But aggregation might increase the chance of physically capturing the AI inside, thus enhancing the NC-AI association which might again create a small pool of NC-associated AI.

## 5.2. Photodegradation

Photodegradation was rather fast, indicating that Clo – irrespective of formulation – is degraded quickly when exposed to direct sunlight.

In aqueous background a protective effect of the NF starts to come into play at Clo concentrations close to and above solubility. Thus, for a foliar spray application at maximum Clo concentrations, reaching 136 mg/L in crops, this effect probably has some relevance, even though further tests would be required to confirm similar behavior on plant surfaces. For some cultivars like grapes and pome fruits even higher spray concentrations are applied and a photoprotective effect would be even more likely.

However, the present NFs did not have much influence on photodegradation, when relating to the maximum occurring soil concentrations during in-furrow application (cClo 13 mg/L). Even though at this concentration NFC was more persistent than the AI, it did not significantly differ from Com. Of course there is no sunlight available within the soil and in-furrow application is not a suitable photodegradation scenario, but it is the scenario producing the maximum Clo concentrations in soil. Thus, it can be concluded for all other soil applications (with even lower spray cClo), that spray drift as well as wash-off to surface waters will not result in Clo concentrations that enable a photoprotective effect of the NF and all the AI is released.

It was shown though, that polymer-based NFs in general have the potential to protect the AI from photodegradation, when the AI is still associated with the NC (at initial testing concentrations above Clo solubility). A polymer-based NF designed for slow release would thus increase the resistance of the AI to photodegradation, if the release rate is slower than the degradation rate (Kah et al. 2014). Such a protection might (e.g. in case of spray drift or soil wash-off) allow enough time for movement of the nanopesticide out of the sunlit surface waters (e.g. with organic particles) to deeper and darker waters where Clo would be persistent, since it is not prone to biodegradation. Release of the AI from the NC in dark waters or sediments would enhance the risk of transport to groundwater, since free Clo is rather mobile (low sorption coefficient). Analogously, photoprotective NFs might increase the amount of AI transported from the soil surface to deeper (dark) layers or increase the persistence on the plant surface, in case of an application as foliar spray. But to infer real behavior on plant surfaces, experiments with slow-release formulations should be repeated under more realistic conditions e.g. because the polymer nanocarrier could also influence the plant uptake of the AI.

The composition/structure of the polymer NC and the location of the AI might influence the degree of protection from photodegradation. Thus, a detailed characterization of NC structure and the location of the AI (inside, at the surface,…) are important to assess protection from radiation. The composition and probably structure of NFA and NFC differed from NFB. However, no significant differences in photodegradation rates could be observed, but this cannot be generalized. In literature hints on stronger protection of the AI within the NC structure were found.

Increasing the salt concentration by addition of PP fertilizer did not trigger an increased protective effect due to NC-association, as NFs did not degrade any slower than the AI/Com. Still, Clo degradation rates were much slower in fertilizer background than in aqueous background for all formulations and the AI, which was attributed to a shading effect. Hence, the presence of inorganic ions, which are omnipresent in natural waters, can decrease the photodegradation rates of Clo. For an application as foliar spray, combining Clo insecticide formulations with liquid fertilizer would probably increase persistence of Clo on the plant surfaces (due to shading) and increase the risk of residues in food produce. The evaporation of water from the spray droplet might even allow for precipitation of the AI and salts on the plant surface and further enhance persistency, at least in dry periods.

Unexpected was the increased photodegradation rate of NFA and NFC, as compared to the other formulations and the AI, in the presence of PP fertilizer, which was attributed to their similar composition. Recalling that those formulations by tendency displayed the lowest k values in aqueous background, underpins that formulation influences can only be assessed, considering interactions with compounds present in the environment. Still concerning the present formulations, the influence of formulation type on photodegradation rate was rather low and negligible when compared to the influence of fertilizer shading in the foliar spray application scenario. Nevertheless, with polymer-based NFs that exhibit a stronger AI-NC association, the situation could be different.

## 5.3. Sorption to Soil

Sorption to soil was much higher in the more sorptive loamy soil than in sand, irrespective of the used method, background solution or formulation and seemed to be dominated by organic matter content. The overarching soil effect indicates that, for purposes of fate assessment, it is most important to test a broad variety of soil types. However, from a mechanistic point of view, also method, background solution and formulation are interesting, as they significantly influenced $K_d$ values.

In the centM evolution of $K_d$ with time could be assessed. For sand-$H_2O$, sand-PP and loam-PP an increased sorption with time was observed and attributed to diffusion into less accessible sorption sites together with physical trapping and increased sorption strength with time. With loam in $H_2O$-background temporal behavior was the opposite: extraction efficiency (and for some formulations solution concentrations) increased with time. The reason for this was hypothesized to be an initial fast diffusion of spiking solution into the loam aggregates due to pre-equilibration with deionized water, followed by a slow back-out diffusion to equilibrate with aggregates non-directly hit by spiking droplets. Under field conditions aggregates would not be pre-equilibrated with deionized water, thus an increase of sorption with time seems likely to be the rule. To rule out any diffusion gradient, the study could be repeated with tap water, ionic solution or an increased pre-equilibration time.

Concerning background solution, in loam stronger sorption occurred with PP-background, whereas in sand the opposite was true. This was probably due to different qualities of organic matter in the different soils. Sand seemed to contain higher fractions of fulvic and humic acids, which were strongly solubilized by monovalent $NH_4^+$ in PP-background, increasing cClo in solution. Organic matter in loam seemed to be dominated by humins which were insoluble in both background solutions but probably became more accessible for sorption in PP-background due to soil aggregate dispersion by $NH_4^+$. The observed effects on $K_d$ confirmed the association of Clo with organic matter and indicate that there is a certain risk of dissolution of humics by ammonium fertilizers, which would co-mobilize associated Clo. On the other hand, in aggregated soils dominated by higher molecular weight organic matter, PP fertilizer could promote retention of Clo. However, for an evaluation of in-furrow application of Clo insecticides with/without fertilizer, this conclusion would be too simplistic, since aggregate destabilization (as in loam) might allow for colloidal transport of organics in soil pores, and dilution of PP fertilizer by soil/rain water could decrease the mobilization of humic/fulvic acids that was observed in sand. Also mobilized humics may be immobilized in deeper layers. Again, more realistic experiments would be necessary.

Comparing the methods used to test sorption showed that $K_d$ values in sand were higher with the batchM, but in loam they were higher with the centM, with the absolute $K_d$ difference between the methods being smaller for sand than for loam. However, when basing the method comparison on percentages adsorbed, rather than on $K_d$, sorption was stronger in the centM for both soils in both background solutions. An explanation for this discrepancy with regards to sand could be an inexactness arising in the centM due to slightly varying extraction efficiencies and corrections for filter prewetting, to which the formulas of $K_d$ and percentage adsorbed react with different sensibility. A higher sorption in the batchM might be explained by a more thorough equilibration due to shaking, while a higher sorption in the centM, especially in a structured aggregated soil like loam, is most likely explained by a quick uptake of spiking solution into unsaturated aggregates and physical protection of the AI within aggregates and zones of immobile water. Other less likely explanations include precipitation of the AI because of local exceedance of Clo solubility and a possible underestimation of $K_d$ in loam with the batchM due to Clo-association with colloidal fractions, being measured as “in solution”.

Considering the percentages adsorbed, sorption was higher in the centM in all cases. Since the centM reflects moisture conditions which are more close to field conditions, one can conclude that the classical batchM underestimates retention of Clo as compared to field conditions. The reason for this is probably that Clo is a rather weak sorbing substance and in the centM also physical retention, like diffusion into non-mobile water, is interpreted as adsorption, not only “real” adsorption. However, considering $K_d$ values would suggest that sorption is slightly overestimated by the batchM in sand, at least shortly after pesticide application, as sorption in the centM increased with time.

Regarding formulation effects, no generally valid nano-effect could be shown during the sorption experiments. In aqueous background, the AI was probably immediately released and also in PP-background no salting-out induced nano-effect could be established, not even with the centM, which tested very high Clo and salt concentrations. Still, ANOVA indicated a significant influence of formulation under (assumed) equilibrium conditions. This could have partly been simple formulation effects (due to introduction of surfactants and polymers into the system), but there were also some significant nano-effects for single NFs in the batchM, e.g. in loam ($H_2O$- and PP-background) NFB sorbed stronger than Com and the AI. NFC was the only formulation exhibiting a nano-effect (stronger sorption than Com) in all soil-background-solution combinations and it also sorbed stronger than the AI in both soils with aqueous background. This was in line with NFC belonging to the most protective formulations during photodegradation experiments and showing the highest aggregation of all the NFs. Together those hints indicate that in NFC a small fraction of the AI stays associated with the NC, e.g. due to physical capturing within aggregates. As all natural soil solutions and waters usually contain loads of ions, aggregation might be a major mechanism in slowing down release and enhancing retention of polymer-based NFs.

A comparison of the methods did not show any consistencies of formulation differences and, other than assumed, the centM exhibited less power to discover formulation effects: After 7 days no significant difference was found between the NFs and Com and the sometimes higher sorption of the AI could be attributed to higher spiking solution amounts and thus better mixing.

Based on the present results, it seems that the batchM had more power to show formulation influences, as it yielded at least some significant differences. It might be that with the present pesticide products the impact of formulation was rather low and additionally masked by other effects in the rather concentrated system of the centM, e.g. by dissolution of soil humics due to PP fertilizer or by physical non-equilibrium in structured soil samples. In the rather dilute system of the batchM, such effects were less powerful and thus some formulation effects remained visible. However, literature revealed that for slow-release formulations, pronounced nano-effects can be demonstrated with both methods. Since the centM reflects more realistic conditions, one can conclude that for the present NFs, under field conditions, formulation influences would be irrelevant as compared to other effects.

The observed interaction between soil formulation and background solution in loam-$H_2O$ at day one in the centM, on the other hand, indicates that the centM might be a nice tool to test time dependent sorption dynamics under realistic conditions, e.g. of slow-release formulations with more frequent sampling intervals.

## 5.4. Future Research Perspectives

Summing up, from the present study, no overarching effect of the present nanoformulations on the environmental sorption or photodegradation behavior of Clo could be deduced, when the products are used on crops at maximum recommended concentrations. The observed differences are small and remain irrelevant compared to other influencing factors in the environment (e.g. soil type or fertilizer impacts). However, this study found some evidence and hints, that polymer-based NFs in general have the potential to influence both sorption and photodegradation when the AI stays associated with the NC for a while.

Concerning photodegradation, further investigations should comprise nanoformulations showing a distinct slow release behavior. With such formulations, photodegradation under more realistic conditions could be studied. It would be for example interesting to do photodegradation studies on plant surfaces to include effects of AI plant-uptake modifications by the polymer nanocarrier or by the presence of fertilizer ions, as well as effects of $H_2O$ evaporation from spray droplets and thus higher AI concentrations on the leaf surfaces.

Furthermore, photodegradation could be studied on soil surfaces imitating alternating sunny and rainy conditions to see whether a slow-release NF has enough photoprotective capacity to increase the amount of AI transported to the dark layers below.

Regarding sorption to soils, further investigations should also be mainly focused on slow-release formulations, to enhance the chance of detecting real nano-effects.

The present study indicates that a batchM approach might be too simplistic and does not properly reflect processes occurring in well-structured soils with rather low moisture contents as usually found in the field. Even though complex interactions between soil physical properties, type of humic substances and introduction of fertilizer salts seemed to be more realistic when using the centM, there are still larger scale processes which should be accounted for. For example the risk of leaching to groundwater due to co-mobilization of humic substances and nanopesticides by fertilizer addition or transport of nanopesticides with organic colloids due to aggregate destabilization upon fertilizer addition could be investigated. To elucidate such processes, slow-release NFs and their transport/relocation behavior could be studied in soil columns or lysimeters, with pulses of fertilizer addition or “rain events”.

The centM could be further refined to investigate sorption dynamics of slow-release formulations over time, e.g. by increasing the sampling frequency. However, one should think about a different approach to determine initial concentrations for $K_d$ calculations, since AcN extraction efficiency also varied with time, impacting on $K_d$ results. One possibility would be e.g. to sterilize the soil to preclude any occurrence of biodegradation and then use measured concentrations and added amounts of spiking solutions to calculate initial concentrations. As another source of error, filter pre-wetting should be avoided, while maintaining a sufficient soil-solution yield. Possible remedies would be to increase the soil amount centrifuged or the soil water content. And especially for highly structured soils like loam a longer period of pre-equilibration with background solution might be advisable, to rule out any diffusion gradients.

In general, it is hard to draw universal conclusions regarding the impact of polymer-based NFs on environmental fate processes, due to the high diversity of nanocarriers, Thus, more comparative studies on the effects of composition, structure and surface-chemical properties of the NC on the fate of the AI would be desirable, especially for slow-release formulations. For example aggregation might be a major mechanism in slowing down release due to the omnipresence of ions in the environment: Studies with slow-release formulations exhibiting different aggregation behavior could be conducted.

And finally, the environmental risk emerging from polymer nanocarriers themselves should not be ignored. Even though it might be sufficient for pesticide risk assessment of fast-release formulations to study the fate of the AI, a regular application of nano-sized polymers to soils via plant protection products might cause additional problems arising with time.

# vii. Literature Cited

Ahmed, M.M. et al., 2014. Solar photo-Fenton using peroxymonosulfate for organic micropollutants removal from domestic wastewater: Comparison with heterogeneous TiO2 photocatalysis. *Chemosphere*, 117(1), pp.256–261.

APVMA, 2009. Trade Advice Note on Clothianidin in the product Sumitomo Samurai Systemic Insecticide. Available at: www.apvma.gov.au/sites/default/files/publication/13161-tan-clothianidin.pdf [Accessed March 17, 2016].

ATSDR, 1997. Public Health Statement for Propylene Glycol. , pp.55–57. Available at: www.atsdr.cdc.gov/toxprofiles/tp189-c1-b.pdf [Accessed May 12, 2016].

Beigel, C., Barriuso, E. & Calvet, R., 1998. Sorption of low levels of nonionic and anionic surfactants on soil: Effects on sorption of triticonazole fungicide. *Pesticide Science*, 54(1), pp.52–60.

Bergstrom, K. & Strandberg, C., 2014. Agrochemical compositions containing naphthalene sulfonate derivatives and nitrogen-containing surfactants. Available at: www.google.ch/patents/US8629085.

Bhattacharjee, S., 2016. DLS and zeta potential – What they are and what they are not? *Journal of Controlled Release*, 235, pp.337–351.

Bindhu, V.. R., Ganga, S. & Dayanandan, S., 2016. Effect of Plant Formulations on Larvae and Adults of Callosobruchus Chinensis. *The Journal of Community Health Management*, 3(1), pp.16–18.

Buck, R.P., Singhadeja, S. & Rogers, L.B., 1954. Ultraviolet Absorption Spectra of Some Inorganic Ions In Aqueous Solutions. *Analytical Chemistry*, 26(7), pp.1240–1242.

Cao, Y. et al., 2005. HPLC/UV analysis of chlorfenapyr residues in cabbage and soil to study the dynamics of different formulations. *Science of the Total Environment*, 350(1), pp.38–46.

Chemtrade International, 2007. Material Safety Data Sheet Sodium Naphthalene Sulfonate Formaldehyde. Available at: www.trade-chem.com/products/MSDS/msds_snf.pdf [Accessed August 12, 2016].

Chern, C.S., 2006. Emulsion polymerization mechanisms and kinetics. *Progress in Polymer Science*, 31(5), pp.443–486.

Ciou, C.T., 2002. *Partition and Adsorption of Organic Contaminants in Environmental Systems*, Hoboken: John Wiley and Sons.

Delle Site, A., 2001. Factors Affecting Sorption of Organic Compounds in Natural Sorbent/Water Systems and Sorption Coefficients for Selected Pollutants. A Review. *Journal of Physical and Chemical Reference Data*, 30(1), pp.187–439.

Deng, Y. et al., 2016. Hollow lignin azo colloids encapsulated avermectin with high anti-photolysis and controlled release performance. *Industrial Crops and Products*, 87, pp.191–197.

EC, 2016a. Definiton of a nanomaterial. Available at: www.ec.europa.eu/environment/chemicals/nanotech/faq/definition_en.htm [Accessed August 31, 2016].

EC, 2016b. Pesticides. Available at: www.ec.europa.eu/food/plant/pesticides/index_en.htm [Accessed August 31, 2016].

EC-SANCO, 2005. Review report for the active substance clothianidin. Available at: www.furs.si/law/EU/ffs/eng/annexI/direktive/RR/clothianidin.doc [Accessed September 4, 2015].

EWG, 2016. Sodium Methyl Oleyl Taurate. Available at: www.ewg.org/skindeep/ingredient/706124/SODIUM_METHYL_OLEYL_TAURATE/ [Accessed August 12, 2016].

FAO, 2015. FAO Specifications and Evaluations for Clothianidin. Available at: www.fao.org/fileadmin/templates/agphome/documents/Pests_Pesticides/Specs/Clothianidin_2015_01.pdf [Accessed July 20, 2016].

FAO and WHO, 2012. Emamectin Benzoate. *Pesticide Residues in Food - JMPR Evaluations 2011: Part I Residues*, pp.231–404. Available at: www.fao.org/fileadmin/templates/agphome/documents/Pests_Pesticides/JMPR/Evaluation11/Emamectin.pdf [Accessed September 5, 2016].

Fish, J.D. et al., 2001. Planting Apparatus with Improved Liquid Pesticide Delivery Device and Related Method for Delivering Liquid Pesticide. Available at: www.google.com/patents/US6289829.

Gamerdinger, A.P. & Kaplan, D.I., 2000. Application of a continuous-flow centrifugation method for solute transport in disturbed, unsaturated sediments and illustration of mobile-immobile water. *Water Resources Research*, 36(7), pp.1747–1755.

Gong, Y. et al., 2012. Separation and Identification of Photolysis Products of Clothianidin by Ultra-Performance Liquid Tandem Mass Spectrometry. *Analytical Letters*, 45(17), pp.2483–2492.

Gooddy, D.C. et al., 2007. The significance of colloids in the transport of pesticides through Chalk. *Science of the Total Environment*, 385(1), pp.262–271.

GraphPad Software Inc., 2014a. GraphPad Curve Fitting Guide. *GraphPad*. Available at: http://cdn.graphpad.com/docs/prism/6/Prism-6-Curve-Fitting-Guide.pdf [Accessed June 7, 2016].

GraphPad Software Inc., 2016. GraphPad Prism 6.

GraphPad Software Inc., 2014b. GraphPad Statistics Guide. Available at: http://cdn.graphpad.com/docs/prism/6/Prism-6-Statistics-Guide.pdf [Accessed June 7, 2016].

Guan, H. et al., 2010. Dynamics of residues from a novel nano-imidacloprid formulation in soyabean fields. *Crop Protection*, 29(9), pp.942–946.

Harvard University, 2007. A Summary of Error Propagation. Available at: http://ipl.physics.harvard.edu/wp-uploads/2013/03/PS3_Error_Propagation_sp13.pdf [Accessed June 15, 2016].

Hechenbichler GmbH, 2012. Label: POWERPHOS liquid fertilizer. Available at: www.kroni.ch/pdfs/Sicherheitsdatenblatt Powerphos1411539861.pdf.

Hergert, G.W. et al., 2012. Using Starter Fertilizers for Corn, Grain Sorghum, and Soybeans. *NebGuide*, (G361). Available at: http://extensionpublications.unl.edu/assets/pdf/g361.pdf.

Hessler, D.P., Gorenflo, V. & Frimmel, F.H., 1993. Degradation of Aqueous Atrazine and Metazachlor Solutions by UV and UV/H2O2 - Influence of pH and Herbicide Concentration. *Acta Hydrochimica et Hydrobiologica*, 21(4), pp.209–214.

Hofmann, T. & von der Kammer, F., 2009. Estimating the relevance of engineered carbonaceous nanoparticle facilitated transport of hydrophobic organic contaminants in porous media. *Environmental Pollution*, 157(4), pp.1117–1126.

Hofmann, T. & Wendelborn, A., 2007. Colloid facilitated transport of polychlorinated dibenzo-p-dioxins and dibenzofurans (PCDD/Fs) to the groundwater at Ma Da area, Vietnam. *Environmental Science and Pollution Research*, 14(4), pp.223–224.

Huang, Q. et al., 2006. Photolysis Behavior of Herbicide Propisochlor in Water Media and Preliminary Analysis of Photoproducts Under Different Light Sources. *Journal of Environmental Science and Health, Part B*, 41(3), pp.253–267.

Innospec, 2015. Taurates. Available at: www.innospecinc.com/our-markets/performance-chemicals/personal-care/surfactants/taurates [Accessed August 12, 2016].

Ishiguro, M. & Koopal, L.K., 2016. Surfactant adsorption to soil components and soils. *Advances in Colloid and Interface Science*, 231, pp.59–102.

ISO 11268-2, 2012. Soil quality - Effects of pollutants on earthworms - Part 2: Determination of effects on reproduction of Eisenia fetida/Eisenia andrei.

de Jonge, H. & Wollesen de Jonge, L., 1999. Influence of pH and solution composition on the sorption of glyphosate and prochloraz to a sandy loam soil. *Chemosphere*, 39(5), pp.753–763.

Kah, M. et al., 2014. Analysing the fate of nanopesticides in soil and the applicability of regulatory protocols using a polymer-based nanoformulation of atrazine. *Environmental Science and Pollution Research*, 21(20), pp.11699–11707.

Kah, M. et al., 2013. Nanopesticides: State of Knowledge, Environmental Fate, and Exposure Modeling. *Critical Reviews in Environmental Science and Technology*, 43(16), pp.1823–1867.

Kah, M. & Brown, C.D., 2007. Changes in pesticide adsorption with time at high soil to solution ratios. *Chemosphere*, 68(7), pp.1335–1343.

Kah, M. & Hofmann, T., 2014. Nanopesticide research: Current trends and future priorities. *Environment*

*International*, 63, pp.224–235.

Kahn, S.U., 1980. *Pesticides in the Soil Environment*, Amsterdam: Elsevier.

Kang, M.A. et al., 2012. Insecticidal activity and feeding behavior of the green peach aphid, Myzus persicae, after treatment with nano types of pyrifluquinazon. *Journal of Asia-Pacific Entomology*, 15(4), pp.533–541.

Kao Corp., 2016. Polymeric Surfactants. Available at: http://chemical.kao.com/tw/products/chemicalname/c030713.html [Accessed August 17, 2016].

Kookana, R.S. et al., 2014. Nanopesticides: Guiding principles for regulatory evaluation of environmental risks. *Journal of Agricultural and Food Chemistry*, 62(19), pp.4227–4240.

Kretzschmar, R. et al., 1999. Mobile Subsurface Colloids and Their Role in Contaminant Transport. *Advances in Agronomy*, 66, pp.121–193.

L.V. Lomas, 2014. Agricultural Markets - Solutions that bring a field of possibilities. Available at: www.lvlomas.com/pdf/LVL895-Line_Card-Natural_Resources-Agricultural_Markets-August_2014.pdf [Accessed August 12, 2016].

Lagaly, G. & Ziesmer, S., 2003. Colloid chemistry of clay minerals: The coagulation of montmorillonite dispersions. *Advances in Colloid and Interface Science*, 100-102, pp.105–128.

Li, K. et al., 2014. Concentration-dependent photodegradation kinetics and hydroxyl-radical oxidation of phenicol antibiotics. *Chemosphere*, 111, pp.278–282.

Liu, Y., Zhang, Y. & Wang, J., 2014. Mesocrystals as a Class of Multifunctional Materials. *CrystEngComm*, 16(27), pp.5948–5967.

LS Instruments, 2016. Dynamic Light Scattering: Measuring the Particle Size Distribution. Available at: www.lsinstruments.ch/technology/dynamic_light_scattering_dls/ [Accessed August 31, 2016].

LWK Nordrhein-Westfalen, 2015. Bestandesdichte und Reihenabstände. Available at: www.landwirtschaftskammer.de/landwirtschaft/ackerbau/mais/bestandsdichte-pdf.pdf [Accessed June 7, 2015].

Mateus, M.C.D.A., Da Silva, A.M. & Burrows, H.D., 2000. Kinetics of photodegradation of the fungicide fenarimol in natural waters and in various salt solutions: Salinity effects and mechanistic considerations. *Water Research*, 34(4), pp.1119–1126.

McNeil-Watson, F., 2013. Electrophoretic Light Scattering. In G. C. K. Roberts, ed. *Encyclopedia of Biophysics*. Heidelberg: Springer, pp. 648–654.

Meunier, F. & Elaissari, A., 2003. Poly(N-nisopropylacrylamide)-Based Particles - Preparation and Colloidal Characterization. In A. Elaissari, ed. *Colloidal Polymers: Synthesis and Characterization*. New York, Basel: Marcel Dekker.

Mulligan, R.A. et al., 2016. Photodegradation of clothianidin under simulated California rice field conditions. *Pest. Manag. Sci.*, 72(7), pp.1322–1327.

Mulligan, R.A., Parikh, S.J. & Tjeerdema, R.S., 2015. Abiotic partitioning of clothianidin under simulated rice field conditions. *Pest Management Science*, 71(10), pp.1419–1424.

NanoComposix, 2015. NanoComposix’s Guide to Dynamic Light Scattering Measurement and Analysis. Available at: http://50.87.149.212/sites/default/files/nanoComposix Guidelines for DLS Measurements and Analysis.pdf [Accessed September 5, 2016].

Nayak, S.R., 2015. *UV induced photolysis of fructose: Generation of reactive oxygen species and their application in photo-degradation of pesticides*. Drexel University.

OECD, 2002. OECD Guidelines for the Testing of Chemicals - Proposal For a New Guideline: Phototransformation of Chemicals in Soil Surface. Available at: www.oecd.org/chemicalsafety/testing/2741541.pdf [Accessed August 23, 2016].

OECD, 2008. OECD Guidelines for the Testing of Chemicals Nr. 316: Phototransformation of Chemicals in Water - Direct Photolysis.

OECD, 2000. OECD Guidline for the Testing of Chemicals Nr. 106: Adsorption - Desorption Using a Batch Equilibrium Method.

Von Oepen, B., Kördel, W. & Klein, W., 1991. Sorption of Nonpolar and Polar Compounds to Soils: Processes, Measurements and Experience with the Applicability of the Modified OECD-Guideline 106. *Chemosphere*, 22(3-4), pp.285 – 304.

Pettit, R.E., 2008. Organic Matter, Humus, Humate, Humic Acid, Fulvic Acid and Humin: Their Importance in Soil Fertility and Plant Health. Available at: www.humates.com/pdf/ORGANICMATTERPettit.pdf [Accessed August 8, 2016].

Piccolo, A. & Mbagwu, J.S.C., 1989. Effects of Humic Substances and Surfactants on the Stability of Soil Aggregates. *Soil Science*, 147(1), pp.47–54.

Pignatello, J.J. & Xing, B., 1996. Mechanisms of slow sorption of organic chemicals to natural particles. *Environmental Science and Technology*, 30(1), pp.1–11.

Ping, L. et al., 2010. Imidacloprid adsorption by soils treated with humic substances under different pH and temperature conditions. *African Journal of Biotechnology*, 9(13), pp.1935–1940.

Quivet, E. et al., 2006. Influence of metal salts on the photodegradation of imazapyr, an imidazolinone pesticide. *Pest Management Science*, 62(5), pp.407–413.

Rao, P.-H. et al., 2006. Effect of an Anionic Surfactant on Hydraulic Conductivities of Sodium- and Calcium-Saturated Soils. *Pedosphere*, 16(5), pp.673–680.

Riyajan, S.A. & Sakdapipanich, J.T., 2009. Encapsulated neem extract containing Azadiractin-A within hydrolyzed poly(vinyl acetate) for controlling its release and photodegradation stability. *Chemical Engineering Journal*, 152(2), pp.591–597.

Röttgers, R. et al., 2010. Pure water spectral absorption, scattering, and real part of refractive index model. Available at: www.brockmann-consult.de/beam-wiki/download/attachments/17563679/ATBD_waterradiance_watermodel_v2.pdf [Accessed April 12, 2016].

Rutesh, D.H., 2008. Overview of pharmaceutical excipients used in tablets and capsules. *Drug Topics*. Available at: www.drugtopics.modernmedicine.com/drug-topics/news/modernmedicine/modern-medicine-news/overview-pharmaceutical-excipients-used-tablets [Accessed August 12, 2016].

Sánchez-Camazano, M. et al., 1995. Effect of Different Surfactants on the Mobility of Selected Nonionic Pesticides in Soil. *Chemosphere*, 31(8), pp.3793–3801.

dos Santos Silva, M. et al., 2011. Paraquat-loaded alginate/chitosan nanoparticles: Preparation, characterization and soil sorption studies. *Journal of Hazardous Materials*, 190(1), pp.366–374.

Shang, Q. et al., 2013. Pesticide-conjugated polyacrylate nanoparticles: Novel opportunities for improving the photostability of emamectin benzoate. *Polymers for Advanced Technologies*, 24(2), pp.137–143.

Shaw, R., 2013. Dynamic Light Scattering Training - Achieving reliable nano particle sizing. Available at: http://149.171.168.221/partcat/wp-content/uploads/Malvern-Zetasizer-LS.pdf [Accessed October 3, 2016].

Shu, Z. et al., 2013. Photodegradation of emerging micropollutants using the medium-pressure UV/H2O2 Advanced Oxidation Process. *Water Research*, 47(8), pp.2881–2889.

Shulgin, A., 2013. Method of Preparing a Humic Acid Extraction. Available at: www.google.com/patents/US8580979.

Stevenson, F.J., 1982. *Humus Chemistry. Genesis, Composition, Reactions* 2nd ed., New York, Toronto: John Wiley and Sons.

Talevi, A., Gantner, M.E. & Ruiz, M.E., 2014. Applications of Nanosystems to Anticancer Drug Therapy (Part I . Nanogels, Nanospheres, Nanocapsules). *Recent Patents on Anti-Cancer Drug Discovery*, 9(1), pp.83–98.

Tjeerdema, R.S. et al., 2014. Annual Report Comprehensive Research on Rice - The environmental Fate of Pesticides Important to Rice Culture. Available at: www.carrb.com/14rpt/2014 Tjeerdema RP-5.pdf [Accessed July 21, 2016].

Uneme, H., 2011. Chemistry of clothianidin and related compounds. *Journal of Agricultural and Food Chemistry*, 59(7), pp.2932–2937.

University of Hertfordshire, 2016. Clothianidin. *IUPAC Pesticide Properties Database*. Available at: http://sitem.herts.ac.uk/aeru/iupac/Reports/409.htm [Accessed August 1, 2016].

US-EPA, 2016. Basic Information about Pesticide Ingredients. Available at: www.epa.gov/ingredients-used-pesticide-products/basic-information-about-pesticide-ingredients [Accessed August 31, 2016].

US-EPA, 2005. EFED Registration Chapter for Clothianidin for use on Potatoes and Grapes as a spray treatment and as a Seed Treatment for Sorghum and Cotton. Available at: www3.epa.gov/pesticides/chem_search/cleared_reviews/csr_PC-044309_28-Sep-05_a.pdf [Accessed April 12, 2016].

Valent USA Corp., 2014. Label: Belay Insecticide. Available at: www.valent.com/Data/Labels/2014-BEL-0001 Belay - form 1681-G.pdf.

Visek, K.E., 1990. Fatty Acid Amide Surfactants. In J. M. Richmond, ed. *Cationic Surfactants: Organic Chemistry*. New York: Marcel Dekker, pp. 2–50.

Walker, A., 2000a. A simple centrifugation technique for the extraction of soil solution to permit direct measurement of aqueous phase concentrations of pesticide. In J. Cornejo & P. Jamet, eds. *pesticide/soil interactions - some current research methods*. Paris: INRA, pp. 173–178.

Walker, A., 2000b. Soil structure and the adsorption and degradation of pesticides. Available at: http://randd.defra.gov.uk/Document.aspx?Document=PL0521_1526_FRP.pdf [Accessed July 15, 2016].

Walker, A. & Jurado-Exposito, M., 1998. Adsorption of isoproturon, diuron and metsulfuron-methyl in two soils at high soil:solution ratios. *Weed Research*, 38(3), pp.229–238.

Wang, P. & Keller, A.A., 2009. Partitioning of hydrophobic pesticides within a soil-water-anionic surfactant system. *Water Research*, 43(3), pp.706–714.

Ware, G.W., 1994. *The Pesticide Book* 4th ed., Fresno: Thomson Publications.

Washington State University, 2004. Cation-Exchange Capacity (CEC). Available at: http://soils.tfrec.wsu.edu/webnutritiongood/soilprops/04CEC.htm [Accessed August 25, 2016].

Weng, L.P., Van Riemsdijk, W.H. & Hiemstra, T., 2007. Adsorption of humic acids onto goethite: Effects of molar mass, pH and ionic strength. *Journal of Colloid and Interface Science*, 314(1), pp.107–118.

Wijayaratne, R.D. & Means, J.C., 1984. Affinity of Hydrophobic Pollutants for Natural Estuarine Colloids in Aquatic Environments. *Environmental Science and Technology*, 18(2), pp.121–123.

Wozniak, B. & Dera, J., 2007. Light Absorption by Water Molecules and Inorganic Substances Dissolved in Sea Water. In *Light Absorption in Sea Water*. New York: Springer, pp. 11–81.

Yang, D. et al., 2014. Synthesis and Characterization of a Molecularly Imprinted Polymer for Preconcentration of Clothianidin in Environmental Samples. *Analytical Letters*, 47(15), pp.2613–2627.

Yazgan, M.S. et al., 2005. Comparison of two methods for estimation of soil sorption for imidacloprid and carbofuran. *Chemosphere*, 60(9), pp.1325–1331.

Zabar, R. et al., 2012. Photocatalytic degradation with immobilised TiO2 of three selected neonicotinoid insecticides: Imidacloprid, thiamethoxam and clothianidin. *Chemosphere*, 89(3), pp.293–301.

Zaiontz, C., 2016. Real Statistics Using Excel. Available at: www.real-statistics.com/two-way-anova/anova-more-than-two-factors/ [Accessed July 17, 2016].

Zhejiang NetSun Co. Ltd., Sodium Naphthalene Sulfonate Formaldehyde Condensate. Available at: www.chemnet.com/chinasuppliers/38129/sodium-naphthalene-sulfonate-formaldehyde-condensate--1628098.html [Accessed August 16, 1990].

Zheng, H. & Ye, C., 2001. Photodegradation of acetochlor and butachlor in waters containing humic acid and inorganic ion. *Bulletin of Environmental Contamination and Toxicology*, 67(4), pp.601–608.

# viii. Annex

# List of Annex

A. Handling of Clothianidin and Nanoformulations ... i
B. HPLC Method Validation ... iv
C. Photodegradation ... viii
D. Batch Method ... x
E. Centrifugation Method ... xii
F. Zusammenfassung ... xv

# List of Tables

Table 1. Linear regression parameters of the calibration curves (±SD) ... iv
Table 2. Deviation of back-calculated cClo from nominal cClo in calibration standards (±SD) ... v
Table 3. Accuracy and precision data for HPLC method validation (±SD) ... v

# List of Figures

Figure 1. Clo stability in $H_2O$ stored in the dark at 4°C ... i
Figure 2. Clo photodegradation test under natural sunlight conditions (windowsill) ... ii
Figure 3. Testing AI losses to different tube materials ... ii
Figure 4. Testing Clo losses of all formulations to different tube materials ... iii
Figure 5. HPLC method calibration curves for quantification of Clo ... iv
Figure 6. Clo stability in AcN stored in the dark at 4°C ... vi
Figure 7. Loam AcN extract: background peak merged with Clo peak (10 min gradient 0-100 % AcN) ... vi
Figure 8. Loam AcN extract: background peak separated from Clo peak (7 min gradient 0-100 % AcN) ... vii
Figure 9. Blank sand AcN extract background peak at retention time 5.5 min (7 min gradient 0-100 % AcN) ... vii
Figure 10. Photodegradation pretest: exponential decay of AI at two concentration levels ... viii
Figure 11. Photodegradation Pretest: formation of degradation products at cClo 6.08 mg/L ... ix
Figure 12. Photolysis rate (k) at cClo ~544 mg/L with and without phosphate buffer ... ix
Figure 13. Setting soil:solution ratio with estimated $K_d$ and intended fraction adsorbed (A) (OECD 2000) ... x
Figure 14. Test on formation of cClo depth gradient due to centrifugation of NFC in $PP_{batch}$ ... xi
Figure 15. Pseudo second-order sorption kinetics of AI in PP-background in sand and loam ... xi
Figure 16. Composition of wet soil mass in centrifugation experiments with PP background solution ... xii

# A. Handling of Clothianidin and Nanoformulations

### Stability of Clo in $H_2O$

Since working solutions for all experimental setups were prepared as aqueous solutions, the stability of Clo in $H_2O$ was tested. Clo did not undergo hydrolysis when stored at 4°C in the dark over a period of 9 months (Figure 32). This confirmed prior findings (US-EPA 2005) and allowed storage and reuse of prepared solutions.

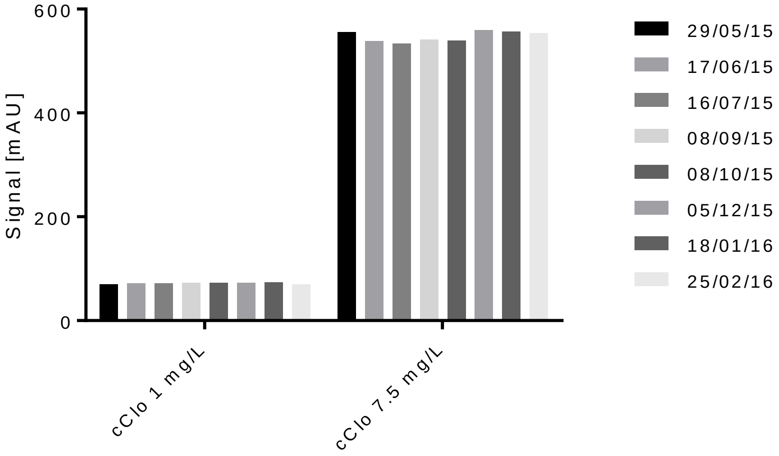

**Figure 32. Clo stability in $H_2O$ stored in the dark at 4°C**

### Risk of Photodegradation

Since Clo is photodegradable, the risk of degradation during handling in the laboratory was tested under “worst case” lab conditions: Transparent and amber vials were filled with Clo solutions at two concentration levels (1 mg/L and 7.5 mg/L) and put in a transparent rack. The samples were exposed to natural sunlight (on a sunny day in May) on the windowsill for 8 h. Every two hours, triplicates of amber and transparent vials were removed and put into the dark fridge. Triplicate controls were kept in the fridge, right from the start.

Linear regression (Figure 33) showed no significant decrease in transparent ($p = 0.15$) and amber ($p = 0.28$) glass vials at cClo 1 mg/L. At the higher concentrations the slope was significantly negative for both transparent ($p = 0.0078$) and amber glass ($p = 0.0149$), with a slightly steeper slope in transparent (-0.110±0.035) than amber glass (-0.050±0.018). The variability among replicates might be due to shading effects, since all samples were placed close together in a rack. The maximum loss was 6.9 % (in transparent glass at cClo 7.5 mg/L). Degradation under “work-bench” light conditions can be assumed to be much lower. Thus, losses during handling of Clo solutions were considered negligible.

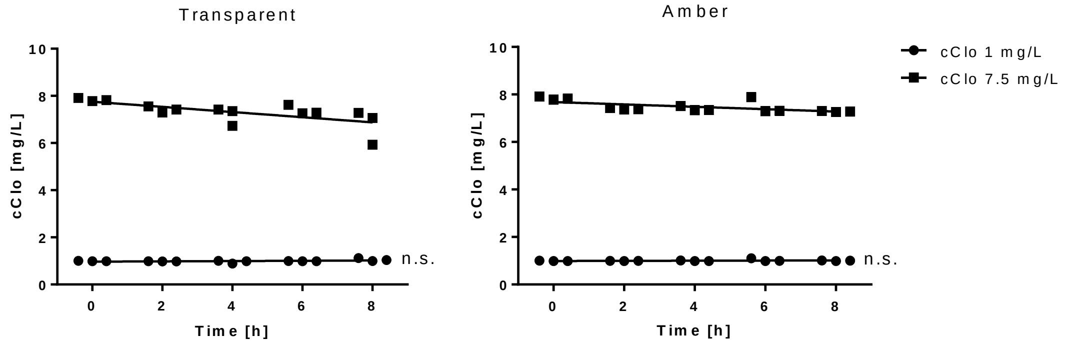

**Figure 33. Clo photodegradation test under natural sunlight conditions (windowsill)**

## Losses to Material Surfaces

Further tests were carried out to choose a tube-material that minimizes Clo losses due to adsorption. Materials tested included Teflon (PFTE) and polypropylene (PP) for the sorption batchM and PVDF tubes with an insert (PVDF+I) for the centM. Glass served as a reference material.

Two concentration levels (0.6 and 3 mg/L) of Clo in 0.01 M $CaCl_2$ solution (imitating soil solution) were used. Triplicates of PP, PFTE and glass tubes were filled with à 30 mL solution, and equilibrated on the side-to-side shaker in the dark for 2 h and 20 min.

In case of the PVDF+I tubes, the inserts of the tubes (à triplicates) were filled with à 20 mL of each solution-concentration, then centrifuged for 30 min like in the centM. Clo concentrations after equilibration were measured by HPLC.

Figure 34 shows no significant cClo difference of PTFE, PP and PVDF+I from glass at both concentration levels.

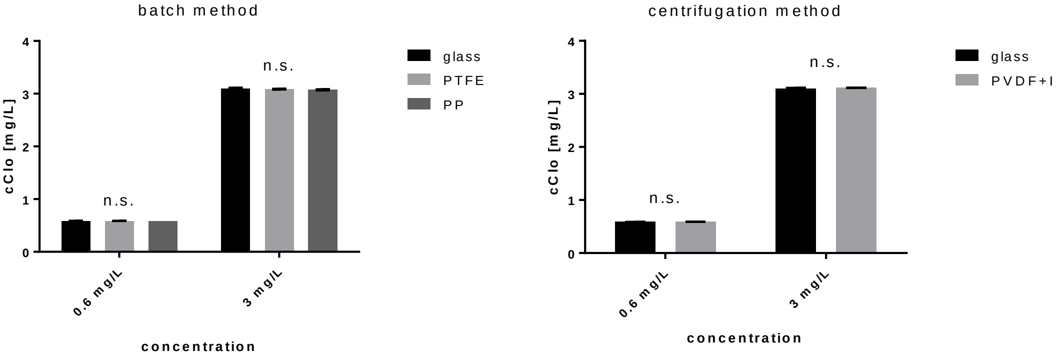

**Figure 34. Testing AI losses to different tube materials**

A similar test was performed with the different formulations to see whether polymer nanocarriers (NC) or other formulation ingredients enhance the risk of Clo losses to plastic tubes.

Working solutions of each formulation were prepared in $H_2O$ at two mass based concentration levels: 5 and 50 mg formulation $L^{-1}$ (≈ cClo 1 mg/L and 10 mg/L). Tubes of different materials were filled with à 20 mL (in duplicates) and agitated on the side-to-side shaker for 3 h. Clo concentration of the initial solution ($cClo_{initial}$) and after tube contact ($cClo_{eq}$) were determined by HPLC after 1:1 (V:V) extraction with AcN. Duplicate blanks confirmed the absence of Clo background. Recoveries were calculated according to Equation 1.

**10)**

$$recovery\ [\%] = \frac{cClo_{eq}}{cClo_{initial}} \times 100$$

$cClo_{eq}$.......concentration of Clo equilibrated with tube material
$cClo_{initial}$ ...concentration of Clo in initial solution

Recoveries ranged from 94 to 105 %, being perfectly within the acceptable range 90-110% (OECD 2000), and were at both concentrations not significantly different between the materials (Figure 35).

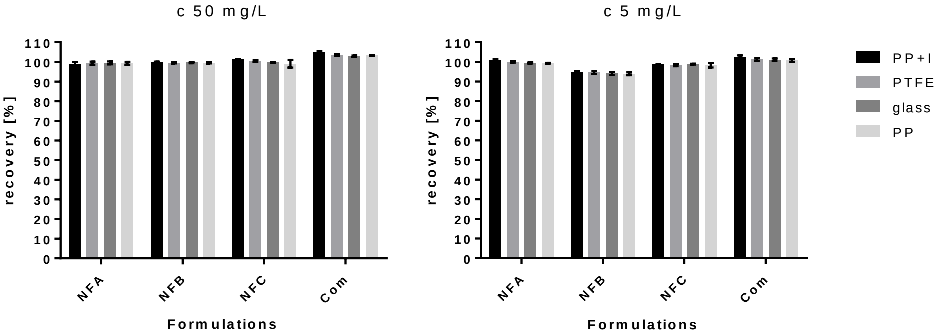

**Figure 35. Testing Clo losses of all formulations to different tube materials**

These tests confirm that losses to tubes are negligible and each material could be used. For the batchM PTFE tubes were chosen due to easier handling (no breakage).

# B. HPLC Method Validation

Three individual calibration curves were prepared, consisting of 6-9 standards in AcN at cClo ranging from 0.1-10 or 15 mg/L (Figure 36).

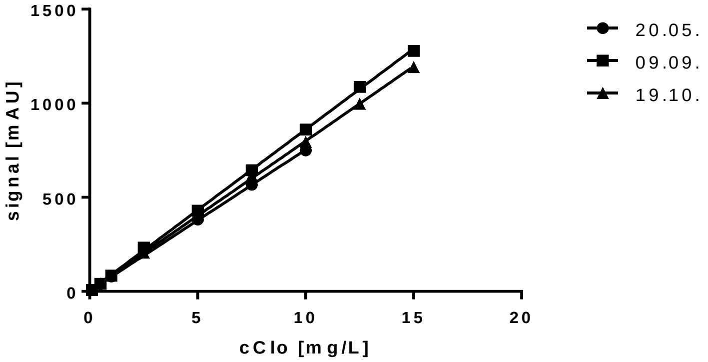

**Figure 36. HPLC method calibration curves for quantification of Clo**

Table 19 summarizes the regression parameters for the three prepared calibration curves (Figure 36). The limits of detection and quantification were calculated based on the signal-to-noise ratio (SN) according to Equations 2 and 3. The SN-ratio was determined by Agilent ChemStation relating the height of the peak to the noise, which is calculated as 6 × SD of the linear regression fit of a defined noise time range in the chromatogram (Agilent Technologies Inc. 2009).

**11)**

$$LOD\ [mg/L] = \frac{3 \times c_{peak}}{SN}$$

LOD.... limit of detection
$c_{peak}$ ..... concentration of Clo (of respective peak) [mg/L]
SN....... signal-to-noise ratio

**12)**

$$LOQ\ [mg/L] = \frac{10 \times c_{peak}}{SN}$$

LOQ.... limit of quantification
$c_{peak}$ ..... concentration of Clo (of respective peak) [mg/L]
SN....... signal-to-noise ratio

**Table 19. Linear regression parameters of the calibration curves (±SD)**

| intercept [mAU] | slope [mAU×L/mg] | $R^2$ | LOD [mg/L] | LOQ [mg/L] |
|---|---|---|---|---|
| 3.40±3.18 | 80.11±4.37 | 0.9998±0.0001 | 0.02±0.01 | 0.08±0.03 |

Blank runs following injections of high concentrations confirmed that there is no carry-over. Back-calculations of cClo with the calibration curves showed that deviations from the nominal cClo were < 9 % for all calibration standards except the lowest (0.1 mg/L) which deviated by 45 % (Table 20).

**Table 20. Deviation of back-calculated cClo from nominal cClo in calibration standards (±SD)**

| $cClo_{nominal}$ [mg/L] | $cClo_{back\ calc.}$ [mg/L] | deviation [%] |
|---|---|---|
| 0.1 | 0.06±0.01 | -44.94±12.40 |
| 0.5 | 0.46±0.02 | -8.71±4.26 |
| 1 | 0.98±0.05 | -1.68±4.60 |
| 2.5 | 2.60±0.10 | +4.17±4.20 |
| 5 | 5.03±0.02 | +0.56±0.41 |
| 7.5 | 7.58±0.08 | +1.02±1.05 |
| 10 | 9.96±0.02 | -0.45±0.15 |
| 12.5 | 12.52±0.04 | +0.19±0.31 |
| 15 | 14.94±0.02 | -0.39±0.11 |

Accuracy is the closeness of a determined value to the nominal value in percent (EMEA 2015). Within-run accuracy was determined in triplicates at four concentration levels. Replicates were prepared from separate stock solutions each. For between-run accuracy, duplicates of separately prepared stocks were measured on three different days.

Within- and between-run precision, defined as the closeness of repeated measures (EMEA 2015), were calculated as coefficients of variance, according to Equation 4, from the same data as accuracy. Results are summarized in Table 21.

**13)**

$$CV\ [\%] = \frac{SD}{mean} \times 100$$

CV ......... coefficient of variance
SD ......... standard deviation

**Table 21. Accuracy and precision data for HPLC method validation (±SD)**

| nominal cClo [mg/L] | accuracy | | precision | |
|---|---|---|---|---|
| | within-run [%] | betw.-run [%] | within-run CV [%] | betw.-run CV [%] |
| 0.1 | -44.78±2.48 | -31.98±16.8 | 4.49 | 24.70 |
| 0.5 | -0.47±8.56 | -5.65±8.95 | 0.09 | 9.49 |
| 5 | +10.62±9.79 | +3.30±12.62 | 8.85 | 12.22 |
| 10 | +7.53±10.25 | -1.15±12.31 | 9.53 | 12.46 |

For accuracy and back-calculated cClo values, deviation from the nominal concentrations should be max. 15 %, also the precision coefficient of variance should be ≤ 15 %. For the lowest concentration level (≤ 3 × LOQ) a deviation of 20 % is allowed (EMEA 2015).

Average deviations were all below 15 % except for concentration 0.1 mg/L. Since this concentration was quite below 3 × LOQ (0.08±0.03 × 3 = 0.24±0.09), it was probably out of the linear calibration range, which would explain the higher deviations. For cClo 0.5 mg/L, deviations were well below the 15 % limit.

Clo proved to be stable in AcN, when stored in the dark at 4°C (Figure 37) over a testing period of four months, which allowed storage and reuse of calibration standards.

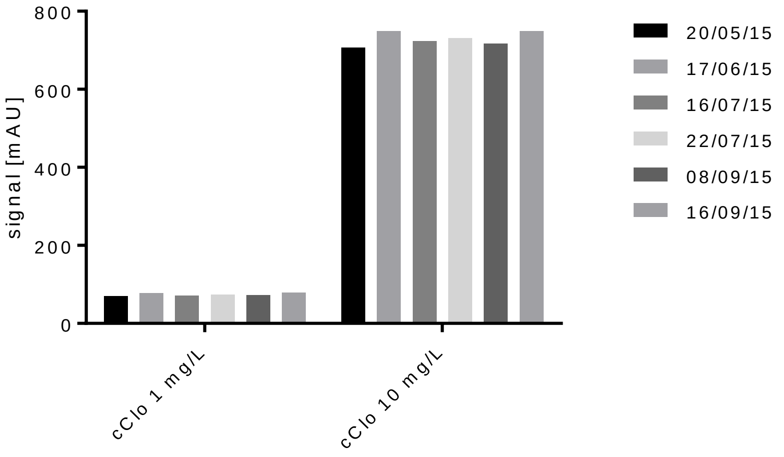

**Figure 37. Clo stability in AcN stored in the dark at 4°C**

The HPLC method was tuned to assure selectivity in all experimental matrices, e.g. aqueous and AcN soil extracts as used in the sorption experiments.

Aqueous soil extracts did not interfere: sand and loam were extracted 1:5 (w:w) with 0.01 M $CaCl_2$ and centrifuged. Subsamples of the supernatants and pure 0.01 M $CaCl_2$ were spiked with AI in AcN to reach final cClo of 0.6 and 3 mg/L (each in triplicates). The matrix effect – calculated by relating the HPLC signal in soil matrix to the signal in pure $CaCl_2$ (Equation 5) – was < 8.4 % in all cases; well below the threshold of 15 % (EMEA 2015).

**14)**

$$\text{matrix effect [\%]} = 100 - \frac{Clo_{matrix}}{Clo_{CaCl_2}} \times 100$$

$Clo_{matrix}$ peak area of Clo in soil matrix [mAU]
$Clo_{CaCl2}$ peak area of Clo in 0.1 M $CaCl_2$ [mAU]

However, AcN soil extracts of loam clearly interfered: À 15 g of air-dry soil were spiked with 3 mL of AI in 0.01 M $CaCl_2$ at cClo 3 and 1.5 mg/L, mixed carefully and incubated for 3 h in the dark at 4°C. Following a 1:1 extraction with AcN, chromatograms were checked for matrix interference. Triplicate blanks confirmed absence of Clo background and served as “pure matrix” baseline. In loam a background peak merged with the Clo peak (Figure 38).

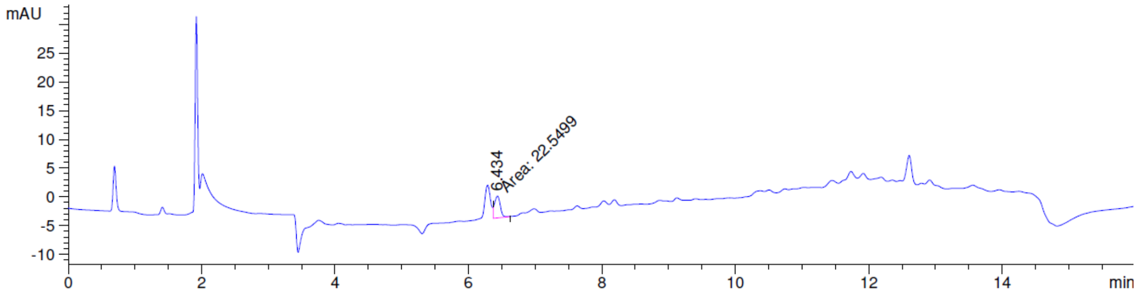

**Figure 38. Loam AcN extract: background peak merged with Clo peak (10 min gradient 0-100 % AcN)**

Varying the gradient allowed for peak separation (Figure 39).

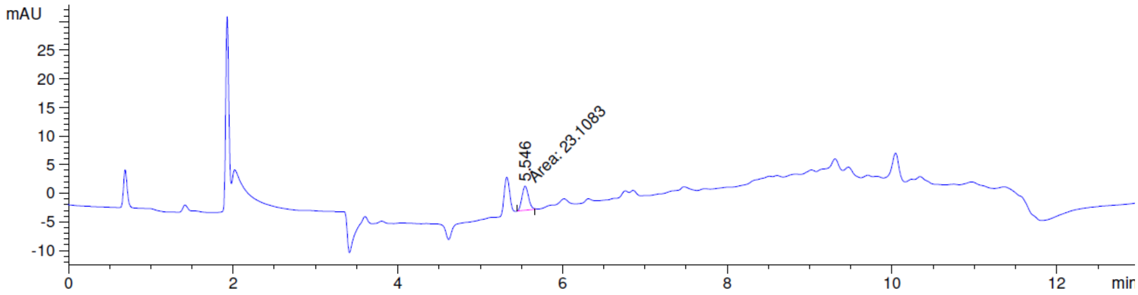

**Figure 39. Loam AcN extract: background peak separated from Clo peak (7 min gradient 0-100 % AcN)**

When applying the same gradient to AcN extracts of sand, the blank soil extracts showed a tiny background peak at retention time 5.5 which overlapped with Clo retention time (Figure 40).

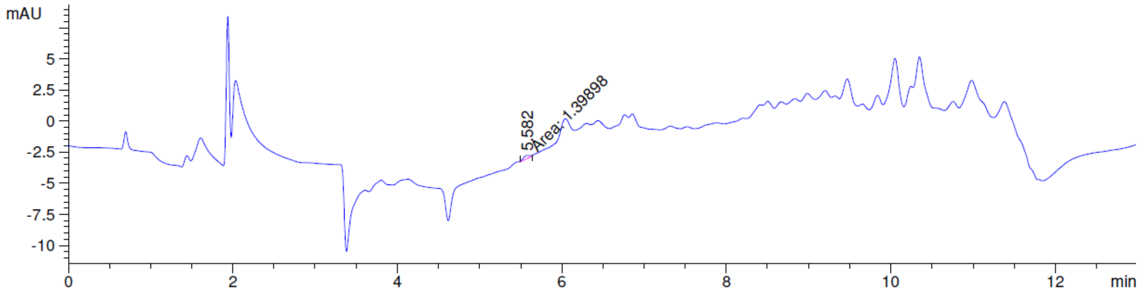

**Figure 40. Blank sand AcN extract background peak at retention time 5.5 min (7 min gradient 0-100 % AcN)**

However, an interference can be considered non-relevant if the response is < 20 % of the LOQ (EMEA 2015). LOQ was 0.08±0.03 which is close to 0.1 mg/L. The mean peak area of cClo 0.1 mg/L was 8.15 mAU. Twenty percent of this value gives 1.63 mAU which is larger than the background peak observed (1.40 mAU). Therefore the HPLC settings were considered selective for both soils and extraction methods.

Finally, the method was tested on the various formulations to preclude interference of formulation ingredients. No interferences were observed.

# C. Photodegradation

To check the suitability of the “Atlas Suntest CPS+” for Clo photodegradation experiments and respective settings of the aging chamber, a pre-test was conducted with AI solutions in $H_2O$ (cClo 0.8 and 6.08 mg/L). Irradiance was controlled in the wave-length range of 300-400 nm and fixed to 65 W/m², BST was set to 40°C. Triplicate transparent HPLC vials per interval contained à 1 mL solution.

Some lessons from these settings were, that regulation of $BST_{max}$ down to 40°C caused Atlas Suntest CPS+ to switch off several times during the test period due to BST-exceedance and that the air space within the HPLC vials allowed for inside misting. Those factors were adjusted in the main experiments.

The system proved suitable to study Clo photodegradation over several half-lives within rather short time-spans: The data followed a first order decay (Figure 41) and a first-order exponential decay fit yielded half-lives of 112.7 (AI 0.8 mg/L) and 115.2 min (AI 6.08 mg/L), which were clearly below the 30 d threshold for insignificant direct photolysis (OECD 2008).

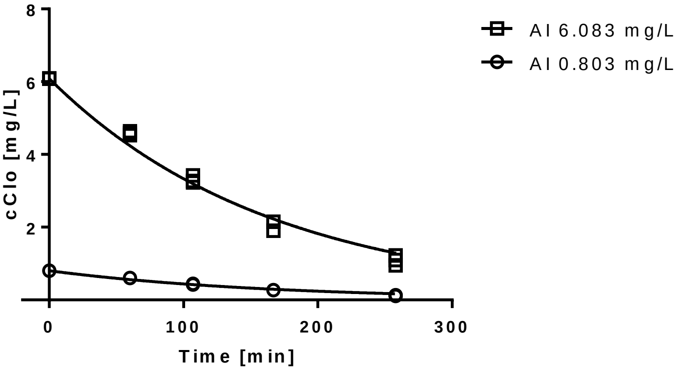

**Figure 41. Photodegradation pretest: exponential decay of AI at two concentration levels**

Having a closer look at the chromatograms, peaks of degradation products appeared with time. At the lower concentration only peaks at retention time 4.9 min were visible, at the higher concentration (cClo 6.08 mg/L) three major peaks were identified at retention time 4.9 min, 5.8 min and 6.3 min (Figure 42). Further investigation (qualification and quantification) of appearing degradation products would have been beyond the focus of this work.

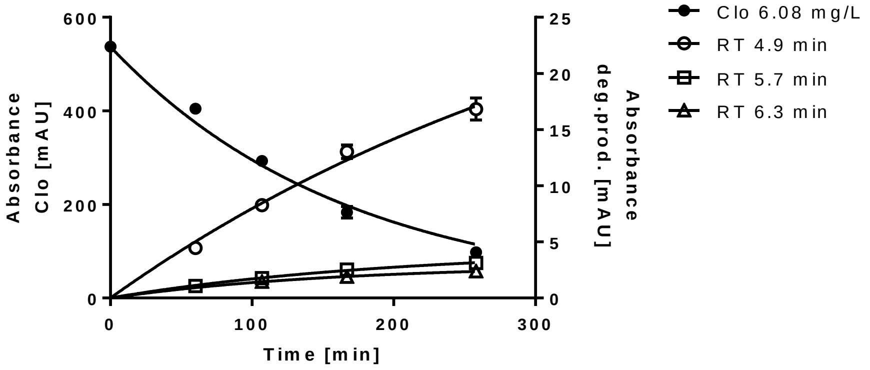

Figure 42. Photodegradation Pretest: formation of degradation products at cClo 6.08 mg/L

Since the OECD (2008) recommends using a phosphate buffer to avoid pH influences on photolysis, a photodegradation run was carried out in buffered background (Na-phosphate buffer, pH 6) at cClo ~544 mg/L and repeated in aqueous background. Figure 43 shows that degradation rates were much higher in buffered solution. Also the difference in k between Com and the NFs was not significant in buffered solution. It seems that the phosphate-buffer either had an influence on polymer stability or acted as a photocatalyst. To avoid these effects, photodegradation experiments were carried out without buffer. Instead pH of the initial solutions was measured to comment on pH influences.

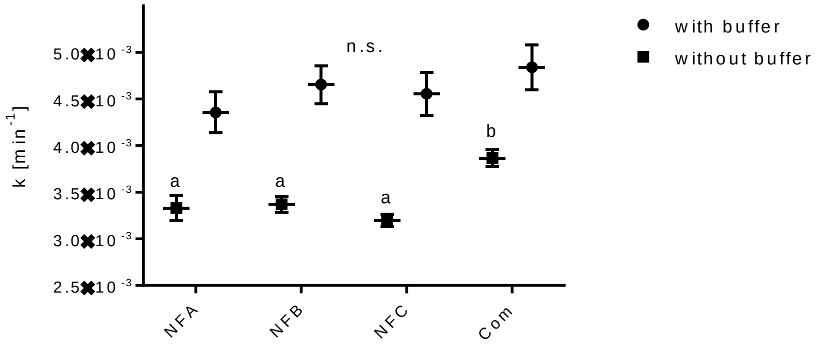

Figure 43. Photolysis rate (k) at cClo ~544 mg/L with and without phosphate buffer

# D. Batch Method

## Choosing Soil:Solution Ratio

According to the OECD guideline on sorption, the fraction adsorbed (A) at equilibrium should be > 20 % or better > 50 %. Based on this and on expected $K_d$ values, the experimental soil:solution ratio can be chosen (OECD 2000). Previously reported $K_d$ values for Clo ranged from 0.52-10.8 (US-EPA 2005; Mulligan et al. 2015) in various soils. Using this range, with a soil:solution ratio of 1:2, the fraction adsorbed (A) would be above 20 % or even above 50 %, as indicated in red (Figure 44).

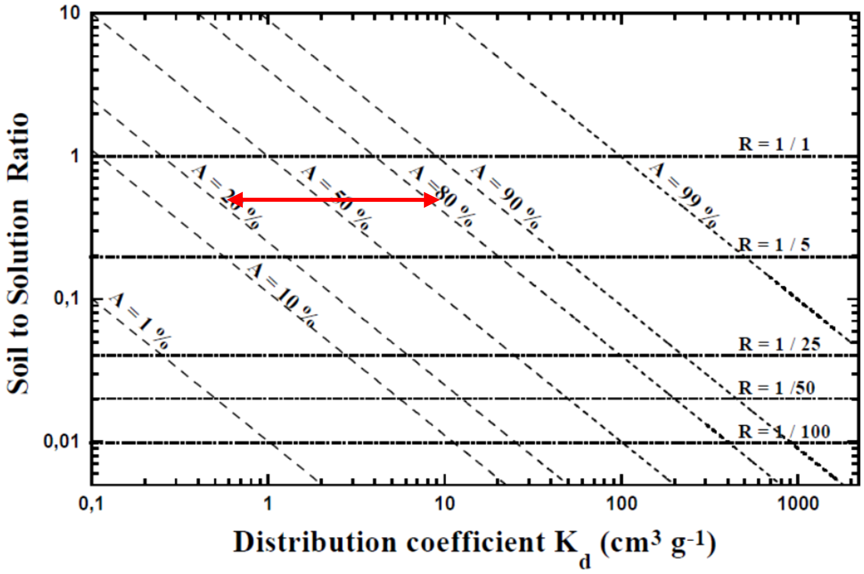

**Figure 44. Setting soil:solution ratio with estimated $K_d$ and intended fraction adsorbed (A) (OECD 2000)**

## Testing Centrifugation Time and Speed

Since the nanocarriers might aggregate in high ionic strength, there is the chance that centrifugation removes NC-attached AI from the solution, which will then be misinterpreted as sorption (Kah et al. 2014).

To check whether this might occur during the batch experiments, a small test was conducted with NFC, which was the formulation that aggregated the most. Three tubes were filled with à 19 mL PPbatch and 0.9 mL H2O and spiked with à 0.1 mL aqueous NFC solution (cClo 1300 mg/L), to end up with the experimental concentrations from the main study. The tubes were centrifuged for 30 min at 4000 g. Then each tube was sampled at a different depth (bottom, middle, top), to see whether a cClo depth gradient is formed, before shaking the tubes and re-sampling for mixed-control. Figure 45 shows that experimental centrifugation force is not strong enough to form a cClo-gradient, perhaps because polymers are too light to be separated and/or because Clo is released from the NC.

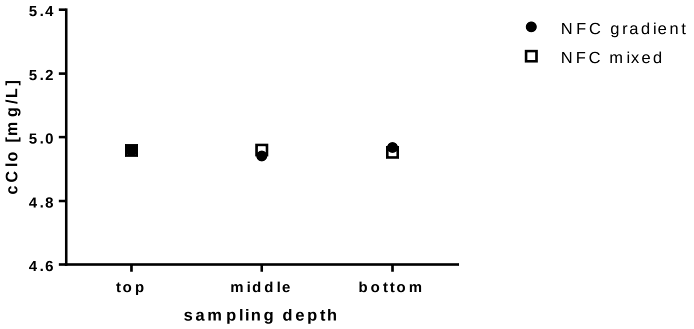

**Figure 45. Test on formation of cClo depth gradient due to centrifugation of NFC in $PP_{batch}$**

### Testing Sorption Kinetics and Equilibration Time

Furthermore, a preliminary study on the equilibration period was conducted with the parallel method (OECD 2000) for AI solution in PP-background. The procedure was the same as in the experimental batchM, just that various equilibration times were tested: After 3, 6, 9, 24 and 48 h duplicates of each soil were taken off the shaker and centrifuged.

The percentages absorbed (A) were calculated according to OECD (2000). The produced data followed “pseudo second order kinetics” (Equation 6) as introduced by Ho & McKay (1998).

**15)**

$$q(t)[mg/kg] = \frac{k_2\, q_e{}^2\, t}{1 + k_2\, q_e\, t}$$

$q(t)$ .....adsorbed amount at time t
$k_2$........pseudo second order rate constant [L $mg^{-1}$ $s^{-1}$]
$q_e$........adsorbed amount at equilibrium [mg/kg]
t..........time [h]

Plotting adsorption percentage over time shows that an equilibration period of 24 h is sufficient (Figure 46).

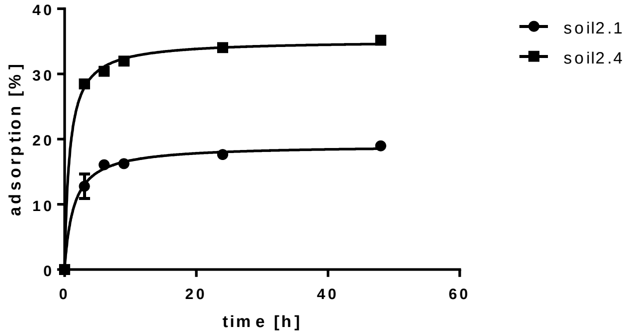

**Figure 46. Pseudo second-order sorption kinetics of AI in PP-background in sand and loam**

Calculated percentages adsorbed reached 17.6±0.2 % in sand and 34.0±0.3 % in loam after 24 h. Although sand was slightly below the recommended min. of 20 % adsorption (OECD 2000), the soil:solution ratio was not increased to 1:1 because with less solution loamy soil forms a slurry which does not mix properly while shaking.

# E. Centrifugation Method

### Choosing Degree of Soil Moisture

The degree of soil moisture for the centM was chosen on the basis of the amount of soil solution collected by centrifugation. A test was conducted with both soils (à 60 g), wetted to 50 % of the respective MWHC (as in Kah et al. (2014)) in a screw-cap glass bottles (250 mL) and incubated for three days in the dark fridge at 4°C. Then triplicate subsamples of à ~10 g were weighed into the inserts of the PVDF centrifuge tubes, equipped with pre-wetted (0.1 mL H2O) glass microfiber filters with a pore size of 1.6 µm, and centrifuged for 30 min at 1500 g. The recovered soil solutions (determined by weighing and normalized to 10 g of soil) amounted to 0.807±0.014 and 0.073±0.005 mL, for sand and loam respectively. Since 73 µL is a very tiny amount for further processing, experimental soil moisture was increased to 60 % of MWHC.

### Accounting for Introduced Salt Mass in Fertilizer Background

In the case of PP-background, salt introduced an additional mass component ($m_{salt}$) to the wet subsamples ($m_{sw}$) weighed in for AcN-extraction and centrifugation (Figure 47).

This salt mass has been excluded when adjusting to 60 % MWHC for incubation. Thus, it was also excluded from the mass of soil solution ($m_{ss}$) and of dry soil ($m_{sd}$) used in $K_d$, percentage absorbed and extraction recovery calculations, so that $m_{ss} = m_{sw} - m_{sd} - m_{salt}$ and $m_{sd} = m_{sw} - m_{ss} - m_{salt}$.

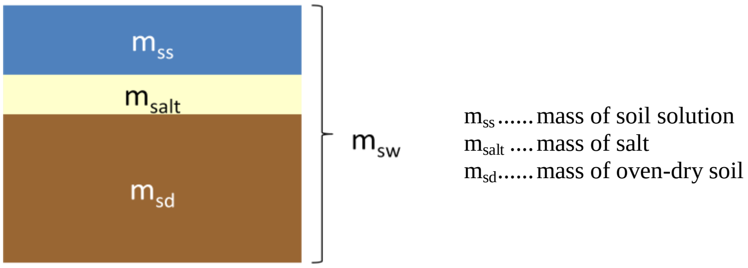

**Figure 47. Composition of wet soil mass in centrifugation experiments with PP background solution**

### Determination of AcN extraction recoveries

The percentage recovery was calculated as the ratio of cClo measured in the AcN extracts and expected nominal cClo in the extracts (Equation 16).

**16)**

$$recovery\ [\%] = \frac{cClo_{measured}\ [mg/L]}{cClo_{nominal}\ [mg/L]} \times 100$$

To derive $cClo_{nominal}$, the Clo concentrations of the working solution ($cClo_{WS}$) used for spiking were determined by HPLC in à triplicate dilutions (1:100 for formulation working solutions with cClo ~1300 mg/L and 1:10 for AI working solution with cClo ~130 mg/L). With the amount of spiking solution added ($V_{WS}$) and the total amount of dry soil weighed in for pre-equilibration ($m_{sd\_tot}$), the Clo concentration on a dry-soil basis ($cClo_{sd}$) was calculated (Equation 17), which was further used to arrive at the nominal cClo in solution (Equation 18). In the case of PP-background, $m_{sd\_tot}$ and $m_{sd\_extr}$ were corrected for the introduced salt mass (see above).

**17)**

$$c_{Clo_{sd}}\ [mg/kg] = \frac{c_{Clo_{WS}} \times V_{WS}}{m_{sd\_tot}}$$

$cClo_{sd}$ .... concentration of Clo in oven-dry soil [mg/kg]
$cClo_{WS}$... concentration of Clo in working solutions [mg/L]
$V_{WS}$ ....... volume of working solution spiked [L]
$m_{sd\_tot}$..... mass of total oven-dry soil weighed in for incubation [kg]

**18)**

$$c_{Clo_{nominal}}\ [\mathrm{mg/L}] = c_{Clo_{sd}} \times \frac{m_{sd\_extr}}{\mathrm{m}_{ss} + V_{AcN}}$$

$cClo_{sd}$..... concentration of Clo in oven-dry soil [mg/kg]
$m_{sd\_extr}$.... mass of oven-dry soil extracted [kg]
$m_{ss}$ ......... mass of soil solution [kg]
$V_{AcN}$....... volume of AcN for extraction [L]

# Literature Cited

Agilent Technologies Inc., 2009. Agilent ChemStation. *Agilent Technologies*. Available at: www.agilent.com/cs/library/usermanuals/.../G2070-91126_Understanding.pdf [Accessed August 17, 2016].

EMEA, 2015. Guideline on bioanalytical method validation. Available at: www.ema.europa.eu/docs/en_GB/document_library/Scientific_guideline/2011/08/WC500109686.pdf [Accessed June 15, 2016].

Ho, Y.S. & McKay, G., 1998. Kinetic model for lead (II) sorption onto peat. *Adsorption Science and Technology*, 16(4), pp.243–255.

Kah, M. et al., 2014. Analysing the fate of nanopesticides in soil and the applicability of regulatory protocols using a polymer-based nanoformulation of atrazine. *Environmental Science and Pollution Research*, 21(20), pp.11699–11707.

Mulligan, R.A., Parikh, S.J. & Tjeerdema, R.S., 2015. Abiotic partitioning of clothianidin under simulated rice field conditions. *Pest management science*, 71(10), pp.1419–1424.

OECD, 2008. OECD Guidelines for the Testing of Chemicals Nr. 316: Phototransformation of Chemicals in Water – Direct Photolysis.

OECD, 2000. OECD Guidline for the Testing of Chemicals Nr. 106: Adsorption - Desorption Using a Batch Equilibrium Method.

US-EPA, 2005. EFED Registration Chapter for Clothianidin for use on Potatoes and Grapes as a spray treatment and as a Seed Treatment for Sorghum and Cotton. Available at: www3.epa.gov/pesticides/chem_search/cleared_reviews/csr_PC-044309_28-Sep-05_a.pdf. [Accessed April 12, 2016].

# F. Zusammenfassung

Die Anzahl an Pestizidprodukten mit Komponenten in der Nano-Größenordnung (bis 1000 nm) nimmt zu. Für solche „Nanoformulierungen“ (NFs) sind Polymer-basierte Trägerpartikel (NCs) besonders vielversprechend, da ihre Eigenschaften gezielt designt werden können, um den Wirkstoff (AI) z.B. langsam oder zielgerichtet freizusetzen, ihn vor vorzeitigem Abbau zu bewahren oder seine Löslichkeit zu erhöhen. Daher haben NFs aber auch das Potential, das Umweltverhalten des AIs zu beeinflussen und könnten eine Anpassung der relevanten Gesetzgebung für die Risikobewertung von Pestiziden erfordern. Der aktuelle Wissensstand scheint jedoch nicht ausreichend, um dies zu beurteilen.

Diese Arbeit untersucht daher den Einfluss von Nanoformulierungen auf (1) die photochemische Abbaurate und (2) das Sorptionsverhalten des Wirkstoffes Clothianidin (Clo), anhand von vergleichenden Laborstudien dreier NFs (NFA, NFB, NFC), einer kommerziell verfügbaren Formulierung (Com) und der reinen Wirkstofflösung (AI).

Die Analyse von Clo erfolgte mit HPLC und UV-Vis Detektion. Die getesteten Clo-Konzentrationen wurden an maximal realistische Ausbringungsmengen für Feldfrüchte bei der Blattspritzung (für den photochem. Abbau) und mit der Saat in der Anbaufurche (für die Sorption) angelehnt. Beide Prozesse (Sorption & Abbau) wurden in zwei Hintergrundlösungen untersucht: entionisiertes Wasser (H2O) einerseits und eine PowerPhos Flüssigdünger-Lösung (PP) andererseits. Letztere sollte die Freisetzung des AI von den NCs durch „Aussalzen“ reduzieren.

Der photochemische Abbau erfolgte durch Bestrahlung von Formulierungs- und AI-Lösungen mit einer Xenonbogenlampe. Anhand der generierten Abbaukurven wurden die Abbauraten bestimmt. Um Konzentrationseffekte zu berücksichtigen, wurden im H2O-Hintergrund mehrere Konzentrationen der Formulierungen unter und über der Löslichkeit von Clo getestet.

Die Ergebnisse zeigten einen Fall der Abbauraten in H2O für alle Formulierungen und den AI mit ansteigenden Clo-Konzentrationen. Nahe und über der Löslichkeit von Clo setzte ein Schutzmechanismus der NFs ein und verlangsamte den Abbau – umso stärker, je höher die Konzentrationen über der Clo-Löslichkeit lagen. Da auch die Freisetzung des AIs von den NCs Löslichkeitsbedingt war, konnte der reduzierte Abbau dem Schutz des AIs durch die NCs zugeordnet werden. In PP-Lösung waren die Abbauraten aller Formulierungen und des AIs stark reduziert, jedoch war der Effekt nicht, wie angenommen, stärker für die NFs als für Com/AI, weshalb der Effekt eher der Strahlungsabsorption durch die Düngersalze geschuldet war und keinem Nanoeffekt durch Aussalzen.

Sorptionsexperimente wurden an unterschiedlichen Böden (Sand und Lehm) mit zwei Methoden durchgeführt: einer klassischen Batch-Equilibrium Methode (batchM) und einer Zentrifugenmethode (centM) die es ermöglicht, Sorption unter realistischen Boden:Lösung-Verhältnissen und über die Zeit zu untersuchen. Aus den generierten Daten wurden Verteilungskoeffizienten (Kd) berechnet.

Drei-faktorielle ANOVAs wiesen in beiden Sorptionsmethoden den Bodentyp als dominierenden Einflussfaktor aus. Dieser erklärte > 90 % der Kd-Varianz in beiden Methoden, wobei die Kd-Werte für Lehm wegen des höheren Organikgehalts in allen Designs höher waren als für Sand. Die Einflussfak-

toren Formulierung, Hintergrundlösung und Faktorinteraktionen beliefen sich auf < 2.3 %. Es konnte kein genereller Nanoeffekt nachgewiesen werden: In H2O löste sich der AI von den NCs da die Clo-Konzentrationen unter der Löslichkeit lagen und auch die Zugabe von PP löste keine Nanoeffekte aus. Nanoeffekte einzelner Formulierungen konnten aber in der batchM beobachtet werden: NFC sorbierte stärker als Com in beiden Böden & Hintergrundlösungen (und stärker als AI in H2O-Hintergrund), und NFB sorbierte generell stärker an Lehm als Com/AI. NFC war gleichzeitig die Formulierung die bei hoher Ionenstärke am stärksten aggregierte, weshalb der physische Einschluss des AI in Aggregaten eine mögliche Erklärung ist. Generell waren Kd-Unterschiede zwischen den Formulierungen aber gering und irrelevant gegenüber anderen Faktoren (z.B. Bodentyp).

Davon abgesehen konnten jedoch Erkenntnisse über die Sorptionsmethoden und Einflüsse von Düngersalzen gewonnen werden. Die Hintergrundlösung hatte stärkeren Einfluss in der centM und verursachte eine gegensätzliche Wirkung in Sand und Lehm: Kd-Werte für Sand waren höher in H2O, jene für Lehm eher in PP. Ersteres kann an den Fulvin- und Huminsäuren liegen, die den Organikanteil im Sand dominierten. Diese Säuren wurden vom NH4+ des Düngers gelöst co-mobilisierten Clo. Zweiteres kann durch die Zerstörung von Lehmaggregaten durch Düngersalze erklärt werden. Aggregate verlangsamen die Equilibrierung mit der Lösung und verringern den Kontakt zwischen Adsorbat und Adsorbenten. Werden Aggregate durch monovalentes NH4+ zerstört, kann das die Sorption erhöhen. Eine längere Inkubationszeit (in der centM) bedeutete grundsätzlich eine erhöhte Sorption durch die langsame Diffusion in feine Poren und Aggregate. Nur in Lehm-H2O wurde das nicht beobachtet, wahrscheinlich wegen des starken Diffusionsgradienten, in den mit entionisiertem Wasser befeuchteten Lehm-Aggregaten.

Der Vergleich der Sorptionsmethoden zeigte, dass die centM eine höhere prozentuelle Clo-Sorption generierte als die batchM. Jedoch waren die Kd-Werte nur für Lehm (in H2O und PP) höher mit der centM, für Sand hingegen im Batch-Versuch. Eine stärkere Sorption in der centM kann bei eigentlich gering sorbierenden Substanzen wie Clo durch den physischen Einschluss in Aggregaten (z.B. in Zonen immobilen Wassers) aufgrund des hohen Boden:Lösung-Verhältnisses erklärt werden.

Zusammenfassend fand die aktuelle Studie keinen Nanoeffekt der stark genug wäre, um für die Risikobewertung der getesteten Formulierungen relevant zu sein, wenn die maximalen Ausbringungsmengen für Feldfrüchte eingehalten werden. Ein verlangsamter photochem. Abbau ist jedoch sehr wahrscheinlich, wenn höhere Spray-Konzentrationen (wie für Trauben und Kernobst empfohlen) verwendet werden. Die getesteten NFs setzten den AI sofort nach Verdünnung unterhalb der Löslichkeit frei, was bedeutet, das Formulierungen mit verzögerter AI-Freisetzung sehr wahrscheinlich mehr Einfluss auf den Verbleib und das Verhalten des AIs in der Umwelt haben.

Bezüglich der Sorptionsmethoden überschätzte die batchM tendenziell die Clo-Mobilität, da physikalische Rückhalteprozesse in strukturierten Böden ignoriert werden. Auch komplexe Interaktionen von Dünger, Organik und Bodenaggregaten, sowie Änderungen über die Zeit wurden in der centM sichtbar und könnten für die Untersuchung von Formulierungen mit langsamer AI-Freisetzung dienlich sein.